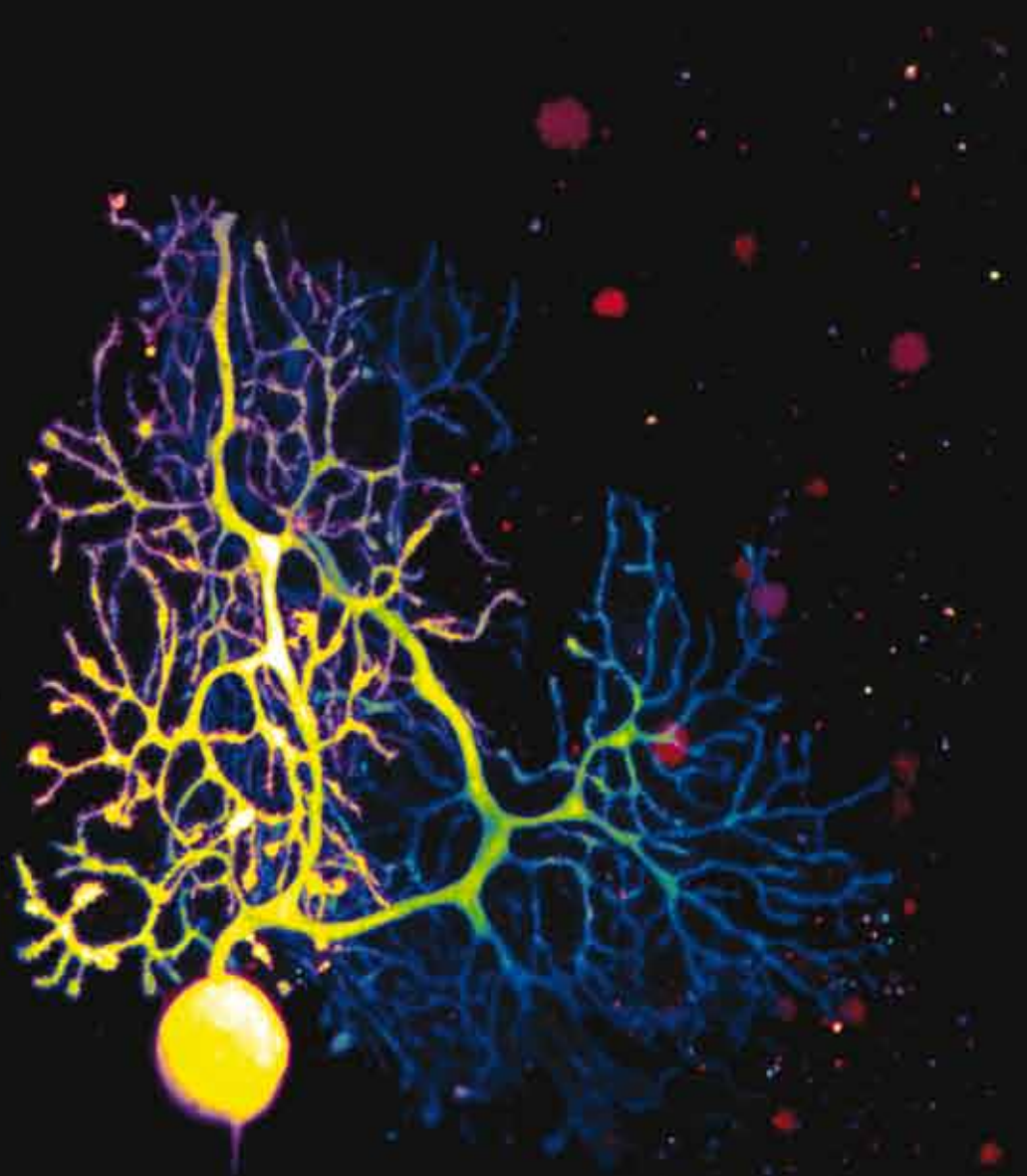


Impact of Signaling and Plasticity on Cerebellar Function and Memory Formation



Boeke J. van Beugen

IMPACT OF SIGNALING AND PLASTICITY ON CEREBELLAR FUNCTION AND MEMORY FORMATION

**Gevolgen van Signaaloverdracht
en Plasticiteit op Cerebellair Functioneren
en Geheugenvorming**

Boeke Job van Beugen

ISBN: 978-94-6182-216-1

Lay-out and printing: Off Page, www.offpage.nl

Cover image: Color-coded representation of a cerebellar Purkinje cell, selectively filled with Oregon Green BAPTA-2 and Alexa-549 *in vitro*, displaying the ever impressive dendritic tree on which it can receive hundreds of thousands of parallel fiber inputs.

Copyright © 2012 by B.J. van Beugen. All rights reserved. No part of this book may be reproduced, stored in a retrieval system, or transmitted in any form or by any means, without prior permission of the author.

IMPACT OF SIGNALING AND PLASTICITY ON CEREBELLAR FUNCTION AND MEMORY FORMATION

**Gevolgen van Signaaloverdracht
en Plasticiteit op Cerebellair Functioneren
en Geheugenvorming**

Proefschrift

Ter verkrijging van de graad van doctor aan de
Erasmus Universiteit Rotterdam
Op gezag van de rector magnificus
Prof. Dr. H.G. Schmidt
En volgens besluit van het college voor Promoties

De openbare verdediging zal plaatsvinden op
Woensdag 19 december 2012 om 09:30

Door
Boeke Job van Beugen
Geboren te Utrecht

Dedicated to my dad.

I was really fortunate to have the perfect tutor as my father.

*Thanks for all the support and guidance you've given me over the years.
No one would have been more proud of this thesis than you.*

Boeke, November 2012



TABLE OF CONTENTS

Chapter I	Introduction	7
1.1.	Cerebellar organization	9
1.1.1.	Layer organization of the cerebellum	9
1.1.2.	Pathways in the cerebellar network	9
1.2.	Synaptic transmission	12
1.2.1.	Basic overview of synaptic transmission	12
1.2.2.	Plasticity of synaptic transmission	12
1.2.3.	Functional role of plasticity	12
1.3.	Plasticity at the parallel fibre–Purkinje cell synapses	13
1.3.1	Postsynaptic LTD	13
1.3.2.	Postsynaptic LTP	15
1.3.3	Presynaptic LTP and LTD	16
1.4.	Scope of this thesis	17
Chapter II	High Frequency Burst Firing Ensures Vesicular Release at the Parallel Fiber to Purkinje Cell Synapse at the Cost of Temporal Coding.	25
Chapter III	Climbing Fiber-Evoked Endocannabinoid Signaling Heterosynaptically Suppresses Presynaptic Cerebellar Long-Term Potentiation	47
Chapter IV	Purkinje cell-specific knockout of the protein phosphatase PP2B impairs potentiation and cerebellar motor learning	63
Chapter V	Enhanced AMPA receptor function promotes cerebellar long-term depression rather than potentiation	89
Chapter VI	General discussion	103
6.1.	Implications of low release probability at the PF-PC synapse on cerebellar function	105
6.2.	Behavioural implication of reversible plasticity at PF-PC synapse	105
6.3.	Network formation under CF control	106
6.3.1.	Endocannabinoids assist climbing fiber driven plasticity at the PF-PC synapse	106
6.3.2.	Function of the Purkinje cell network: Creating output by selecting input	106
6.3.3.	Distributed synergistic plasticity	108
6.4	Ampakines: the potential to promote cerebellar learning	111
Publications		115
Acknowledgements		117

INTRODUCTION

Boeke J. van Beugen

parts of this introduction are adapted from
Gao, van Beugen and De Zeeuw, 2012



I. INTRODUCTION

Although the full extent of cerebellar involvement in the many aspects of behaviour remains elusive, its role in the control of movement has been known for more than a century (Glickstein et al., 2009). Positioned as an isolated network superimposed on other structures within the brain, the cerebellum is typically regarded as a ‘controller’ of ongoing processes, such as the fine-tuning of movement and posture (Fig 1). As a controller, the output of the cerebellum needs to be flexible and constantly adapt to (re-)establish the desired level of control. It is generally believed that plasticity (*i.e.* the ability of a synapse to alter its connective strength) underlies the process of adaptation and embodies the structural substrate of learning and memory formation.

1.1. Cerebellar organization

1.1.1. Layer organization of the cerebellum

Although voluntary and involuntary movements can be initiated without a cerebellum, the proper execution of movements as well as their adaptive modification and possibly cognitive preparation require an intact cerebellum (De Zeeuw et al., 2011). This agrees with the position and connectivity of the cerebellum: it is superimposed on, but not an essential part of, the brain systems that are required for the initiation and occurrence of movements (see Fig 1, part a).

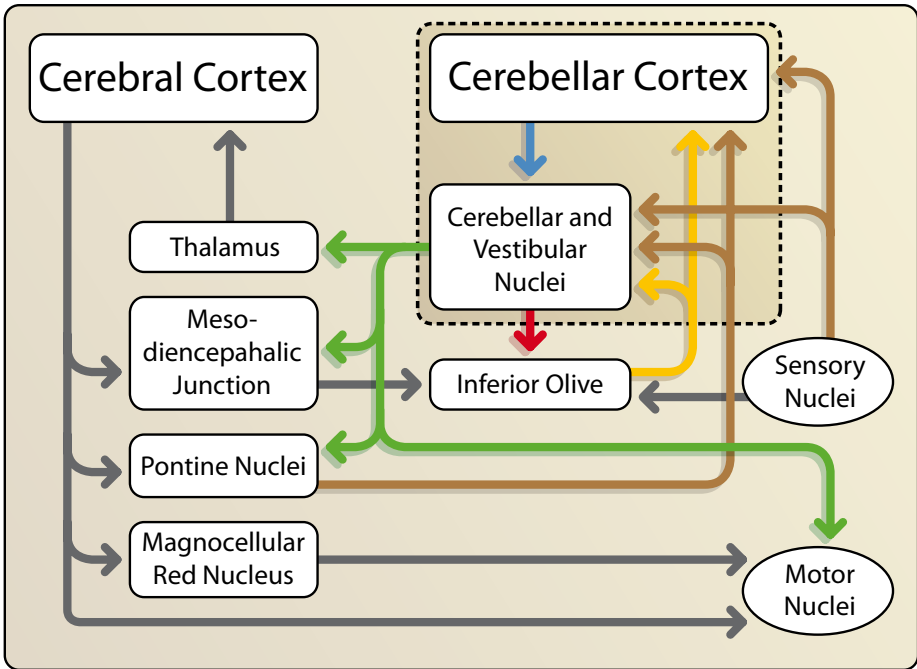
The cerebellum is itself composed of layered networks (see Fig 1, part b): first, the cerebellar cortex is superimposed on cerebellar and vestibular nuclei, to which it projects and via which it exerts all its effects; second, the granular layer of the cerebellar cortex contains the mossy fibre (MF) – granule cell (GrC) pathway on which Golgi cells (GoC) and unipolar brush cells (UBCs) (both interneurons) are superimposed (Geurts et al., 2003; van Versendaal et al., 2012) ; and third, in the molecular layer another group of interneurons (molecular-layer interneurons (MLI)), formed by stellate cells and basket cells, is superimposed on Purkinje cells (PC)(Jorntell et al., 2010). Finally, the cerebellar cortex contains a type of interneuron, the Lugaro cell (LC), that is superimposed on all other types of interneurons in both the granular and molecular layers (Geurts et al., 2003).

Because of the layered character of its networks, the cerebellar cortex is well suited to be dissected into cellular components so that their individual functional contributions within the networks can be analyzed. Such an approach follows the concept that during CNS evolution the implementation of new functions involves imposing new networks onto existing circuitries and/or expanding existing circuitries (Nakanishi, 2009; Simat et al., 2007). Specific functions may thus be attributed to separate network layers in the cerebellar cortex and their target neurons in cerebellar and vestibular nuclei.

1.1.2. Pathways in the cerebellar network

In part a (Fig 1), pathways directly involved in olivocerebellar processing are shown in individual colours, and other pathways are indicated in dark grey. Mossy fibres (brown arrow) and climbing fibres (CF) (yellow arrow) convey their input to both the nuclei and cortex of the cerebellum (dashed border). Purkinje cells in turn project from the

a



b

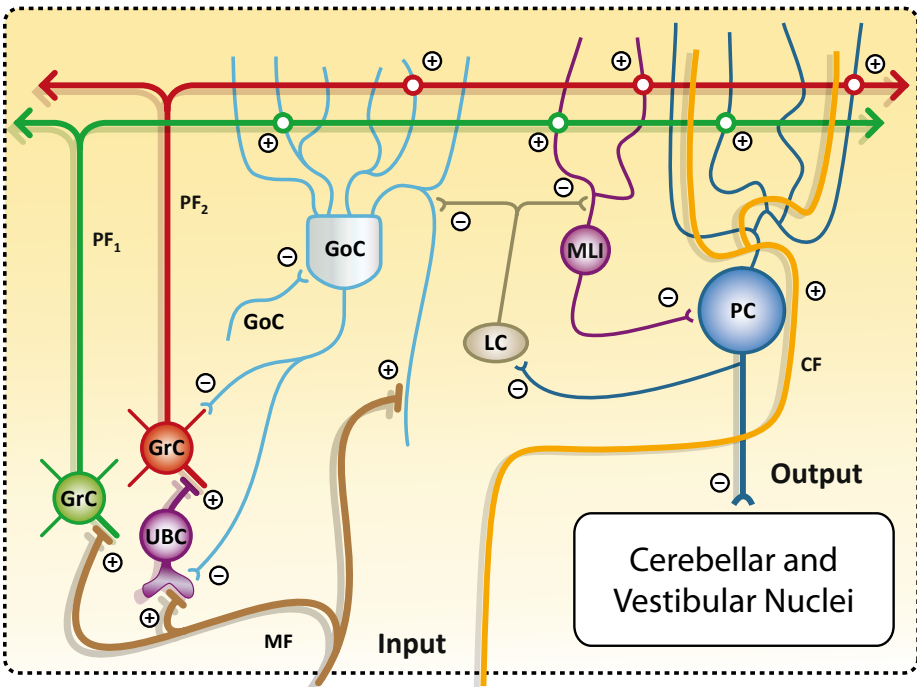


Fig 1 Intro (on the previous page): Layered character of the cerebellum and its position in the brain. Although voluntary and involuntary movements can be initiated without a cerebellum, the proper execution of movements as well as their adaptive modification and possibly cognitive preparation require an intact cerebellum. This accords with the position and connectivity of the cerebellum: it is superimposed on, but not an essential part of, the brain systems that are required for the initiation and occurrence of movements (see the figure, part **a**). The cerebellum is itself composed of layered networks (see the figure, part **b**): first, the cerebellar cortex is superimposed on cerebellar and vestibular nuclei, to which it projects and via which it exerts all its effects; second, the granular layer of the cerebellar cortex contains the mossy fibre (MF) – granule cell (GrC) pathway on which Golgi cells (GoC) and unipolar brush cells (UBCs) (both interneurons) are superimposed; and third, in the molecular layer another group of interneurons (molecular-layer interneurons (MLI)), formed by stellate cells and basket cells, is superimposed on Purkinje cells (PC). Finally, the cerebellar cortex contains a type of interneuron, the Lugaro cell (LC), that is superimposed on all other types of interneurons in both the granular and molecular layers. Because of the layered character of its networks, the cerebellar cortex is well suited to be dissected into cellular components so that their individual functional contributions within the networks can be analyzed. Such an approach follows the concept that during CNS evolution the implementation of new functions involves imposing new networks onto existing circuitries and/or expanding existing circuitries. Specific functions may thus be attributed to separate network layers in the cerebellar cortex and their target neurons in cerebellar and vestibular nuclei. In part **a**, pathways directly involved in olivocerebellar processing are shown in individual colours, and other pathways are indicated in dark grey. Mossy fibres (brown arrow) and climbing fibres (CF) (yellow arrow) convey their input to both the nuclei and cortex of the cerebellum (dashed border). Purkinje cells in turn project from the cerebellar cortex to the cerebellar and vestibular nuclei (blue arrow). From these nuclei, projections are provided to the inferior olive for inhibitory feedback (red arrow) and to other extracerebellar sites for control of motor behaviour and/or cognitive functions. The direct projections in the figure from the cerebellar and vestibular nuclei to the motor nuclei reflect the direct projections towards the oculomotor nuclei; direct connections to other motor nuclei have so far not been identified. In part **b** excitatory and inhibitory synaptic connections are indicated by “+” and “-”, respectively. The cerebellar cortex has many potential sites for synaptic plasticity at both excitatory and inhibitory terminals, but it may also regulate plasticity downstream, in the cerebellar and vestibular nuclei. In general, deficits in motor consolidation, motor learning and motor performance result from mild, mediocre, and severe problems in cerebellar function, respectively; thus, the larger the number of sites of synaptic plasticity are affected in the cerebellar circuitry, the more severe the impairment in motor function.

cerebellar cortex to the cerebellar and vestibular nuclei (blue arrow). From these nuclei, projections are provided to the inferior olive for inhibitory feedback (red arrow) and to other extracerebellar sites for control of motor behaviour and/or cognitive functions. The direct projections in the figure from the cerebellar and vestibular nuclei to the motor nuclei reflect the direct projections towards the oculomotor nuclei; direct connections to other motor nuclei have so far not been identified.

In part **b** (Fig 1) excitatory and inhibitory synaptic connections are indicated by “+” and “-”, respectively. The cerebellar cortex has many potential sites for synaptic plasticity at both excitatory and inhibitory terminals, but it may also regulate plasticity downstream, in the cerebellar and vestibular nuclei. In general, deficits in motor consolidation, motor learning and motor performance result from mild, mediocre, and severe problems in

cerebellar function, respectively; thus, the more sites of synaptic plasticity are affected in the cerebellar circuitry, the more severe the impairment in motor function.

1.2. Synaptic transmission

1.2.1. Basic overview of synaptic transmission

Both electrical and neuronal circuits process a given input by guiding the flow of information over specific relays. In electrical circuits, these relays are often subject to all-or-none characteristics, whereas in neuronal networks these connections display a graded range of responses, allowing for a higher level of detail that can be carried over a single relay.

Signalling between neurons occurs predominantly over synapses. Whereas other forms of transmission exist, synapses provide the potential to adjust connective strength, making them the perfect tool for a network to alter its computational properties.

A synapse consists of a presynaptic and a postsynaptic site. The presynaptic site, also known as the presynaptic terminal, is a specialized structure of the ‘sending’ neuron in which electrical signals (action potentials) are translated into a local rise of free calcium ions. Sensitive to relative fluctuations in the calcium concentration, small pockets (vesicles) release their content of freely diffusible molecules (neurotransmitter) into the synaptic cleft. The postsynaptic site (spine) is a specialized structure belonging to the ‘receiving’ neuron. Here, neurotransmitters bind to receptors, which translate this signal back into an electrical current and/or activate molecular signalling pathways.

1.2.2. Plasticity of synaptic transmission

This structural organisation provides numerous potential sites at which small alterations can affect synaptic behaviour (Hebb, 1949). For example, addition of a presynaptic calcium buffer will reduce responsiveness by ‘filtering’ fluctuations in the calcium concentration to individual action potentials; altering vesicular content or changing the total number of postsynaptic receptors will modify the amplitude of transmission. Depending on preceding activity, synapses can adapt their connective strength (Bliss and Lomo, 1973). Such adaptations can be transitory (short-term plasticity) or long-lasting (long-term plasticity). Generally, persistent activity will strengthen a connection (potentiation), whereas absence of activity while neighbouring synapses are responsive leads to weakening (depression), as predicted by Hebb.

1.2.3. Functional role of plasticity

Historically, declarative and procedural memory formations in cortical structures have been proposed to be predominantly mediated by a specific, monosynaptic form of plasticity. Long-term potentiation (LTP) at synapses of CA3 axons onto CA1 pyramidal cells was originally considered the sole substrate for hippocampal learning (Neves et al., 2008), whereas long-term depression (LTD) at the parallel fibre–Purkinje-cell synapse has been proposed to be the dominant type of plasticity for cerebellar learning (Ito, 2001). However, different forms of plasticity can occur at multiple, synaptic and extrasynaptic sites within the same network and serve complementary or overlapping functions. For example, evidence is now emerging that LTD in the hippocampus and intrinsic plasticity in the cerebral cortex are likely to contribute to particular components of

spatial and visual learning (Collingridge et al., 2010; Feldman, 2009; Griffiths et al., 2000; Kessels and Malinow, 2009; Luscher and Huber, 2010; Malenka and Bear, 2004). Likewise, procedural memory formation, which underlies the coordination of movements, may be mediated by multiple forms of plasticity including those occurring in the cerebellum (Belmeguenai et al., 2010; Ito and Kano, 1982; Lev-Ram et al., 2002).

Neurons in cerebellar cortex and neurons in cerebellar and vestibular nuclei show various forms of synaptic and intrinsic plasticity (Bagnall and du Lac, 2006; Hansel et al., 2001; Pugh and Raman, 2009), and neurons in both regions are innervated by axons from the mossy fibre and climbing fibre system (Fig 1). This raises the possibility that the various forms of plasticity induced in the cerebellar cortex and nuclei are not independent, but are finely regulated in a coordinated fashion (De Zeeuw et al., 2011; Kassardjian et al., 2005), and that some of the memories that are formed in the cerebellar cortex ultimately are also consolidated and stored in the cerebellar and vestibular nuclei (Kassardjian et al., 2005; Kellett et al., 2010; Shutoh et al., 2006).

Cerebellar research has benefitted from discoveries of cell-specific promoters for the neurons that form the main chain of information through the different layers in the cerebellar cortex. These include both the promoter for gamma-aminobutyric-acid type-A-receptor (GABA_A) $\alpha 6$ -subunit, which is specific for cerebellar granule cells (Bahn et al., 1997), and the *Pcp2* promoter L7, which is specific for Purkinje cells (Oberdick et al., 1990). These tools have enabled the creation of transgenic animals with cell-specific deletions in both the granular or molecular layer. As a result, one can specifically and directly manipulate the output of the granule cells and Purkinje cells themselves (De Zeeuw et al., 1998; Schonewille et al., 2010; Seja et al., 2012). Moreover, by manipulating postsynaptic receptors and/or second messenger systems inside these cells, one can in effect also make a specific interruption of the output of presynaptic interneurons involved (Wulff et al., 2009).

1.3. Plasticity at the parallel fibre–Purkinje cell synapses

Purkinje cells receive their input from granule cells via thousands of parallel fibre varicosities (Palay and Chan-Palay, 1974). All four forms of long-term plasticity that can occur at a synapse — postsynaptic LTD (Ito and Kano, 1982), postsynaptic LTP (Coesmans et al., 2004; Lev-Ram et al., 2002), presynaptic LTP (Salin et al., 1996) and presynaptic LTD (Qiu and Knöpfel, 2009) — have been described for the parallel fibre–Purkinje cell contacts. Whereas the functional relevance of the presynaptic forms of plasticity remains to be largely demonstrated at the behavioural level (Le Guen and De Zeeuw, 2010; Neher and Sakaba, 2008), the postsynaptic forms of plasticity have been implicated in learning.

1.3.1 Postsynaptic LTD

Postsynaptic LTD at the parallel fibre–Purkinje cell synapse is typically induced by paired stimulation of parallel fibres and climbing fibres. This combined stimulation induces a large Ca^{2+} influx and activates both AMPA and mGluR1 receptors (Fig 2), which in turn facilitate phospholipase C to produce inositol-1,4,5-triphosphate (IP_3) (Hartell, 1994; Khodakhah and Armstrong, 1997; Linden and Connor, 1991). Boosted by IP_3 - and Ca^{2+} -

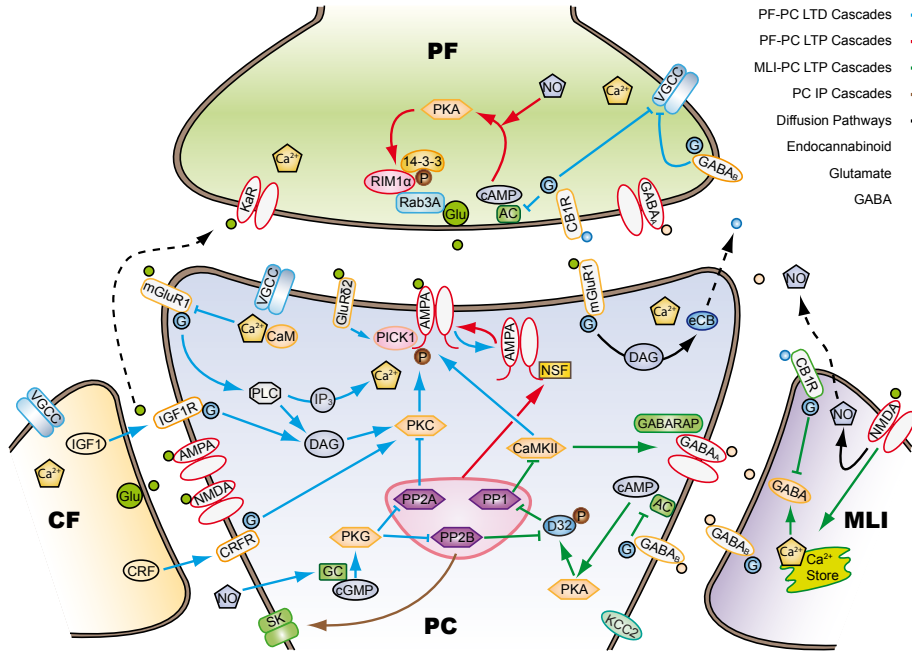


Fig 2 Intro. Molecular mechanisms underlying plasticity in Purkinje cells. The schematic drawing presents the main molecules and pathways involved in the various forms of synaptic plasticity that can occur at synapses between parallel fibres (PF), climbing fibres (CF) or molecular-layer interneurons (MLI) and Purkinje cells (PC). Pathways involved in long-term depression (LTD) at PF–PC synapses are marked in blue, and pathways involved in long-term potentiation (LTP) at PF–PC synapses are marked in red. Green arrows indicate pathways involved in LTP at MLI–PC synapses, and the brown arrow indicates the molecular cascade for intrinsic plasticity. All freely diffusing messenger pathways are marked in black. AC, adenylyl cyclase; AMPA, α -amino-3-hydroxy-5-methyl-4-isoxazolepropionic acid receptor; CaMKII, Calcium/calmodulin activated kinase II; cAMP, cyclic adenosine mono-phosphate; CB1R, cannabinoid receptor 1; cGMP, cyclic guanosine mono-phosphate; CRF, corticotropin-releasing factor; CRFR, corticotropin-releasing factor receptor; D32, DARPP-32; DAG, diacyl glycerol; eCB, endocannabinoid; GABA, gamma-aminobutyric acid; GABA_A, gamma-aminobutyric acid type A receptor; GABA_B, gamma-aminobutyric acid type B receptor; GABARAP, GABA_A-R-associated protein; GC, guanylate cyclase; Glu, glutamate; GluR δ 2, Glutamate receptor delta2; IGF1, insulin-like growth factor 1; IGF1R, insulin-like growth factor 1 receptor; IP₃, inositol trisphosphate; K_aR, Kainate receptor; Kcc2, K⁺-Cl⁻ cotransporter 2; mGluR1, metabotropic glutamate receptor-1; NMDAR, N-methyl D-aspartate receptor; NSF, N-ethylmaleimide-sensitive factor; PICK1, protein interacting with C kinase 1; PKA, protein kinase A; PKC, protein kinase C; PKG, protein kinase G; PLC, phospholipase C; PPI, protein phosphatase 1; PP2A, protein phosphatase 2A; PP2B, protein phosphatase 2B; RIM1 α , Rab3-interacting molecule 1alpha; SK, small conductance Ca²⁺ activated K⁺ channel; and VGCC, voltage gated Ca²⁺ channel.

mediated Ca^{2+} release from the endoplasmatic reticulum, the postsynaptic Ca^{2+} transient becomes supralinear (Wang et al., 2000), and this in turn activates protein kinase Ca (PKCa) (Leitges et al., 2004) and alpha-calcium/calmodulin-dependent-protein-kinase-II (αCaMKII) (Hansel et al., 2006). Ultimately, PKCa phosphorylates Ser-880 of the GluR2-subunit (Chung et al., 2003), which causes dissociation of GluR2-subunit-containing AMPA receptors from glutamate receptor interacting-protein' (GRIP) (Matsuda et al., 1999) and facilitates their interaction with protein-interacting with C kinase 1 (PICK1) (Xia et al., 2000), allowing receptor internalization via a clathrin-dependent process (Wang and Linden, 2000; Xia et al., 2000). In addition to this general pathway, several factors, such as GluR δ 2 receptors (Yamasaki et al., 2011; Yawata et al., 2006), nitric oxide (NO) and cyclic guanylate monophosphate (cGMP)-dependent protein kinase (PKG) (Lev-Ram et al., 1997; Safo and Regehr, 2005), endocannabinoids (Miyata et al., 1999), corticotropin-releasing factor (Hartmann et al., 2008; Sawada et al., 2008) and, possibly, NMDA-receptors (Piochon et al., 2010), may play a facilitating or permissive role in the induction of postsynaptic LTD (Fig 2). Studies aimed at elucidating the effect of postsynaptic LTD at the parallel fibre-Purkinje cell synapse on behaviour have received a lot of attention (Ito, 2001). Purkinje cell-specific and global (that is, brain-wide) manipulation of cytosolic enzymes like PKC, PKG, αCaMKII or CaMKIV induce impairments in both LTD induction in Purkinje cells and VOR adaptation (Boyden et al., 2006; De Zeeuw et al., 1998; Feil et al., 2003; Hansel et al., 2006). However, in more recent studies in which the expression of parallel fibre LTD was blocked by modifying AMPA receptors (mice with a mutant form of the GluR2 AMPA receptor subunit lacking the last seven amino acids (*GluR2D7* mice) and mice with a mutant form of GluR2 designed to prevent PKCa-mediated phosphorylation at S880 (*GluR2K882A* mice) or their endocytosis downstream of the molecular cytosolic pathway at the level of the membranes (mice lacking PICK1 (*PICK1*^{-/-} mice)) (Steinberg et al., 2006), mice did not show deficits in learning, at least not during low-frequency gain-increase, gain-decrease and phase-reversal learning (Schonewille et al., 2011). These results suggest that the behavioural phenotypes that have been obtained by manipulating the LTD pathway upstream result at least in part from deficits in cell physiological processes other than LTD.

1.3.2. Postsynaptic LTP

Postsynaptic LTP can be reliably induced by low-frequency parallel-fibre stimulation without climbing fibre stimulation (Coesmans et al., 2004; Lev-Ram et al., 2002). Induction of postsynaptic LTP requires a postsynaptic Ca^{2+} transient that is relatively small compared to that for LTD induction (Coesmans et al., 2004; Miyata et al., 2000). Following such a transient, calcium/calmodulin-activated protein phosphatase 2B (PP2B) activates protein phosphatase 1 (PP1) by releasing the block of PP1 by protein phosphatase inhibitor 1 (DARPP32), which itself is under control of PP2B and cAMP-activated PKA (FIG. 3). Indeed, selective inhibition of phosphatases PP1, PP2A or PP2B prevents postsynaptic LTP (Belmeguenai and Hansel, 2005). The trafficking of AMPA receptors to the synapse — the structural correlate of LTP expression — is controlled by Ca^{2+} -sensitive n-ethylmaleimide

sensitive factor (NSF) (Gardner et al., 2005; Steinberg et al., 2004). As climbing fibre activity can reverse the induction of postsynaptic LTP into LTD and at the same time alter postsynaptic Ca^{2+} -transients (Coemans et al., 2004), these transients may have an important role in determining the direction of plasticity at the parallel fibre–Purkinje cell synapse. Further evidence that Ca^{2+} -sensitive phosphatases and kinases act together to control postsynaptic plasticity is provided by analyses of mice with a global knockout of βCaMKII (van Woerden et al., 2009). In such mice (*Camk2b*^{-/-} mice) LTP and LTD stimulation protocols induce LTD and LTP, respectively, which can be normalized by inhibiting the pathways involved (*i.e.* kinases and phosphatases). LTP induction at the parallel fibre–Purkinje cell synapse may contribute to cerebellar motor learning. This is supported by the finding that mice lacking βCaMKII are ataxic and show deficits in the acquisition of new motor tasks (van Woerden et al., 2009). In addition, mutant mice in which LTP induction is blocked by deleting PP2B specifically in Purkinje cells (*L7-PP2B* mice) show pronounced deficits in motor coordination. These mice show abnormalities in motor performance during both VOR and optokinetic reflex (OKR), VOR gain decrease and gain-increase learning, and VOR phase reversal (Schonewille et al., 2010). Finally, natural changes in VOR learning capabilities during the oestrous cycle in female mice can be correlated with the level of LTP induction at the parallel fibre–Purkinje cell synapse (Andreescu et al., 2007).

1.3.3 Presynaptic LTP and LTD

At the presynaptic site, plasticity at the parallel fibre–Purkinje cell synapse is dominated by potentiation and the control thereof by endocannabinoids (Le Guen and De Zeeuw, 2010). Presynaptic LTP, which is independent of postsynaptic activity, can be elicited by a relatively short period of activity in parallel fibres (Salin et al., 1996). This induces a presynaptic calcium influx that activates a pathway involving Ca^{2+} /calmodulin-sensitive adenylyl cyclase, which in turn leads to a rise in cAMP and subsequent activation of cAMP-dependent PKA (Salin et al., 1996; Storm et al., 1998). PKA activation may further increase the number and size of presynaptic Ca^{2+} -transients, thereby probably further strengthening the potentiation (Qiu and Knöpfel, 2009). In addition, nitric oxide (NO) released from other synapses may contribute, through diffusion, to the induction of presynaptic LTP in non-activated parallel fibre terminals. This NO release might be initiated by activation of NMDARs at sites other than parallel fibres (Jacoby et al., 2001; Qiu and Knöpfel, 2009). It is possible that a short-lasting form of presynaptic potentiation, which can be induced by a periodic burst pattern of homosynaptic stimulation of parallel fibres, can facilitate the initiation of presynaptic LTP at the parallel fibre–Purkinje cell synapse (Goto et al., 2006). A recent study (Qiu and Knöpfel, 2009) reported a form of presynaptic LTD that is expressed at the parallel fibres. Strikingly, this type of plasticity — which is most efficiently induced using a parallel fibre stimulation protocol that is similar to that for presynaptic LTP — can only be revealed when presynaptic LTP is pharmacologically prevented by inhibiting PKA or NO. It requires activation of CB1 receptors in an NMDAR, but not mGluR1, dependent fashion. Thus, in principle, bidirectional mechanisms exist for both postsynaptic and presynaptic

plasticity at the parallel fibre–Purkinje cell synapse, but it remains to be shown whether presynaptic LTD has a behaviourally relevant function. The potential impact of presynaptic LTP at parallel fibre–Purkinje cell synapses during cerebellar learning may be indirectly assessed by evaluating granule cell-specific *A6-ΔCacna1a* mutant mice, in which synaptic transmission of the majority of parallel fibre–Purkinje cell synapses is impaired (Galliano et al., 2009). As indicated above, these mutants show specific deficits in VOR learning and consolidation (Galliano et al., 2009).

1.4. Scope of this thesis

This thesis is aimed at further clarifying the functional properties of the PF-PC synapse, how the interplay between molecular pathways regulates the direction of plasticity at this synapse and whether therapeutic intervention can facilitate memory formation. Together this will further define the role of the PF-PC synapse in cerebellar function and memory formation.

The MF-GrC synapse is capable of signalling reliably at extremely high frequencies up to 1kHz (Rancz et al., 2007). Recent observations have indicated that granule cells themselves generate action potentials at similarly high frequencies (Chadderton et al., 2004). Even though such burst can reliably elicit presynaptic calcium transients in PF terminals, initial release probability is thought to be relatively low around 0.05 (Dittman et al., 2000). Considering this apparent discrepancy, burst firing could have either one of two implications: 1) reliable signalling at the PF-PC synapse allows the cerebellum to compute with high temporal precision; 2) consecutive action potential within a burst can overcome a low initial release probability to ensure signalling in a noise-free environment at the cost of temporal precision. To differentiate between these two options and elucidate if the cerebellum is capable of processing information with high temporal precision, we test the ability of the PF-PC synapse to convey information at high frequency.

The stimulus protocols to induce presynaptic LTP and postsynaptic LTD share a low stimulus frequency (8Hz PF stimulation alone for 15 sec and 1Hz PF+CF for 5 min, respectively) (Coemans et al., 2004; Salin et al., 1996). Postsynaptic LTD demands activation of the CF, while PF stimulation is relatively similar in both protocols. This raises the possibility of counterproductive expression of presynaptic LTP during the induction of postsynaptic LTD. Endocannabinoids possess the potential to function as a suppressor of this undesirable presynaptic LTP when postsynaptic LTD is induced; 1) their release from PC is elicited by CF activity (van Beugen et al., 2006); 2) presynaptically, endocannabinoids suppress the formation of cAMP, preventing downstream activation of PKA (Salin et al., 1996; Storm et al., 1998). Because PKA is critical for the induction of LTP, through this pathway, CF activity could directly inhibit congruent induction of presynaptic LTP when postsynaptic LTD is expressed.

Following the inverted BCM-rule, *in vitro* experiments have shown that the direction of postsynaptic plasticity at the PF-PC synapse is directed by the balance between kinases and phosphatases (van Woerden et al., 2009). Whereas postsynaptic LTD has been proven to be essential for cerebellar function *in vivo* (Boyden et al., 2006; De Zeeuw et al., 1998; Feil et al.,

2003; Hansel et al., 2006), it is unknown if postsynaptic LTP has any functional relevance. By creating a cell specific knock-out mouse in which PP2B is selectively removed from PCs, one can test motor performance while both postsynaptic LTP and intrinsic plasticity are affected.

Ampakines are a recently developed group of memory enhancing drugs designed to augment glutamatergic synapses. Their effectiveness to improve memory test scores in Alzheimer patients has already been proven in clinical trials (Ingvar et al., 1997; Lynch et al., 1997). As allosteric modulators, they prevent AMPA receptors to go into the desensitized state, allowing them to either transfer into the open state or immediately become available for glutamate binding again. This enhances synaptic transmission by enlarging and prolonging the synaptic response, temporally potentiating glutamatergic transmission during the drugs presence. However, ampakines might also influence long-term plasticity, as larger and longer depolarization could affect voltage sensitive calcium influx, raising postsynaptic calcium transients. Because the PF-PC synapse adheres to an inverted BCM-rule (Coessmans et al., 2004), according to which low and high calcium levels will induce LTP and LTD, respectively, we test if ampakines can enhance calcium transients and promote LTD over LTP, potentially benefitting motor performance.

Together, these questions will elucidate how signalling and plasticity at the PF-PC synapse affect cerebellar function and memory formation. This will greatly benefit our understanding of how the cerebellum processes information and how this relates to its function as a controller of ongoing cerebral processes.

REFERENCES

1. Andreescu, C.E., Milojkovic, B.A., Haasdijk, E.D., Kramer, P., De Jong, F.H., Krust, A., De Zeeuw, C.I., and De Jeu, M.T. (2007). Estradiol improves cerebellar memory formation by activating estrogen receptor beta. *J Neurosci* 27, 10832-10839.
2. Bagnall, M.W., and du Lac, S. (2006). A new locus for synaptic plasticity in cerebellar circuits. *Neuron* 51, 5-7.
3. Bahn, S., Jones, A., and Wisden, W. (1997). Directing gene expression to cerebellar granule cells using gamma-aminobutyric acid type A receptor alpha6 subunit transgenes. *Proc Natl Acad Sci U S A* 94, 9417-9421.
4. Belmeguenai, A., and Hansel, C. (2005). A role for protein phosphatases 1, 2A, and 2B in cerebellar long-term potentiation. *J Neurosci* 25, 10768-10772.
5. Belmeguenai, A., Hosy, E., Bengtsson, F., Pedroarena, C.M., Piochon, C., Teuling, E., He, Q., Ohtsuki, G., De Jeu, M.T., Elgersma, Y., *et al.* (2010). Intrinsic plasticity complements long-term potentiation in parallel fiber input gain control in cerebellar Purkinje cells. *J Neurosci* 30, 13630-13643.
6. Bliss, T.V., and Lomo, T. (1973). Long-lasting potentiation of synaptic transmission in the dentate area of the anaesthetized rabbit following stimulation of the perforant path. *J Physiol* 232, 331-356.
7. Boyden, E.S., Katoh, A., Pyle, J.L., Chatila, T.A., Tsien, R.W., and Raymond, J.L. (2006). Selective engagement of plasticity mechanisms for motor memory storage. *Neuron* 51, 823-834.
8. Chadderton, P., Margrie, T.W., and Hausser, M. (2004). Integration of quanta in cerebellar granule cells during sensory processing. *Nature* 428, 856-860.
9. Chung, H.J., Steinberg, J.P., Hugarir, R.L., and Linden, D.J. (2003). Requirement of AMPA receptor GluR2 phosphorylation for cerebellar long-term depression. *Science* 300, 1751-1755.
10. Coesmans, M., Weber, J.T., De Zeeuw, C.I., and Hansel, C. (2004). Bidirectional parallel fiber plasticity in the cerebellum under climbing fiber control. *Neuron* 44, 691-700.
11. Collingridge, G.L., Peineau, S., Howland, J.G., and Wang, Y.T. (2010). Long-term depression in the CNS. *Nat Rev Neurosci* 11, 459-473.
12. De Zeeuw, C.I., Hansel, C., Bian, F., Koekkoek, S.K., van Alphen, A.M., Linden, D.J., and Oberdick, J. (1998). Expression of a protein kinase C inhibitor in Purkinje cells blocks cerebellar LTD and adaptation of the vestibulo-ocular reflex. *Neuron* 20, 495-508.
13. De Zeeuw, C.I., Hoebeek, F.E., Bosman, L.W., Schonewille, M., Witter, L., and Koekkoek, S.K. (2011). Spatiotemporal firing patterns in the cerebellum. *Nat Rev Neurosci*.
14. Dittman, J.S., Kreitzer, A.C., and Regehr, W.G. (2000). Interplay between facilitation, depression, and residual calcium at three presynaptic terminals. *J Neurosci* 20, 1374-1385.
15. Feil, R., Hartmann, J., Luo, C., Wolfsgruber, W., Schilling, K., Feil, S., Barski, J.J., Meyer, M., Konnerth, A., De Zeeuw, C.I., *et al.* (2003). Impairment of LTD and cerebellar learning by Purkinje cell-specific ablation of cGMP-dependent protein kinase I. *J Cell Biol* 163, 295-302.
16. Feldman, D.E. (2009). Synaptic mechanisms for plasticity in neocortex. *Annu Rev Neurosci* 32, 33-55.
17. Galliano, E., Hoebeek, F.E., Gao, Z., Schonewille, M., Todorov, B., Van Beugen, B.J., Pop, A., D'Angelo, E., Van den Maagdenberg, A.M., and De Zeeuw, C.I. (2009). Granule cell output mediates phase reversal learning and consolidation of gain learning by altering the regularity of Purkinje cell firing patterns. In *Society of Neuroscience (Chicago: 660.2 / CC19)*.
18. Gardner, S.M., Takamiya, K., Xia, J., Suh, J.G., Johnson, R., Yu, S., and Hugarir, R.L. (2005). Calcium-permeable AMPA receptor plasticity is mediated by subunit-specific interactions with PICK1 and NSF. *Neuron* 45, 903-915.
19. Geurts, F.J., De Schutter, E., and Dieudonne, S. (2003). Unraveling the cerebellar cortex: cytology and cellular physiology of large-sized interneurons in the granular layer. *Cerebellum* 2, 290-299.
20. Glickstein, M., Strata, P., and Voogd, J. (2009). Cerebellum: history. *Neuroscience* 162, 549-559.
21. Goto, J., Inoue, T., Kuruma, A., and Mikoshiba, K. (2006). Short-term potentiation at the parallel fiber-Purkinje cell synapse. *Neurosci Res* 55, 28-33.
22. Griffiths, M.R., Cooper, A.J., Barber, D.J., and Mitchell, I.J. (2000). Pharmacological mechanisms mediating phencyclidine-induced apoptosis of striatopallidal neurons:

- the roles of glutamate, dopamine, acetylcholine and corticosteroids. *Brain Res* 855, 1-10.
23. Hansel, C., de Jeu, M., Belmeguenaï, A., Houtman, S.H., Buitendijk, G.H., Andreev, D., De Zeeuw, C.I., and Elgersma, Y. (2006). α CaMKII Is essential for cerebellar LTD and motor learning. *Neuron* 51, 835-843.
 24. Hansel, C., Linden, D.J., and D'Angelo, E. (2001). Beyond parallel fiber LTD: the diversity of synaptic and non-synaptic plasticity in the cerebellum. *Nat Neurosci* 4, 467-475.
 25. Hartell, N.A. (1994). Induction of cerebellar long-term depression requires activation of glutamate metabotropic receptors. *Neuroreport* 5, 913-916.
 26. Hartmann, J., Dragicevic, E., Adelsberger, H., Henning, H.A., Sumser, M., Abramowitz, J., Blum, R., Dietrich, A., Freichel, M., Flockerzi, V., *et al.* (2008). TRPC3 channels are required for synaptic transmission and motor coordination. *Neuron* 59, 392-398.
 27. Hebb, D.O. (1949). *The organization of behavior* (New York: Wiley & Sons).
 28. Ingvar, M., Ambros-Ingerson, J., Davis, M., Granger, R., Kessler, M., Rogers, G.A., Schehr, R.S., and Lynch, G. (1997). Enhancement by an ampkine of memory encoding in humans. *Experimental neurology* 146, 553-559.
 29. Ito, M. (2001). Cerebellar long-term depression: characterization, signal transduction, and functional roles. *Physiol Rev* 81, 1143-1195.
 30. Ito, M., and Kano, M. (1982). Long-lasting depression of parallel fiber-Purkinje cell transmission induced by conjunctive stimulation of parallel fibers and climbing fibers in the cerebellar cortex. *Neurosci Lett* 33, 253-258.
 31. Jacoby, S., Sims, R.E., and Hartell, N.A. (2001). Nitric oxide is required for the induction and heterosynaptic spread of long-term potentiation in rat cerebellar slices. *J Physiol* 535, 825-839.
 32. Jorntell, H., Bengtsson, F., Schonewille, M., and De Zeeuw, C.I. (2010). Cerebellar molecular layer interneurons - computational properties and roles in learning. *Trends Neurosci* 33, 524-532.
 33. Kassardjian, C.D., Tan, Y.F., Chung, J.Y., Heskin, R., Peterson, M.J., and Broussard, D.M. (2005). The site of a motor memory shifts with consolidation. *J Neurosci* 25, 7979-7985.
 34. Kellett, D.O., Fukunaga, I., Chen-Kubota, E., Dean, P., and Yeo, C.H. (2010). Memory consolidation in the cerebellar cortex. *PLoS One* 5, e11737.
 35. Kessels, H.W., and Malinow, R. (2009). Synaptic AMPA receptor plasticity and behavior. *Neuron* 61, 340-350.
 36. Khodakhah, K., and Armstrong, C.M. (1997). Induction of long-term depression and rebound potentiation by inositol trisphosphate in cerebellar Purkinje neurons. *Proc Natl Acad Sci U S A* 94, 14009-14014.
 37. Le Guen, M.C., and De Zeeuw, C.I. (2010). Presynaptic plasticity at cerebellar parallel fiber terminals. *Funct Neurol* 25, 141-151.
 38. Leitges, M., Kovac, J., Plomann, M., and Linden, D.J. (2004). A unique PDZ ligand in PKC α confers induction of cerebellar long-term synaptic depression. *Neuron* 44, 585-594.
 39. Lev-Ram, V., Jiang, T., Wood, J., Lawrence, D.S., and Tsien, R.Y. (1997). Synergies and coincidence requirements between NO, cGMP, and Ca $^{2+}$ in the induction of cerebellar long-term depression. *Neuron* 18, 1025-1038.
 40. Lev-Ram, V., Wong, S.T., Storm, D.R., and Tsien, R.Y. (2002). A new form of cerebellar long-term potentiation is postsynaptic and depends on nitric oxide but not cAMP. *Proc Natl Acad Sci U S A* 99, 8389-8393.
 41. Linden, D.J., and Connor, J.A. (1991). Participation of postsynaptic PKC in cerebellar long-term depression in culture. *Science* 254, 1656-1659.
 42. Luscher, C., and Huber, K.M. (2010). Group 1 mGluR-dependent synaptic long-term depression: mechanisms and implications for circuitry and disease. *Neuron* 65, 445-459.
 43. Lynch, G., Granger, R., Ambros-Ingerson, J., Davis, C.M., Kessler, M., and Schehr, R. (1997). Evidence that a positive modulator of AMPA-type glutamate receptors improves delayed recall in aged humans. *Experimental neurology* 145, 89-92.
 44. Malenka, R.C., and Bear, M.F. (2004). LTP and LTD: an embarrassment of riches. *Neuron* 44, 5-21.
 45. Matsuda, S., Mikawa, S., and Hirai, H. (1999). Phosphorylation of serine-880 in GluR2 by protein kinase C prevents its C terminus from binding with glutamate receptor-interacting protein. *J Neurochem* 73, 1765-1768.
 46. Miyata, M., Finch, E.A., Khiroug, L., Hashimoto, K., Hayasaka, S., Oda, S.I., Inouye, M., Takagishi, Y., Augustine, G.J., and Kano, M. (2000). Local calcium release

- in dendritic spines required for long-term synaptic depression. *Neuron* 28, 233-244.
47. Miyata, M., Okada, D., Hashimoto, K., Kano, M., and Ito, M. (1999). Corticotropin-releasing factor plays a permissive role in cerebellar long-term depression. *Neuron* 22, 763-775.
 48. Nakanishi, S. (2009). Genetic manipulation study of information processing in the cerebellum. *Neuroscience* 162, 723-731.
 49. Neher, E., and Sakaba, T. (2008). Multiple roles of calcium ions in the regulation of neurotransmitter release. *Neuron* 59, 861-872.
 50. Neves, G., Cooke, S.F., and Bliss, T.V. (2008). Synaptic plasticity, memory and the hippocampus: a neural network approach to causality. *Nat Rev Neurosci* 9, 65-75.
 51. Oberdick, J., Smeyne, R.J., Mann, J.R., Zackson, S., and Morgan, J.I. (1990). A promoter that drives transgene expression in cerebellar Purkinje and retinal bipolar neurons. *Science* 248, 223-226.
 52. Palay, S.L., and Chan-Palay, V. (1974). *Cerebellar cortex: cytology and organization* (Berlin, Heidelberg, New York; Springer).
 53. Piochon, C., Levenes, C., Ohtsuki, G., and Hansel, C. (2010). Purkinje cell NMDA receptors assume a key role in synaptic gain control in the mature cerebellum. *J Neurosci* 30, 15330-15335.
 54. Pugh, J.R., and Raman, I.M. (2009). Nothing can be coincidence: synaptic inhibition and plasticity in the cerebellar nuclei. *Trends Neurosci* 32, 170-177.
 55. Qiu, D.L., and Knöpfel, T. (2009). Presynaptically expressed long-term depression at cerebellar parallel fiber synapses. *Pflugers Arch* 457, 865-875.
 56. Rancz, E.A., Ishikawa, T., Duguid, I., Chadderton, P., Mahon, S., and Hausser, M. (2007). High-fidelity transmission of sensory information by single cerebellar mossy fibre boutons. *Nature* 450, 1245-1248.
 57. Safo, P.K., and Regehr, W.G. (2005). Endocannabinoids control the induction of cerebellar LTD. *Neuron* 48, 647-659.
 58. Salin, P.A., Malenka, R.C., and Nicoll, R.A. (1996). Cyclic AMP mediates a presynaptic form of LTP at cerebellar parallel fiber synapses. *Neuron* 16, 797-803.
 59. Sawada, K., Fukui, Y., and Hawkes, R. (2008). Spatial distribution of corticotropin-releasing factor immunopositive climbing fibers in the mouse cerebellum: analysis by whole mount immunohistochemistry. *Brain Res* 1222, 106-117.
 60. Schonewille, M., Belmuguenai, A., Koekkoek, S.K., Houtman, S.H., Boele, H.J., van Beugen, B.J., Gao, Z., Badura, A., Ohtsuki, G., Amerika, W.E., *et al.* (2010). Purkinje cell-specific knockout of the protein phosphatase PP2B impairs potentiation and cerebellar motor learning. *Neuron* 67, 618-628.
 61. Schonewille, M., Gao, Z., Boele, H.J., Veloz, M.F., Amerika, W.E., Simek, A.A., De Jeu, M.T., Steinberg, J.P., Takamiya, K., Hoebeek, F.E., *et al.* (2011). Reevaluating the role of LTD in cerebellar motor learning. *Neuron* 70, 43-50.
 62. Seja, P., Schonewille, M., Spitzmaul, G., Badura, A., Klein, I., Rudhard, Y., Wisden, W., Hübner, C.A., De Zeeuw, C.I., and Jentsch, T.J. (2012). Raising cytosolic Cl⁻ in cerebellar granule cells affects their excitability and vestibulo-ocular learning. *EMBO* 17, 1217-1230.
 63. Shutoh, F., Ohki, M., Kitazawa, H., Itohara, S., and Nagao, S. (2006). Memory trace of motor learning shifts transsynaptically from cerebellar cortex to nuclei for consolidation. *Neuroscience* 139, 767-777.
 64. Simat, M., Ambrosetti, L., Lardi-Studler, B., and Fritschy, J.M. (2007). GABAergic synaptogenesis marks the onset of differentiation of basket and stellate cells in mouse cerebellum. *Eur J Neurosci* 26, 2239-2256.
 65. Steinberg, J.P., Huganir, R.L., and Linden, D.J. (2004). N-ethylmaleimide-sensitive factor is required for the synaptic incorporation and removal of AMPA receptors during cerebellar long-term depression. *Proc Natl Acad Sci U S A* 101, 18212-18216.
 66. Steinberg, J.P., Takamiya, K., Shen, Y., Xia, J., Rubio, M.E., Yu, S., Jin, W., Thomas, G.M., Linden, D.J., and Huganir, R.L. (2006). Targeted in vivo mutations of the AMPA receptor subunit GluR2 and its interacting protein PICK1 eliminate cerebellar long-term depression. *Neuron* 49, 845-860.
 67. Storm, D.R., Hansel, C., Hacker, B., Parent, A., and Linden, D.J. (1998). Impaired cerebellar long-term potentiation in type I adenylyl cyclase mutant mice. *Neuron* 20, 1199-1210.
 68. van Beugen, B.J., Nagaraja, R.Y., and Hansel, C. (2006). Climbing fiber-evoked endocannabinoid signaling heterosynaptically suppresses presynaptic cerebellar long-term potentiation. *J Neurosci* 26, 8289-8294.
 69. van Versendaal, D., Rajendran, R., Saiepour, M.H., Klooster, J., Smit-Rigter, L., Sommeijer, J.P., De Zeeuw, C.I., Hofer, S.B., Heimel, J.A., and

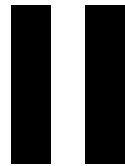
- Levelt, C.N. (2012). Elimination of inhibitory synapses is a major component of adult ocular dominance plasticity. *Neuron* 74, 374-383.
70. van Woerden, G.M., Hoebeek, F.E., Gao, Z., Nagaraja, R.Y., Hoogenraad, C.C., Kushner, S.A., Hansel, C., De Zeeuw, C.I., and Elgersma, Y. (2009). betaCaMKII controls the direction of plasticity at parallel fiber-Purkinje cell synapses. *Nat Neurosci* 12, 823-825.
71. Wang, S.S., Denk, W., and Häusser, M. (2000). Coincidence detection in single dendritic spines mediated by calcium release. *Nat Neurosci* 3, 1266-1273.
72. Wang, Y.T., and Linden, D.J. (2000). Expression of cerebellar long-term depression requires postsynaptic clathrin-mediated endocytosis. *Neuron* 25, 635-647.
73. Wulff, P., Schonewille, M., Renzi, M., Viltono, L., Sassoe-Pognetto, M., Badura, A., Gao, Z., Hoebeek, F.E., van Dorp, S., Wisden, W., *et al.* (2009). Synaptic inhibition of Purkinje cells mediates consolidation of vestibulo-cerebellar motor learning. *Nat Neurosci* 12, 1042-1049.
74. Xia, J., Chung, H.J., Wihler, C., Huganir, R.L., and Linden, D.J. (2000). Cerebellar long-term depression requires PKC-regulated interactions between GluR2/3 and PDZ domain-containing proteins. *Neuron* 28, 499-510.
75. Yamasaki, M., Miyazaki, T., Azechi, H., Abe, M., Natsume, R., Hagiwara, T., Aiba, A., Mishina, M., Sakimura, K., and Watanabe, M. (2011). Glutamate receptor delta2 is essential for input pathway-dependent regulation of synaptic AMPAR contents in cerebellar Purkinje cells. *J Neurosci* 31, 3362-3374.
76. Yawata, S., Tsuchida, H., Kengaku, M., and Hirano, T. (2006). Membrane-proximal region of glutamate receptor delta2 subunit is critical for long-term depression and interaction with protein interacting with C kinase 1 in a cerebellar Purkinje neuron. *J Neurosci* 26, 3626-3633.

**HIGH FREQUENCY
BURST FIRING ENSURES
VESICULAR RELEASE
AT THE PARALLEL FIBER TO
PURKINJE CELL SYNAPSE
AT THE COST
OF TEMPORAL CODING.**

Boeke J. van Beugen¹, Zhenyu Gao¹,
Laurens Witter², Freek Hoebeek¹
and Chris I. De Zeeuw^{1,2}

¹ Department of Neuroscience, Erasmus MC, 3000
DR Rotterdam, The Netherlands

² Netherlands Institute for Neuroscience, Royal
Dutch Academy of Arts & Sciences (KNAW), 1105
BA Amsterdam, The Netherlands



ABSTRACT

Cerebellar granule cells (GCs) convey information from mossy fibers (MFs) to Purkinje cells (PCs) via their parallel fibers (PFs). MF to GC signaling allows transmission of frequencies up to 1 kHz, and GCs themselves can also fire bursts of action potentials with instantaneous frequencies up to 1 kHz. This has been demonstrated in various mammals, but it remains to be shown whether high-frequency GC bursts also occur in mice, and if so, to what extent high-frequency information can also be conveyed onto their PCs. Here, we show that GCs in mice can also show high-frequency bursting, but that signaling at the murine PF-PC synapse is limited. The relative peak amplitude of EPSCs of PC responses increased with stimulus frequency following stimulation of a group of PFs up to a frequency of 300 Hz. Moreover, the slopes of the virtually linear correlations between relative charge in PCs and PF burst duration overlapped at stimulus frequencies > 300 Hz due to insufficient glutamate release. Recordings from individual GC-PC pairs revealed connections with a low or high release probability possibly reflecting depressed and potentiated synapses, respectively. Our data indicate that high-frequency bursting at PF-PC synapses facilitates release during the first few spikes ensuring signaling, but that vesicular release falls behind in response to enduring high-frequency activity patterns and that the responsiveness of individual connections differs substantially supporting the possibility that the cerebellar granular layer acts as a differential filter between MF input and PC output.

INTRODUCTION

Understanding synaptic efficacy is a critical step towards unraveling the computational properties of a neuronal network. In the cerebellum, the cortical network is fed by two distinct inputs including mossy fibers (MFs) and climbing fibers (CFs), both known to fire action potentials at high frequencies paired with a high probability of vesicular release (Saviane and Silver, 2006; De Zeeuw et al., 2011). Even though both projections share these characteristics, each has a very distinct way of transmitting information to their postsynaptic targets; whereas CF-terminals display rapid vesicular depletion when they elicit a complex spike composed of multiple spikelets in a Purkinje cell (PC) (Schmolesky et al., 2005), thus loosing synaptic power with consecutive action potentials, MF-terminals are remarkably well equipped to facilitate reliable signaling at a high frequency up to 1 kHz (Sargent et al., 2005; Saviane and Silver, 2006; Hallerman et al., 2010). Together, CFs and MFs represent both ends of the spectrum of high-frequency coding, namely reliability versus temporal precision, respectively.

Mossy fibers (MFs) convey their information to the Purkinje cells (PCs) via the granule cells (GCs), each of which provides a single ascending axon that bifurcates into a parallel fiber (PF). Like MF to GC signaling, GCs themselves can also fire bursts of action potentials (Chadderton et al., 2004; Hensbroek et al., 2005; Jörntell and Ekerot, 2006). At rest they are rather silent, but following sensory activation GCs display bursts of tens of action potentials with instantaneous frequencies up to 1kHz (Isope and Barbour, 2002; Chadderton et al., 2004). This burst-like mode of activation may have two potential functional implications: 1) when paired with a high synaptic release probability, it would allow granule cells to act as a relay, preserving frequency-coded information from MFs; and/or 2) when paired with a low synaptic release probability, it would allow granule cells to function as low-pass filters, reducing noise from spontaneous activity and signal only when strongly activated, albeit at the expense of temporal precision. The burst-like activity in GCs has been demonstrated in various mammals such as rats, rabbits and cats (Chadderton et al., 2004; Hensbroek et al., 2006; Jörntell and Ekerot, 2006). However, it remains to be shown whether high-frequency GC bursts can also be induced in mice, and if so, to what extent high-frequency information can also be conveyed onto their PCs. This question is not only relevant because of the advent of mouse transgenics, but also because different results have been found for different strains of rats in this respect. For example, release probability at the PF-PC synapse ranges from 0.05 to 0.9 among different rat strains and different experimental protocols (Dittman et al., 2000; Isope and Barbour, 2002; Valera et al., 2012). We therefore set out experiments in mice to investigate the occurrence of bursting activity of GCs at rest using patch clamp recordings *in vivo*, to study the impact of bursting activity in groups of PFs on the EPSCs of PCs using whole cell recordings *in vitro* and to examine the unitary impact of a burst within a single PF on a PC using paired GC – PC recordings.

MATERIAL & METHODS

In vivo recordings in rabbits. Experiments were performed as described in Ruigrok, Hensbroek and Simpson (2011). In short, extracellular recordings of cerebellar granule cells located in the flocculus were acquired from awake, behaving Dutch-belted rabbit (3-6months of age) using fine-tipped glass microelectrodes (~ 1 μ m diameter). Given the predominant silent behavior of granule cells at rest, cells were located while the animal was stimulated by rotation around the vertical axis. While characteristic spiking behavior was often suggestive of the cells subtype, further identification was confirmed by comparison of spontaneous spiking behavior to the algorithm as described (Ruigrok et al., 2011) Recordings were filtered below 100Hz and above 3 kHz and sampled at 20kHz (CED power 1401, Cambridge Electronic Design, United Kingdom).

In vivo recordings in mice. Adult (4-10 weeks) C57Bl/6 mice were prepared for in-vivo patch clamp recordings by placing a pedestal on the skull under general anesthesia with isoflurane/O₂. On the day of the experiment, animals were anesthetized with an initial intraperitoneal injection of ketamine/xylazine (75 and 12 mg/kg, respectively). Throughout the experiment, anesthesia was sustained by supplemental dosages when needed. Animals were kept at 37°C body-temperature via a feedback-controlled heating pad. For experiments in the awake, a dam of dental cement was built around the occipital bone under anesthesia, while the bone and dura were left intact. Prior to the experiment, mice were anaesthetized with isoflurane/O₂, then quickly fixated in the setup via the pedestal and a tubular body restrainer. Access to the cerebellar cortex was obtain via an occipital craniotomy. Once the dura mater was removed, animals were allowed to wake up. Electrodes were pulled from borosilicate glass (1.5 OD x 0.86 ID, 1-2 μ m tips, 8-12 M Ω). filled with internal solution (in mM: 10 KOH, 3.48 MgCl₂, 4 NaCl, 129 K-Gluconate, 10 hepes, 17.5 glucose 4 Na₂ATP, and 0.4 Na₃GTP) and inserted under positive pressure into the cerebellar cortex. After the electrode was positioned in the target area, pressure was lowered and cells were patched in voltage-clamp. Granule cells were identified by their high input resistance (>350m Ω) and low capacitance (<10pF). Signals were amplified using a Multiclamp 700B amplifier (Axon Instruments) and digitized for storage with a Digidata 1440 (Axon Instruments). Junction potential between the electrode and the extracellular milieu was determined to be 8.53 \pm 0.87 mV.

In vitro patch clamp recordings from PCs following grouped PF stimulation. Sagittal slices (200-250 μ m thickness) of the cerebellar vermis of adult male C57Bl/6 wild-type mice (8-30 weeks) were prepared in ice-cold aCSF and stored at room temperature in carbogen-bubbled (95% O₂ and 5% CO₂) aCSF containing (in mM): 124 NaCl, 5 KCl, 1.25 Na₂HPO₄, 2 MgSO₄, 2 CaCl₂, 26 NaHCO₃, and 10 d-glucose. Whole-cell patch clamp recordings were acquired 1-6 hrs after slice preparation from Purkinje cells using a HEKA EPC-10 amplifier (HEKA Electronics, Germany) at near physiological temperature (34 \pm 1°C). Recording electrodes (2.5-4.0 M Ω) were filled with a solution containing (in mM): 9 KCl, 10 KOH, 3.48 MgCl₂, 4 NaCl, 120 K-gluconate, 10 HEPES, 4 Na₂ATP, 0.4 Na₃GTP and 28.5 sucrose (pH-adjusted to 7.25 \pm 0.05). For experiments conducted in current clamp, the membrane-impermeable

voltage gated sodium channel blocker QX314 was added to prevent generation of action potentials. Throughout recordings, slices were perfused with carbogen bubbled aCSF to which picrotoxin (100 μ M) was supplemented in order to isolate excitatory inputs. All drugs were acquired from Sigma-Aldrich, except γ DGG (Tocris). Recorded currents were filtered (low-pass Bessel, 3 kHz) and sampled at 20 kHz through Pulse-software (HEKA Electronics, Germany). PFs were activated by current injection (100 μ s, 0.5-2.0 mA) (ISO-flex current generator, A.M.P.I., Israel) using a bipolar glass microelectrode positioned in the molecular layer. Input and series resistance were monitored in each experiment and cells were rejected if a change of > 10 % occurred. In general, the stimulus protocol consisted of a sequence of high-frequency bursts of (1), 2, 3, 4, 5, 10, 15 and 20 pulses. This sequence was tested with burst-frequencies varying between 100, 300, 500 and 700 Hz (with a 10, 3.33, 2, and 1.47 ms interstimulus interval, respectively) and repeated 3 times. Consecutive bursts were given at 0.05 Hz to minimize residual effects. For some experiments responses were also tested with bursts at 200 Hz (5 ms stimulus interval). To minimize the possibility of recruiting additional PFs with consecutive pulses in a burst and to promote reproducibility between recordings we applied several strategies: 1) a low-resistance bipolar stimulus electrode was used to reduce stimulus width and minimize current build-up within a burst keeping the stimulus region restricted; 2) the stimulus electrode was positioned close to the pial surface of the molecular layer where PF density is lowest; and 3) stimulus strength was adjusted to elicit a response of \sim 100 pA to a single stimulus.

In vitro double patch clamp recordings from GC-PC pairs. A double patch clamp configuration was favored over the 'loose-cell-attached'-configuration to exclude the possibility of exciting more than a single granule cell. Transverse slices and electrodes were prepared under similar conditions as mentioned above. Granule cell patch pipettes had a resistance of 8-10 M Ω and contained the same internal solution as mentioned above. After the double patch clamp configuration was established, spike trains were elicited by somatic current injections for 50 ms in the granule cell. The amplitude was adjusted such that spiking occurred at \sim 200 Hz. During the experiment connectivity was confirmed by eye when an EPSC was detected in the Purkinje cell after averaging a minimum of 10 trains.

Analyses

In vivo recordings. Mice data were analyzed using Clampfit (Axon Instruments) and custom written routines in MATLAB (Mathworks). Extracellular recordings from the rabbit were acquired using Spike 2 (Cambridge Electronic Design). Spikes were separated upon waveform templates and values were exported to Excel (Microsoft) for further analysis.

PF group stimulation and in vitro recordings. Measurements of peak amplitude and charge were averaged over three recordings to minimize variance and then normalized to the response elicited by 2 pulses at 300 Hz to allow comparison between cells. For those experiments in which individual EPSC amplitudes were measured, the derivative of the stimulus artifact was used to define intervals. Amplitudes were calculated as the difference between the local minimum and the current directly preceding the artifact. When stimuli

took place within the rise phase of the preceding EPSC (which was especially prominent at the higher frequencies) and the response to the first pulse in the burst was more than 10% smaller than the response measured for a single stimulus, the recordings were excluded from analysis. The plateau level during prolonged activation was defined as the average of all values measured directly preceding all stimulus artifacts within a 50 ms time window.

Double patch granule cell - Purkinje cell recordings. After connectivity was confirmed, high-frequency noise was eliminated offline from individual recordings using a running average (1 ms width). The recording was further processed by averaging the measured current over 800 μ s creating virtual bins. Whenever the derivative of these values was negative over 2 or more consecutive bins, events were considered for analysis and both amplitude and derivative of the rise-phase were measured. Baseline values of these parameters were determined over a 50 ms period preceding the current injection. Detected events were considered evoked responses when both amplitude and derivative exceeded 1 x SD over baseline levels and the detected amplitude rose 2 x SD above background noise levels. This method proved very effective to detect wider EPSCs while simultaneously rejecting high-frequency background noise. As an indicator of sensitivity, detected EPSC amplitudes were 5.2 ± 0.2 x SD larger than baseline events. Detection thresholds were -5.76 ± 0.32 pA and -5.9 ± 1.4 pA for 'Low Release Probability (RP)' and 'High RP' pairs, respectively (see text); these values did not differ significantly ($p > 0.05$). Significance was tested using (un-)paired Students' t-test or ANOVA where applicable. All values are expressed as average \pm SEM unless otherwise noted.

RESULTS

Bursting activity in vivo

For long, it was believed that cerebellar granule cells operate at low firing frequencies (but see Eccles, 1969). However, most of these assumptions were based on indirect calculations, for acquiring direct recordings had proven difficult as a result of the small somatic size of granule cells (Roth and Häusser, 2001; Chadderton et al., 2004). It is only since the last decade that more observations have been made that indicate that granule cells can fire bursts of action potentials at surprisingly high frequencies of several hundred hertz with instantaneous frequencies up to 1kHz (Chadderton et al., 2004; Hensbroek et al., 2005; Jörntell and Ekerot, 2006). To underline the intensity of GrC burst firing, we've included examples of burst recorded in vivo both in rabbits and mice (fig 1). The cell taken from the rabbit did not show any activity when the animal was at rest, whereas vestibular stimulation via sigmoidal rotation around the vertical axis caused it to fire bursts of action potentials both during movement in the contralateral direction and while the animal was stationary in the contralateral position. Bursts were defined as a group of >2 spikes separated by less than 50ms between spikes (i.e. >20 Hz). A total of 31 burst were fired over 6 cycles. Bursts had an average firing frequency of 529.8 ± 45.7 Hz, contained 11.6 ± 6.6 spikes and were 23.66 ± 15.86 ms in length (all values AVG \pm SD). Surprisingly, for this particular cell, timing of burst onset was variable (1.49 ± 0.80 ms from start of movement (AVG \pm SD), $n=31$) and multiple

bursts could occur within a single movement. Due to this inconsistent behavior, bursting did not directly relate to either velocity, acceleration, position of the table or position of the eye, but rather seemed to signal movement in the ipsilateral direction indistinctively.

To confirm that GrC are capable of displaying similar characteristics in mice, we've evoked spiking by current injection in vivo. Fig. 1D shows an example of sustained, regular activity under anesthesia. This particular burst contained 21 spikes at an average frequency of $219.6 \pm 21.2\text{Hz}$ (AVG \pm SD). Although less regular, the example from the awake displays

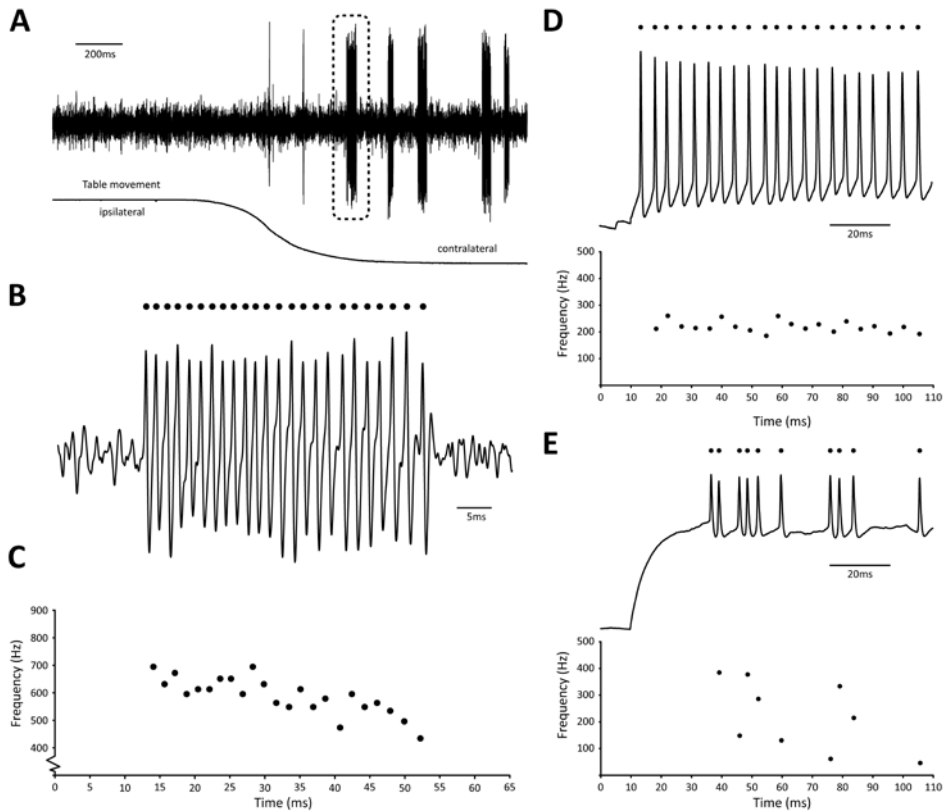


Figure 1. Examples of burst firing in a cerebellar granule cell. **A**, (top) Extracellular recording of granule cell in the flocculus of a Dutch-belted rabbit during vestibular stimulation around the vertical axis. Note absence of activity prior to movement onset, whereas several distinct, high frequency bursts occur during rotation (table position is displayed at bottom). **B**, Burst demarked in **A** shown at larger scale. Identified spikes are indicated by dots. **C**, Instantaneous frequency plot of burst shown in **B**. This particular burst consisted of 24 consecutive spikes with instantaneous frequencies as high as 694Hz and had an average firing frequency of 589Hz. **D**, Burst elicited in anesthetized mouse by current injection (50pA) shows regular firing pattern at high frequency ($219.6 \pm 21.2\text{Hz}$, AVG \pm SD). **E**, Burst elicited in awake mouse by current injection (25pA) shows irregular firing pattern at high frequency ($220.2 \pm 131.2\text{Hz}$, AVG \pm SD) with instantaneous frequencies up to 384.6Hz.

a similar average frequency of 220.2 ± 131.2 Hz (AVG \pm SD) with instantaneous frequencies up to 384.6 Hz (fig. 1E).

While these results confirm that GrC are capable of firing action potentials in high-frequency bursts as reported previously in other species, it should be noted that these bursts are elicited by mild somatic current injection and do not represent actual physiological responses.

Impact of bursting activity in groups of PFs in vitro

We performed whole cell somatic patch-clamp recordings from PCs to measure EPSCs evoked by extracellular stimulation of groups of PFs. Bursts of 2, 3, 4, 5, 10, 15 and 20 pulses were given at frequencies of 100, 200, 300, 500 and 700 Hz (Fig. 2; data obtained at 200 Hz and 700 Hz are only shown in part of the panels). The peak amplitude of the EPSCs showed a significant increase with each additional stimulus ($p < 0.05$ for all frequencies) until a maximum level was reached at 10 pulses (Fig. 2A); additional pulses did not contribute to a significant increase in peak amplitudes ($p > 0.05$ for all frequencies). When comparing bursts of equal numbers of stimuli over different frequencies (Fig. 2B), a significant increase in the relative peak amplitude of the EPSCs (i.e. relative to the 2 pulses at 300 Hz condition, which was set at 100%) was seen for each condition between 100 Hz and 300 Hz ($p < 0.05$ for all numbers of stimulus pulses). Surprisingly, no further enhancing effect on EPSC amplitudes could be observed for stimulus frequencies higher than 300 Hz ($p > 0.05$ for all numbers of stimulus pulses). In fact, the EPSCs following bursts of 2, 3 and 4 stimuli at 700 Hz were significantly smaller compared to those at 300 Hz and 500 Hz ($p < 0.05$ for all comparisons) possibly reflecting insufficient, presynaptic calcium entry, which may occur at higher frequencies (Brenowitz and Regehr, 2007).

The impact of temporal summation at higher frequencies on the peak amplitude of EPSCs was also evident when we studied the relevance of the moment of onset of the second stimulus in relation to the phase of the EPSC evoked by the first stimulus of a burst. For example, the second stimulus always occurred late in the decay phase of an EPSC at a burst of 100 Hz, whereas at 500 Hz the second stimulus usually occurred around the peak of the response (Fig. 2A). Thus, especially at higher frequencies, stimuli could take place within the rise phase of the preceding EPSC. As a result, many of the recordings at the higher frequencies had to be rejected from the analyses of the amplitude, because this effect would have directly biased the measurements (see Analysis section in Methods). Of all the recordings that were included in the analysis none of the first EPSCs showed a significant attenuation ($p > 0.05$ for all frequencies) (Fig. 2A and C).

Remarkably, while the amplitudes of the EPSCs of all frequencies initially showed facilitation for the first stimuli, these amplitudes could only be maintained at 100 Hz (Fig. 2C, top graph); at higher frequencies a rapid decline was observed. With an increasing number of pulses (up to 20), the currents eventually reached a stable amplitude, but these levels reduced progressively with increases in frequency and at 700 Hz virtually no current could be detected. The levels at the different frequencies were all significantly different from each other ($p < 0.05$ at 20 pulses for all comparisons). When these values were expressed

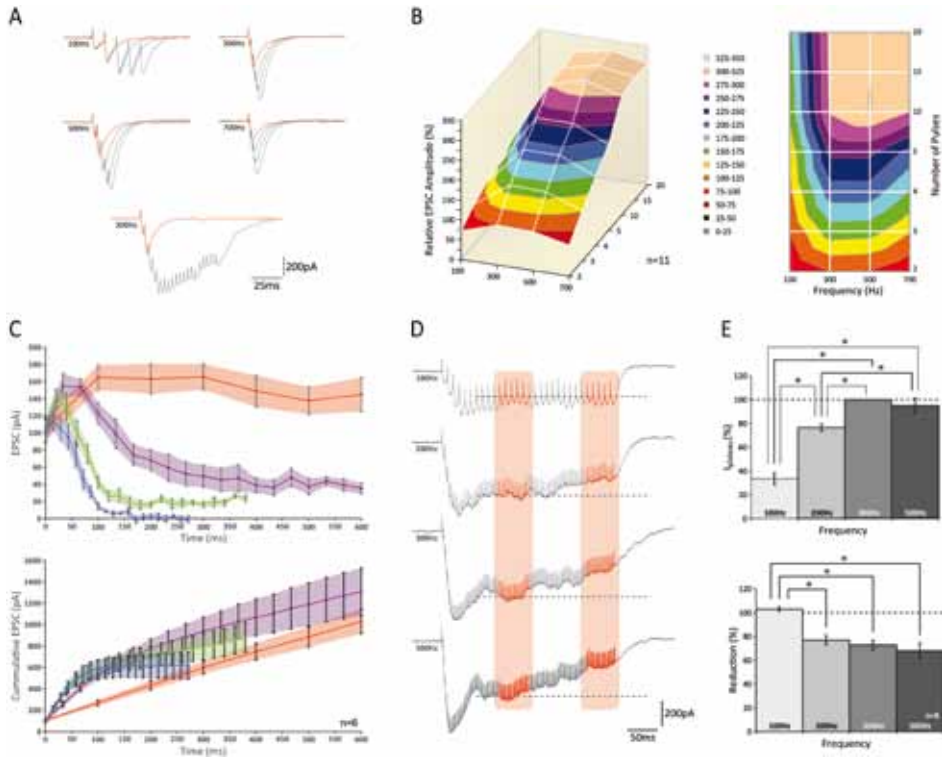


Figure 2. PCs can increase the peak amplitude of their EPSCs following high frequency stimulation of groups of PFs up to 300 Hz. **A**, (top) Traces of PC EPSCs following stimulus bursts of 2, 3, 4, or 5 stimuli at 100, 300, 500 or 700 Hz. Response to 2 stimuli is shown in red for reference. Note the effect of temporal summation on peak amplitude at higher frequencies. (bottom) Recordings of 2 and 20 stimuli at 300 Hz. Note how in the last half of the long burst no robust responses can be distinguished. **B**, 3D representation (left) and top-down view (right) relative peak amplitudes of EPSCs with respect to different stimulus conditions. No increase in EPSC amplitude was observed for bursts of more than 10 stimuli at any of the stimulus frequencies ($p > 0.05$). For bursts with equal number of stimuli, no significant increases were observed for frequencies higher than 300 Hz (for all comparisons, $p > 0.05$). In fact, bursts of 2, 3 and 4 stimuli at 700 Hz were all significantly smaller than those at 300 and 500 Hz ($p < 0.05$). **C**, Relative EPSC increases per stimulus (top) and cumulative EPSC (bottom) over time. **D**, Example traces of EPSCs following prolonged stimulation for 300 ms at 100, 200, 300 and 500 Hz. A plateau establishes after ~100ms for all frequencies. Average current levels were measured early (left orange column) and late (right orange column) during the plateau over a 50 ms time period. Levels measured during first period are indicated by dashed lines for reference. **E**, (top) Bar graph of early plateau current levels; no significant increase was observed between 300 and 500 Hz ($p < 0.05$). (bottom) Relative reduction of plateau current levels (i.e. difference between late and early levels); only at 100 Hz no reduction was observed ($p > 0.05$).

as cumulative responses over burst duration (Fig. 2C, bottom graph), the slope measured over the first 10 ms significantly increased with increasing frequency up to 300 Hz ($p < 0.05$ between frequencies of 100, 200 and 300 Hz), while no rise was seen above 300 Hz ($p > 0.05$).

Prolonged stimulation for 300 ms at 100, 200, 300 and 500 Hz produced a plateau in the amplitude of the EPSCs at all stimulus frequencies after approximately 100 ms (Fig. 2D). All responses initially showed a rise phase, followed by a decay phase until the plateau was reached. The level of the plateau, which was measured as the average of current recorded prior to each stimulus over a 50 ms period (indicated by left red column in Fig. 2D), was lowest for 100 Hz and significantly increased with stimulations at 200 Hz and 300 Hz ($p < 0.05$; Fig. 2E, top graph). No further significant increase was observed between 300 Hz and 500 Hz ($p > 0.05$). As stimulation continued, the level of the plateau was maintained up to the end of the burst at 100 Hz, but not at the higher frequencies where levels showed a significant reduction at the end of the burst suggestive of presynaptic depletion (Fig. 2E). It should be noted though that frequency-dependent limitation of release and depletion probably occur at frequencies lower than reported here, because the effects following stimulation described above apply to PF-activity *as a bundle*; inactivity of a particular fiber can be compensated for by activity from others and therefore, unless all fibers are continuously active, equilibrium can be established at a higher level than would be possible for fibers independently.

To compensate for temporal summation in the rise phase of the response and to capture ongoing activity in the decay phase during prolonged stimulation we calculated the total charge elicited by a burst (i.e. 'area-under-the curve' of EPSCs) as an indicator of ongoing activity during a particular period. Correlating the total charge to burst duration revealed a remarkable near-perfect linear fit for all frequencies (R^2 -values 0.990 ± 0.002 ; Fig. 3A). We saw a significant increase in the slope of the correlation at 300 Hz compared to that at 100 Hz and 200 Hz (in both cases $p < 0.05$) indicating increased ability for a bundle of PFs to maintain activity. However, in accordance with our observations described above, we found no further rise for the slopes at frequencies higher than 300 Hz ($p < 0.05$ for all frequencies). This finding indicates that, within a given time period, stimuli given at a frequency higher than 300 Hz are ineffective in eliciting any additional activity. These 'false' stimuli occur at a rate faster than a bundle of PFs can compensate for. Considering the compensatory mechanism of alternate activity that occurs within a group of fibers, the maximum frequency for individual fibers is likely lower. These results are a first indicator that burst firing at frequencies higher than 300 Hz cannot relay temporally coded information from MFs to PCs. To exclude the possibility that these findings resulted from our whole-cell patch clamp recording conditions, we repeated the experiment in current-clamp mode so as not to restrict PC behavior. No differences were found (fig 3B, $p < 0.05$ for 100 against 300/500/700, $p > 0.05$ between 300,500 and 700). To confirm a transitional trajectory before the observed limit is reached, we also included 200Hz (fig 3C). The slope measured for 200Hz was indeed larger than 100Hz ($p < 0.05$), yet smaller than 300 and 500Hz ($p < 0.05$).

To detect any involvement of postsynaptic receptor desensitization on signaling, we compared the charge with and without application of CX546, which acts as an allosteric

modulator and prevents AMPARs to reside in the desensitized state. With CX546 present (200 μ M) the data did not fall along a linear fit as perfect as without (R^2 -values 0.974 ± 0.004), due to a small facilitation in responses to stimulus bursts smaller than 20 ms in duration (Fig. 3D). However, over the first 20 ms the slope with CX546 still displayed a rather linear relation (R^2 -values 0.989 ± 0.002) and differed only significantly from that without CX546 at 100 Hz ($p < 0.05$). No differences were found for the remaining frequencies ($p > 0.05$). While these results suggest some role of AMPAR desensitization in PF-PC signaling, it cannot explain the restrictions in signaling found for stimulus frequencies over 300 Hz.

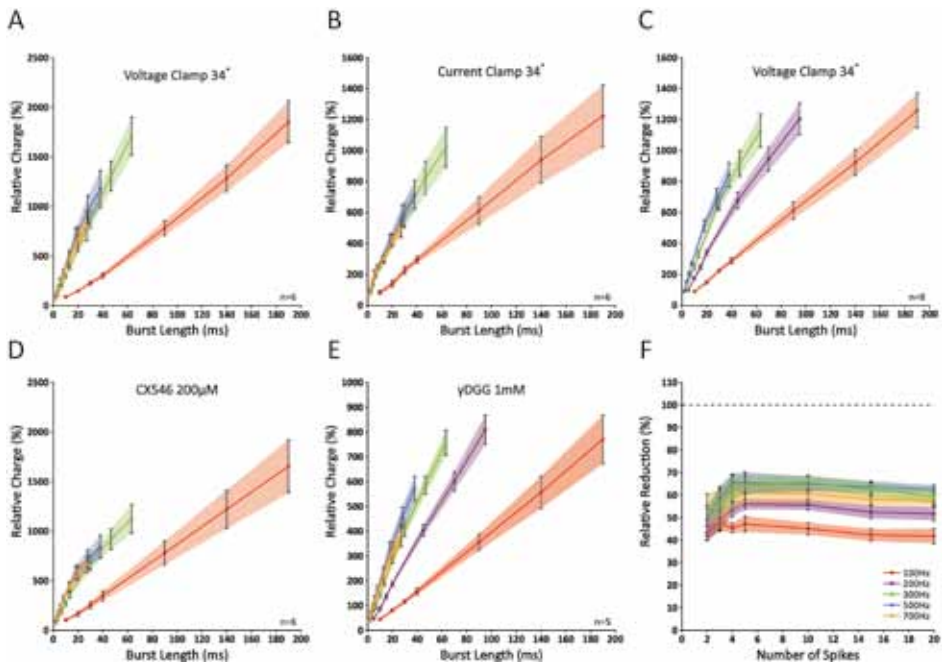


Figure 3. Slopes of near-perfect linear correlations between charge and burst length reveal limited signaling for frequencies higher than 300 Hz as a result of insufficient glutamate release. **A**, Correlations between relative charge and burst length at 100, 300, 500 and 700 Hz; no differences were seen in the slopes between 300, 500 and 700 Hz ($p > 0.05$). The slopes represent the ability for a bundle of PFs to maintain activity at the given frequency. Note that the slope measured for 200 Hz differed significantly from that at 100, 300 and 500 Hz ($p < 0.05$). **B**, Similar experiment as shown in A repeated in current clamp. Recording conditions had no effect on the outcome. **C**, When CX546 was applied, correlations were less linear as a result of small facilitations for bursts smaller than 20 ms. However, bursts that were shorter than 20 ms in duration still displayed a linear relationship and the slopes at 300, 500 and 700 Hz still did not differ significantly from each other ($p > 0.05$). **D**, Application of yDGG (1 mM) did not affect the observed limitation of signaling at frequencies higher than 300 Hz. **E**, yDGG (1 mM) effectively suppressed all responses by more than 35%. Relative suppression was significantly smaller after 5 stimuli at 200, 300 and 500 Hz, although no further decrease was observed for longer stimulus trains. This indicates that additional release might occur with the first few stimuli, but quickly reaches its optimum.

Next, to exclude any major involvement of postsynaptic receptor saturation we investigated the impact of application of γ DGG, which is a competitive antagonist of AMPAR by occupying a portion of the available AMPARs, effectively suppressing EPSCs. Because of its competitive behavior and fast unbinding rate, γ DGG is a perfect reporter of glutamate transients. In the case of postsynaptic receptor saturation, excessive glutamate will compete with γ DGG to overcome its suppressive effect and EPSCs will be unaffected by its presence. At 1mM, γ DGG effectively suppressed all responses to <65% of their original size. However, no effect was observed on the linear behavior of responses (R^2 -values 0.993 ± 0.001). In addition, similar to the data described above, slopes were significantly different at 100 and 200 Hz compared to those at other frequencies ($p < 0.05$), yet those at 300, 500 and 700 Hz were indistinguishable from each other (Fig. 3E). Interestingly, the relative reduction was strongest for short bursts, but showed a gradual decrease towards bursts of 5 pulses at 200, 300 and 500 Hz ($p < 0.05$ for responses of 2 versus 5 pulses at all three frequencies) (Fig. 3F), indicative of additional glutamate release with consecutive pulses. However, no further decrease was observed for longer bursts ($p < 0.05$ for responses of 5 versus 20 pulses), meaning that release had reached its optimum within 5 pulses. Together, these results indicate that signaling at high frequency between PF-PC is restricted to the presynaptic site by insufficient release. While some additional release might occur within the first few pulses of a burst, prolonged activation cannot be maintained.

Impact of bursting activity on release probability from paired recordings of GCs and PCs in vitro

The results described above showed the implications of grouped activity from synchronously activated granule cells, but they failed to accurately describe the behavior of individual connections. We therefore performed paired whole-cell patch clamp recordings from 13 connected GC - PC pairs. Because this configuration turned out to be relatively short-lived, we couldn't test responses for the same wide range of stimuli as with extracellular stimulation. We chose to elicit bursts of action potentials at 200 Hz, because at this frequency, on the one hand, we had found some limitations such as depletion with prolonged activity, while on the other hand we had observed room for additional signaling at higher frequencies (up to 300 Hz; see above).

Recordings from individual GC-PC pairs confirmed a low initial release probability, yet strong differences were observed between these pairs (Fig. 4A-D). Whereas some connections could only be revealed by averaging multiple recordings, others showed clearly recognizable events in individual traces. Overall, we found an initial failure rate (FR) of 0.83 ± 0.01 (Fig. 4D). With consecutive action potentials this FR was significantly reduced to a minimum of 0.66 ± 0.02 at the third action potential ($p < 0.05$). However, from the third action potential on, FR began to show a gradual increase again to return to baseline level at the sixth action potential ($p > 0.05$ 1st versus 6th action potential, $p < 0.05$ 3rd versus 6th action potential). On the basis of cumulative release probability over the first 3 action potentials ($RP_{\text{cumulative } 1-3} = 1 - (FR_1 * FR_2 * FR_3)$), pairs could be separated in a 'Low RP'-group

($RP_{\text{cumulative 1-3}} < 0.55$, average $RP_{\text{cumulative 1-3}} = 0.41 \pm 0.05$, $n=8$) and a 'High RP'-group ($RP_{\text{cumulative 1-3}} > 0.8$, average $RP_{\text{cumulative 1-3}} = 0.86 \pm 0.02$, $n=4$) (Fig. 4A). Even though the initial FR was similar between the 2 groups ($p > 0.05$), a dramatic difference was observed for the FR of the 2nd and 3rd spike ($p > 0.05$, 0.86 ± 0.01 and 0.78 ± 0.01 for Low RP; 0.48 ± 0.03 and 0.43 ± 0.05 for High RP, respectively) (Fig. 4D). No difference in FR was observed after the 3rd spike ($p > 0.05$). The cumulative release probability ($RP_{\text{cumulative 1-n}} = 1 - (FR_1 * FR_2 * FR_{n...})$), unveiled a striking difference between the 2 groups (Fig. 4E); whereas the chance of release for at least one of the action potentials reached $> 90\%$ for the 'High RP'-group at the fourth AP, this chance only reached the level of $\sim 50\%$ for the 'Low RP'-group and only had reached a level of $\sim 75\%$ at the 7th AP.

The EPSC amplitude of the response to the first action potential was $-8.54 \text{ pA} \pm 0.22$ for the 'Low RP'-group (Fig. 4C). No further change in amplitude occurred throughout the burst. Amplitudes in the 'High RP'-group were significantly larger for the 2nd, 3rd and 6th action potential ($p < 0.05$). It should be noted, however, that it is likely that amplitudes of the 4th and 5th were larger as well, although significance could not be reached as a result of a relatively low number of events. Causal to this amplitude difference can be many factors, such as proximal vs distal connections, ascending versus branching segments of the PF or potentiated versus depressed synapses. However, the combined observation that larger EPSC amplitudes coincided with a higher RP raises the intriguing possibility of multi-vesicular release in the 'High RP'-group. Multi-vesicular release is promoted by LTP (Bender et al., 2009) and therefore, the observed heterogeneity could result from a difference between potentiated and depressed synapses. Thus, in short, from the paired recordings we conclude that bursting may facilitate release within the first few spikes in both the Low RP and High RP groups, and result in a high cumulative release probability especially in the responsive 'High RP' group to ensure signaling and overcome a low initial release probability.

DISCUSSION

For a long time, it was believed that cerebellar GCs operate at low firing frequencies (but see Eccles, 1969). However, most of these assumptions were based on indirect calculations, for acquiring direct recordings had proven difficult as a result of their small somatic size (Roth and Häusser, 2001; Chadderton et al., 2004). It is only due to recent technical advances that GCs have been shown to fire bursts of action potentials at surprisingly high frequencies of several hundred Hz with instantaneous frequencies up to 1 kHz (Chadderton et al., 2004; Hensbroek et al., 2006; Jörntell and Ekerot, 2006; Valera et al., 2012) and that individual action potentials in high-frequency bursts of GCs are reliably translated into consistent calcium transients at presynaptic PF varicosities, showing only minor attenuation for intervals starting at approximately 500 Hz (Brenowitz and Regehr, 2007). Here, we demonstrate mice can also show bursts of GC activity at high frequency, but that the capability of their PFs to relay information to the PCs is limited to ~ 300 Hz. In line with previous studies in rat (Brenowitz and Regehr, 2007; for review see Le Guen and De Zeeuw,

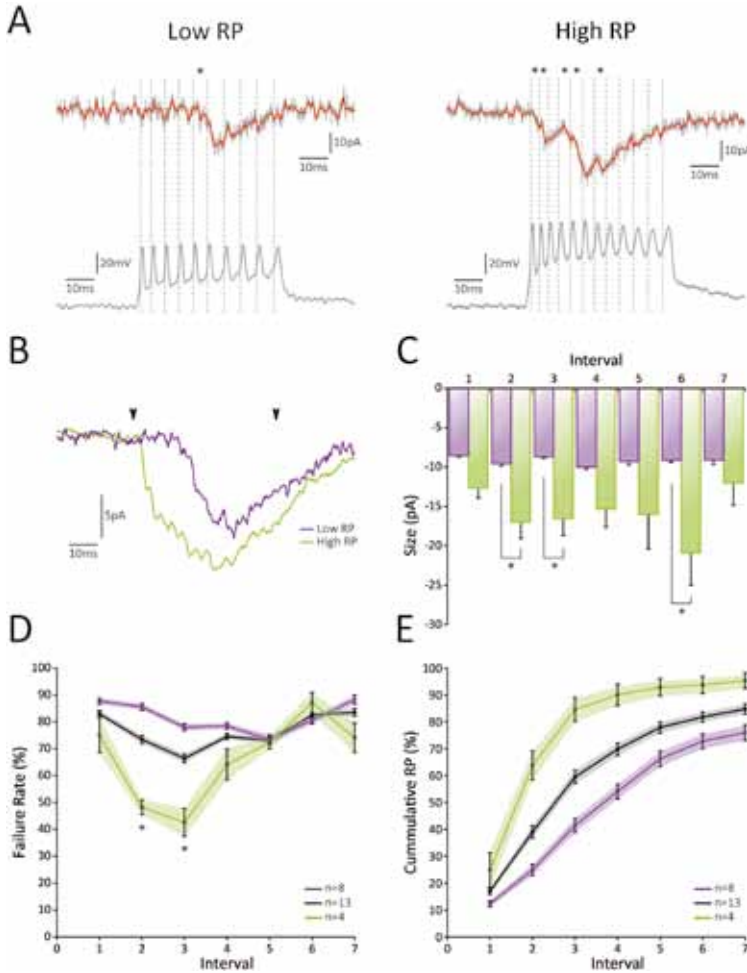


Figure 4. Paired GC-PC recordings reveal heterogeneity in PF release probability. **A**, Examples of paired recordings. Based on the cumulative release probability over the first 3 spikes, pairs could be subdivided into a 'Low RP' group (left) and 'High RP' group (right). (top traces) Original voltage clamp recordings from PCs (gray) and their processed signals used for analysis (red); asterisks indicate detected events. (bottom traces) Current clamp recordings from GCs. Spiking is induced via current injection. Dashed lines indicate detected spikes. **B**, Averaged responses over all recordings from cells shown in **A**. Beginning and end of current injections are indicated by arrowheads. Note a faster overall response in the 'High RP' cell (green). **C**, EPSC amplitudes did not change in size during the burst for 'Low RP' connections (purple, $p > 0.05$ for all comparisons). However, for the 'High RP' group (green) EPSCs elicited by the 2nd, 3rd and 6th spike were significantly larger than that by the 1st spike. No significant difference was observed for responses to the first spike between the 'Low RP' and 'High RP' groups. **D**, Failure rate for all recorded pairs (gray), 'Low RP' group (purple) and 'High RP' group (green). The 'High RP' group showed a short-lift facilitation for the 2nd and 3rd spike, resulting in a significantly smaller failure rate compared to that of the 'Low RP' group ($p < 0.05$). **E**, Cumulative probability of release for all recorded pairs (gray), 'Low RP' group (purple) and 'High RP' group (green).

2010), murine PF inputs constitute a heterogenic group of terminals with various levels of release probability allowing differential filtering. Our data suggest that high-frequency PF activity may facilitate transmitter release during initial spiking ensuring signaling onto PCs, but that variability is too high to allow temporally coded signaling.

Limitations of vesicular release at the murine PF-PC synapse. Our main finding demonstrates that vesicular release from PF terminals onto PC dendrites is limited during physiologically relevant high-frequency bursts. Although the current observations in awake behaving mice and those of others in anesthetized rats and rabbits indicate that cerebellar GCs can fire bursts of action potentials with instantaneous frequencies up to ~ 1 kHz (Chadderton et al., 2004; Ruigrok et al., 2011), our in vitro results following stimulation of bundles of PFs show that signaling at the murine PF-PC synapse is confined to ~ 300 Hz at best. This maximal limit is probably even an overestimation, because the stimulus conditions under which these results were obtained allow for different PFs to be active at different time points within a burst. In this manner, a group of PFs can maintain a highly effective activity pattern, while the effective activity of each individual terminal is in fact substantially lower (see also below). Indeed, our double patch clamp recordings of connected GC-PC pairs in mice confirmed a relatively low RP for most of the individual PF terminals. These recordings showed a low average initial RP of ~ 0.17 , which is in line with previous observations in rat by Dittman and colleagues (2000), but not by those of Valera and colleagues (2012), who reported a RP of 0.44 at a calcium concentration of 1.5 mM. The differences with the latter study may be partially due to the specific strains of rodents used, differences in extracellular calcium concentration in the bath, and/or the approach used to calculate the RP. Valera and colleagues (2012) calculated RP with the Multi-Probability-Fluctuation-Analysis (MPFA), a method that relies on a presumed distribution of Pr_{site} (i.e. the probability for a single vesicle to be released at a particular site) to calculate RP from the quantal distribution. However, this approach does not take into account heterogeneity between synapses that arise from differential factors such as presynaptic calcium transients (Mitchell and Silver, 2003) and/or build-up of residual calcium (Brenowitz and Regehr, 2007). Moreover, whereas Valera and colleagues (2012) used a noise-based signal-to-noise ratio to discriminate events in paired recordings, we applied a noise-based multi-variable threshold detection method; both methods have the potential to misrepresent RP either by missing small events or detecting noise, resulting in an underestimation or overestimation, respectively.

PF terminals in mice are heterogenic. We noticed a clear heterogeneous distribution between release properties of individual connected pairs of GCs and PCs. Given that larger EPSC amplitudes coincided with a higher RP, this difference might reflect diversity between potentiated and depressed synapses (Bender et al., 2009). However, we cannot exclude the possibility that this heterogeneity partly also results from differences between terminals from the ascending versus the horizontal segment of parallel fibers (Sims and Hartell, 2005; Sims and Hartell, 2006). In addition, the heterogeneity may result from the fact that there is great diversity in presynaptic calcium transients in PF terminals, which can account for a ten-fold range in levels of RP (Brenowitz and Regehr, 2007). This enormous range

may result from the fact that the probability of vesicular release for a given PF terminal is dynamic and depends on preceding activity as well as terminal specific parameters such as initial release probability, calcium buffering capacity, number of release sites and the size of the readily releasable pool. Moreover, the differences in synaptic responses will also depend on vesicular depletion, rate of vesicular replenishment, transmitter re-uptake and receptor saturation/desensitization (Neher and Sakaba, 2008). Despite a heterogeneous distribution, we found a low initial release probability for all PF-PC synapses; whereas the PF to Golgi cell synapse is considered to be weak (Dieudonne et al., 1998; Robberechts et al., 2010), the PF to molecular layer interneuron synapse has been shown to be more reliable (Crowley et al., 2007; Satake et al., 2012). These observations are remarkable, because all types of PF connections mentioned above probably persist along a single PF Palay and Chan-Palay, 1974; Napper and Harvey, 1988). It will be interesting to find out to what extent the heterogeneity in RP will have impact on the ability of PFs to signal at high frequencies, not only at their input to PCs but also to Golgi cells and molecular layer interneurons. Moreover, it will be interesting to find out how the plasticity rules that control efficacy at the PF-PC synapse compare to those controlling the PF-interneuron synapses (Gao et al., 2012).

Technical limitations and caveats. We took three different approaches in the current study to investigate GC-PC interactions; these included whole cell patch recordings of GCs in vivo, recordings of intracellular PC responses in vitro following extracellular stimulation of bundles of PFs, and intracellular recordings of individual GC-PC pairs in vitro. Each of these three approaches presented particular technical limitations and caveats. First, the whole-cell patch clamp approach in mice *in vivo* was necessary to verify the identity of GCs, but this configuration disrupts natural behavior. Second, recording EPSCs from PCs following PF activity is notoriously complicated by several factors (Roth and Häusser, 2001): the large dimension of a PC prevents the desired control over electrical properties in patch-clamp experiments; extensive dendritic arborization filters postsynaptic currents; the small size and condense packing of PFs make isolated activation difficult; and spontaneously active inputs obscure individually evoked events. These complications probably had impact on the measurements following PF bundle stimulations as well as those during the paired recordings. When stimulating a bundle of PFs, the elicited response will be the multiplication of dynamic stochastic variables and, given a relatively low release probability, will only reflect activity from a subset of all the stimulated PFs. Considering the heterogenic behavior, where some fibers might show activity to a substantial portion of the stimuli in a burst, and others might respond only periodically, the composed response will not reflect activity from a constant number of terminals. Because the total number of stimulated fibers is unknown, it is unclear what proportion is unresponsive. When, for example, a burst of ten stimuli is given, the response to the 4th and 5th stimulus can be made up by a completely different subset of parallel fibers. As a result, heterogeneity greatly limits the possibilities for group analysis and, in fact, limits applicability of methods proven effective at other release sites (Saviane and Silver, 2007; Valera et al., 2012). Yet, an equilibrium between driving and suppressing forces will establish as sustained activity and heterogenic differences will at least partly be averaged

out. Thus, the measurements following extracellular bundle stimulation may to some degree be subject to misrepresentation, but the established plateau current can probably serve as an indirect indicator of overall synaptic efficacy (Saviane and Silver, 2006; Valera et al., 2012). Finally, finding connected pairs of GCs and PCs was difficult indeed and holding on to both cells for long periods of time proved even more challenging. These technical difficulties forced us to restrict ourselves to investigate only the most physiologically relevant stimulus parameters and limited the power of our statistical analyses.

Functional implications. The notion that frequency coding is partially lost in individual GC firing patterns has interesting implications for the cerebellar network as a whole and challenges the idea that GCs merely act as interposed relay-neurons. What is the purpose for a GC to fire a high-frequency burst when actual vesicular release partly falls behind? The main benefit of a relatively low release probability is that few spontaneous events occur, creating a relatively noise-free background of activity. However, this comes at the expense of reliability and consistency; such a system is not well designed to employ rate coding over its entire frequency range in a linear fashion. Nevertheless, as depicted in Figure 4, the cumulative probability of release at the murine PF-PC synapse reached nearly 1 within a few spikes for the 'High RP'-group. This means that a brief PF burst could overcome the initial low release probability to ensure release within the time window of the burst. Moreover, as the presynaptic insufficiency caused a rapid fall in release probability, restricted release probably prevented immediate saturation of the postsynaptic site and thereby left room for temporal summation at a lower rate. Ultimately, these characteristics point towards a non-linear mode of synaptic transmission, in which the actual occurrence of a synaptic event bears significance as well as its timing within a burst.

GC activity is tightly controlled by tonic inhibition from Golgi cells, resulting in few action potentials at rest (Mapelli and D'Angelo, 2007; Hensbroek et al., 2006); GCs can be relieved from this inhibition when Golgi cell activity is diminished or when excitatory MF input exceeds the inhibiting force. Moreover, glutamate released by MFs can directly act on Golgi cell terminals and suppress GABA release, forming an activity-dependent feed-forward loop (Gao et al., 2012). When the balance is shifted from inhibition to excitation, a time window is created in which a GC can fire a burst of action potentials (D'Angelo and De Zeeuw, 2009). As such, the granular layer can be regarded as a 'gate-keeper' that can selectively allow information to pass from MFs to PCs. Because MF terminals are well tailored to maintain reliable signaling at very high frequencies (Sargent et al., 2005; Hallermann et al., 2010), it is remarkable that rate coding is to some extent lost down the line. This implies that the information encoded by high-frequency firing of MFs may have limited value for PCs, but rather shapes the time window in which GCs can produce a burst of activity. Thus, combining strong inhibition together with a relatively low release probability may result in a system in which synaptic events are restricted and a high signal-to-noise ratio is effectuated.

Our finding that bundles of PFs can display a near-linear, frequency-sensitive relationship between burst duration and total synaptic charge bears some physiological

relevance, because there is strong evidence that PFs are active in bundles (Ebner et al., 2005). Moreover, GCs are also prone to fire together in groups, because of the impact of Golgi cell inhibition, which can produce a center-surround pattern of activity in the granular layer further enhancing the filter function of the granular layer (Mapelli and D'Angelo, 2007). This leads to the interesting possibility that, while output from individual PFs can be relatively insignificant and poorly timed, a group of selectively activated PFs can reliably convey and maintain frequency coded MF activity while further reducing background noise.

In conclusion, our findings indicate that the firing mode of granule cells in high-frequency bursts of action potentials overcome the unreliability and inconsistency of PF terminals to ensure signaling at the partial cost of rate coding. Together with strong Golgi cell inhibition and center-surround group activation this creates an environment in which the granular layer forms a strong spatio-temporal filter, and, while a single GC action potential can become insignificant, controlled bursting can reliably convey selective information from MF input to PC output.

ACKNOWLEDGEMENTS:

We kindly thank the Dutch Organization for Medical Sciences (ZonMw; CIDZ), Life Sciences (ALW; CIDZ, ZG, BvB), Senter (NeuroBasic; CIDZ), and the ERC-advanced, CEREBNET and C7 programs of the European Community (CIDZ) for their financial support. The extracellular data recorded in the rabbit were acquired with the help of R. Hensbroek and J.I. Simpson and are included with their consent. We thank C. Hansel for helpful discussions and critically reviewing the paper. The authors declare no competing financial interest.

REFERENCES

1. Barmack NH, Yakhnitsa V (2008) Functions of interneurons in mouse cerebellum. *J Neurosci* 28 (5), 1140.
2. Bender VA, Pugh JR, Jahr CE (2009) Presynaptically expressed long-term potentiation increases multivesicular release at parallel fiber synapses. *J Neurosci*. Sep 2;29(35):10974-8.
3. Brenowitz SD, Regehr WG (2007) Reliability and heterogeneity of calcium signaling at single presynaptic boutons of cerebellar granule cells. *J Neurosci*. Jul 25;27(30):7888-98.
4. Brickley SG, Cull-Candy SG, Farrant M (1996) Development of a tonic form of synaptic inhibition in rat cerebellar granule cells resulting from persistent activation of GABAA receptors. *J Physiol*. Dec 15;497 (Pt 3):753-9.
5. Chadderton P, Margrie TW, Häusser M (2004) Integration of quanta in cerebellar granule cells during sensory processing. *Nature* 428, 856-860.
6. Crowley JJ, Carter AG, Regehr WG (2007) Fast vesicle replenishment and rapid recovery from desensitization at a single synaptic release site. *J Neurosci*. May 16;27(20):5448-60.
7. D'Angelo E, De Zeeuw CI (2009) Timing and plasticity in the cerebellum: focus on the granular layer. *Trends Neurosci*. Jan;32(1):30-40.
8. Dieudonne S (1998) Submillisecond kinetics and low efficacy of parallel fibre-Golgi cell synaptic currents in the rat cerebellum. *J Physiol*. Aug 1;510 (Pt 3):845-66.
9. Dittman JS, Kreitzer AC, Regehr WG (2000) Interplay between facilitation, depression, and residual calcium at three presynaptic terminals. *J Neurosci*. Feb 15;20(4):1374-85.
10. Ebner TJ, Chen G, Gao W, Reinert K (2005) Optical imaging of cerebellar functional architectures: parallel fiber beams, parasagittal bands and spreading acidification. *Prog Brain Res*. 148:125-38.
11. Eccles JC (1969) The development of the cerebellum of vertebrates in relation to the control of movement. *Naturwissenschaften* 56 (11), 525.
12. Hallermann S, Fejtova A, Schmidt H, Weyhersmüller A, Silver RA, Gundelfinger ED, Eilers J (2010) Bassoon speeds vesicle reloading at a central excitatory synapse. *Neuron*. Nov 18;68(4):710-23.
13. Hensbroek RA, Ruigrok TJH, van Beugen BJ, Simpson JI (2005) Burst modulation of cerebellar granule cells during vestibular stimulation. *Soc Neurosci Abstr* 297.4
14. Hensbroek RA, van Beugen BJ, Ruigrok TJH, Simpson JI (2006) Spike modulation of unipolar brush cells and granule cells in the awake rabbit. *Soc Neurosci Abstr* 740.2
15. Isope P, Barbour B (2002) Properties of unitary granule cell->Purkinje cell synapses in adult rat cerebellar slices. *J Neurosci* 22 (22), 9668.
16. Jakab RL, Hámori J (1988) Quantitative morphology and synaptology of cerebellar glomeruli in the rat. *Anat Embryol (Berl)*. 179(1):81-8.
17. Jörntell H, Ekerot CF (2006) Properties of somatosensory synaptic integration in cerebellar granule cells in vivo. *J Neurosci*. Nov 8;26(45):11786-97.
18. Mapelli J, D'Angelo E (2007) The spatial organization of long-term synaptic plasticity at the input stage of cerebellum. *J Neurosci*. Feb 7;27(6):1285-96.
19. Marr D (1969) A theory of cerebellar cortex. *J Physiol* 202 (2), 437.
20. Napper RM, Harvey RJ (1988) Number of Parallel Fiber Synapses on an Individual Purkinje cell in the Cerebellum of the Rat. *J Comp Neurol*. Aug 8;274(2):168-77.
21. Neher E and Sakaba T (2008) Multiple Roles of Calcium Ions in the Regulation of Neurotransmitter Release. *Neuron* Sep 25;59(6):861-72.
22. Palay SL, Chan-Palay V (1974) *Cerebellar Cortex: Cytology and Organization*. (Springer).
23. Rancz EA, Ishikawa T, Duguid I, Chadderton P, Mahon S, Häusser M (2007) High-fidelity transmission of sensory information by single cerebellar mossy fibre boutons. *Nature*. Dec 20;450(7173):1245-8.
24. Robberechts Q, Wijnants M, Guigliano M, De Schutter E (2010) Long-term depression at parallel fiber to Golgi cell synapses. *J Neurophysiol*. Dec; 104(6):3413-23.
25. Rossi DJ, Hamann M (1998) Spillover-mediated transmission at inhibitory synapses promoted by high affinity alpha6 subunit GABA(A) receptors and glomerular geometry. *Neuron*. Apr;20(4):783-95.
26. Roth A, Häusser M (2001) Compartmental models of rat cerebellar Purkinje cells based on simultaneous somatic and dendritic patch-clamp recordings. *J Physiol*. Sep 1;535(Pt 2):445-72.

27. Sargent PB, Saviane C, Nielsen TA, DiGregorio DA, Silver RA (2005) Rapid vesicular release, quantal variability, and spillover contribute to the precision and reliability of transmission at a glomerular synapse. *J Neurosci.* Sep 7;25(36):8173-87.
28. Satake S, Inoue T, Imoto K. (2012) Paired-pulse facilitation of multivesicular release and intersynaptic spillover of glutamate at rat cerebellar granule cell-interneurone synapses. *J. Physiol.* 2012 Aug 28.
29. Saviane C, Silver RA (2006) Fast vesicle reloading and a large pool sustain high bandwidth transmission at a central synapse. *Nature.* Feb 23;439(7079):983.
30. Saviane C, Silver RA (2007) Estimation of Quantal Parameters with Multiple-Probability Fluctuation Analysis. *Methods Mol Biol.* 403:303-17.
31. Valera AM, Doussau F, Poulain B, Barbour B, Isope P (2012) Adaptation of granule cell to Purkinje cell synapses to high-frequency transmission. *J Neurosci.* Feb 29;32(9):3267-80.

**CLIMBING FIBER-EVOKED
ENDOCANNABINOID
SIGNALING
HETEROSYNAPTICALLY
SUPPRESSES PRESYNAPTIC
CEREBELLAR LONG-TERM
POTENTIATION**

Boeke J. van Beugen*,
Raghavendra Y. Nagaraja*,
and Christian Hansel

Department of Neuroscience, Erasmus University
Medical Center, 3000 DR Rotterdam, The
Netherlands

* These authors contributed equally



ABSTRACT

Endocannabinoid signaling has been demonstrated to mediate depolarization-induced suppression of excitation at climbing fiber (CF) and parallel fiber (PF) synapses onto cerebellar Purkinje cells. Here, we show that CF-evoked release of cannabinoids (CBs) additionally suppresses a presynaptic form of long-term potentiation (LTP) at PF synapses. PF-LTP can be induced by 8 Hz PF tetanization but is blocked when the PF tetanization is paired with 4 or 1 Hz CF coactivation. CF activity can be substituted for by bath application of the CB receptor agonist WIN55,212-2 [*R*(+)-[2,3-dihydro-5-methyl-3-[(morpholinyl)methyl]pyrrolo[1,2,3-de]-1,4-benzoxazinyl]-(1-naphthalenyl) methanone]. In the presence of the CB1 receptor antagonist AM251 [*N*-1-(2,4-dichlorophenyl)-5-(4-iodophenyl)-4-methyl-*N*-1-piperidinyl-1*H*-pyrazole-3-carboxamide], CF activity no longer suppresses PF-LTP. Presynaptic potentiation can also be obtained by the adenylyl cyclase activator forskolin. WIN55,212-2 blocked this forskolin-mediated enhancement, showing that CB1 receptor activation interferes with the adenylyl cyclase–protein kinase A cascade, which participates in LTP induction. CF activity has been described to promote the induction of postsynaptic PF-long-term depression (LTD) and to impair postsynaptic PF-LTP. Our observation that CF activity blocks the induction of presynaptic LTP suggests that the CF input controls all forms of presynaptic and postsynaptic PF plasticity and that CF activity provides a “safety lock” to prevent an enhancement of transmitter release while postsynaptic AMPA receptor function is downregulated during LTD.

INTRODUCTION

Long-term depression (LTD) at cerebellar parallel fiber (PF)–Purkinje cell (PC) synapses is considered a cellular correlate of cerebellar motor learning (Hansel et al., 2001; Ito, 2001). Whereas PF-LTD induction requires the simultaneous activity of the PF and the climbing fiber (CF) inputs onto PCs at low frequencies (e.g., 1 Hz for 5 min), PF stimulation alone leads to the induction of long-term potentiation (LTP) (Lev-Ram et al., 2002; Coesmans et al., 2004). The CF acts as a heterosynaptic control switch for postsynaptic PF plasticity: CF-evoked complex spikes evoke large dendritic calcium transients that trigger LTD induction, whereas LTP results from smaller calcium transients in the absence of complex spikes (Coemans et al., 2004). PF stimulation alone can also elicit a presynaptically expressed form of PF-LTP when applied for short durations at high frequencies (e.g., 8 Hz for 15 s) (Salin et al., 1996). Induction of presynaptic PF-LTP depends on the activation of calcium/calmodulin-sensitive adenylyl cyclase I and the subsequent activation of cAMP-dependent kinase [protein kinase A (PKA)] (Salin et al., 1996; Chen and Regehr, 1997; Linden, 1997; Storm et al., 1998; Jacoby et al., 2001).

In postsynaptic PF plasticity, CF activity determines whether LTD or LTP is induced (Lev-Ram et al., 2002; Coesmans et al., 2004). So far, it has not been examined whether CF activity can suppress presynaptic LTP. We reasoned that such a “safety lock” might exist to prevent the induction of presynaptic LTP while LTD is expressed postsynaptically, because the postsynaptic downregulation of response amplitudes might otherwise be accompanied by an increase in transmitter release. Retrograde endocannabinoid signaling might provide a possible link between CF activity and the suppression of presynaptic PF-LTP. At cerebellar and hippocampal synapses, dendritically released endocannabinoids can bind to presynaptically located CB1 receptors (Diana et al., 2002) and cause depolarization-induced suppression of inhibition (Llano et al., 1991; Pitler and Alger, 1992; Wilson et al., 2001), or its equivalent at excitatory synapses, depolarization-induced suppression of excitation (DSE) (Kreitzer and Regehr, 2001). The release of endocannabinoids involved in DSE at PF–PC synapses can be activated by CF activity (Brenowitz and Regehr, 2005), suggesting that complex spike-associated calcium transients in PC dendrites are sufficient to initiate the release process.

There have been contradictory reports on the effects of retrograde endocannabinoid signaling on synaptic plasticity in the cerebellum. It has been demonstrated that cannabinoids impair PF-LTD induction (Levenes et al., 1998), but also that cannabinoid signaling is required for PF-LTD induction (Safó and Regehr, 2005). The suppressive effect was explained by a reduction in transmitter release during tetanization, and the permissive effect was explained by a CB1 receptor-mediated release of nitric oxide (NO) from PF terminals. Here, we demonstrate that endocannabinoid signaling can suppress presynaptic PF-LTP. We show that this retrograde signaling mechanism is recruited by CF activity to suppress presynaptic PF-LTP and that this effect can be attributed to the CB1 receptor-mediated blockade of adenylyl cyclase. This CB1 receptor-mediated suppression of

presynaptic LTP provides an alternative explanation for the permissive effect of retrograde endocannabinoid signaling in PF-LTD induction.

MATERIALS AND METHODS

Slice preparation

Sagittal slices of the cerebellar vermis (200–250 μm thick) were prepared from postnatal day 18–25 Sprague Dawley rats in ice-cold artificial CSF (ACSF). The slices were kept in ACSF containing the following (in mM): 124 NaCl, 5 KCl, 1.25 Na_2HPO_4 , 2 MgSO_4 , 2 CaCl_2 , 26 NaHCO_3 , and 10 d-glucose bubbled with 95% O_2 and 5% CO_2 . The ACSF used for perfusion was supplemented with 20 μM bicuculline methiodide to block GABA_A receptors. Whole-cell patch-clamp recordings were performed at room temperature using an EPC-9 amplifier (HEKA Elektronik, Lambrecht/Pfalz, Germany). Recording electrodes were filled with a solution containing the following (in mM): 9 KCl, 10 KOH, 108 K-gluconate, 3.48 MgCl_2 , 10 HEPES, 4 NaCl, 4 Na_2ATP , 0.4 Na_3GTP , 5 BAPTA (K_4^+ salt), and 17.5 sucrose, pH 7.25. When the BAPTA concentration was raised to 30 mM (see Fig. 1B,D), 15 mM CaCl_2 was added to maintain the resting calcium concentration. The K-gluconate concentration was lowered to maintain the desired osmolarity and ionic strength. All drugs were purchased from Sigma (St. Louis, MO), except for BAPTA (Invitrogen, Eugene, OR), AM251 [*N*-1-(2,4-dichlorophenyl)-5-(4-iodophenyl)-4-methyl-*N*-1-piperidinyl-1*H*-pyrazole-3-carboxamide; Tocris, Bristol, UK], and PKC [19-36] (Calbiochem, La Jolla, CA). AM251, WIN55,212-2 [*R*(+)-[2,3-dihydro-5-methyl-3-[(morpholinyl)methyl]pyrrolo[1,2,3-de]-1,4-benzoxazinyl]-(1-naphthalenyl) methanone], and forskolin were dissolved in DMSO and kept as stock solution at -20°C .

Electrophysiology

Currents were filtered at 3 kHz, digitized at 8 kHz, and acquired using PULSE software (HEKA Elektronik). During voltage-clamp experiments, PCs were held at potentials in the range of -60 to -70 mV. For extracellular stimulation, standard patch pipettes were filled with external saline. The CF input was activated in the granule cell layer, and the PF input was activated in the molecular layer. Test responses (typically ~ 200 pA) were evoked at a frequency of 0.05 Hz using 0.5–2 μA pulses. To evoke EPSCs, paired pulses (100 ms interpulse interval) were applied to the PF input. In all experiments, cells were switched to current-clamp mode during tetanization. The protocol for inducing presynaptic LTP consisted of 120 pulses at 8 Hz to the PFs. In experiments in which the CF was coactivated, the presence of a CF response was confirmed in the beginning of the recording, but CF stimulation was subsequently only resumed for tetanization. Recordings were excluded from the study if the series or the input resistance varied by $>15\%$ over the course of the experiments. All values are shown as percentage of baseline \pm SEM. For statistical analysis, we used the paired Student's *t* test and the Mann–Whitney U test where appropriate.

RESULTS

To characterize the effect of CF-evoked cannabinoid signaling on presynaptic PF-LTP, we performed whole-cell patch-clamp recordings from PCs in rat cerebellar slices. During the test periods before and after tetanization, EPSCs were monitored in voltage-clamp mode. For tetanization, recordings were switched to current-clamp mode. LTP was observed after 8 Hz PF tetanization for 15 s. This manipulation resulted in a potentiation of EPSC amplitudes ($120.2 \pm 6.3\%$ of baseline; $n = 12$; last 5 min) (Fig. 1A) that reached statistical significance ($p < 0.01$; paired Student's *t* test). The LTP protocol used has been described to induce a presynaptically expressed form of PF-LTP (Salin et al., 1996). The presynaptic origin of the potentiation was confirmed by activating PF–EPSC pairs at an interpulse interval of 100 ms and monitoring the paired-pulse facilitation (PPF) ratio. The LTP observed after tetanization was associated with a modest reduction in the PPF ratio ($94.3 \pm 2.9\%$ of baseline; $n = 12$; last 5 min) (Fig. 1C), which reached statistical significance ($p < 0.01$; paired Student's *t* test), indicating a significant presynaptic component of the potentiation. In subsequent experimental groups (see below), we restricted measurements of the PPF ratio to test for the efficacies of drugs known to act presynaptically. The reason is that the PPF ratio is a simple, but rather unreliable, indicator of the expression site of synaptic gain changes. To obtain independent proof of the presynaptic origin of this form of LTP, we applied the 8 Hz PF tetanization protocol when the calcium chelator BAPTA (30 μM) was added to the internal saline. At this concentration, BAPTA blocks the induction of postsynaptic LTP (Coessmans et al., 2004). In the presence of BAPTA, EPSC amplitudes were still potentiated ($124.7 \pm 7.9\%$ of baseline; $n = 5$; last 5 min; $p < 0.05$) (Fig. 1B), and the PPF ratio was reduced ($92.2 \pm 3.4\%$; $n = 5$; last 5 min; $p < 0.05$) (Fig. 1D). Neither the changes in the EPSC amplitudes nor the PPF alterations differed between the control group and the BAPTA group ($p > 0.05$; Mann–Whitney *U* test). These results suggest that the LTP obtained with 8 Hz PF tetanization is indeed presynaptically expressed.

To examine whether paired CF activity impairs the probability to induce LTP, we costimulated the PF and CF inputs. The same PF tetanization protocol was applied as described above, but now the CF input was coactivated with every second PF stimulation pulse, effectively resulting in a 4 Hz stimulation for 15 s. Although the PF activation pattern was the same, application of this pairing protocol did not result in PF-LTP induction ($92.9 \pm 4.6\%$ of baseline; $n = 7$; last 5 min; $p > 0.05$) (Fig. 1E). This difference in LTP observed in the absence of paired CF stimulation was statistically significant ($p < 0.01$, Mann–Whitney *U* test). To be able to exclude the possibility that paired PF and CF stimulation led to the induction of postsynaptic LTD, which might simply mask presynaptic LTP, we applied the same stimulus protocol when LTD induction was blocked by adding the PKC inhibitory peptide PKC [19–36] (100 μM) to the internal saline (Hansel et al., 2001). In the presence of PKC [19–36], paired stimulation still did not elicit LTP ($93.4 \pm 7.9\%$ of baseline; $n = 6$; last 5 min; $p > 0.05$) (Fig. 1E), indicating that LTD did not mask presynaptic LTP.

Paired PF and CF stimulation also blocks the induction of presynaptic LTP when the frequency of CF stimulation is reduced to 1 Hz, which is in the range of spontaneous complex spike activity observed *in vivo* ($98.4 \pm 3.8\%$ of baseline; $n = 7$; last 5 min) (Fig. 1F). However, the transient EPSC depression seen after pairing with CF stimulation at 4 Hz was not observed after 1 Hz CF stimulation. Thus, it seems that this short-term depression depends on the level of CF activity, but it might not transfer into LTD because of the short duration of tetanization applied here.

Retrograde endocannabinoid signaling can provide a link between CF activity and inhibition of transmitter release at PF terminals (Brenowitz and Regehr, 2005). To test whether the CF-mediated suppression of PF-LTP involves the activation of CB1 receptors, we applied paired 8 Hz PF and 4 Hz CF tetanization, while the CB1 receptor antagonist AM251 was present in the bath ($5 \mu\text{M}$). In the presence of AM251, PF-LTP was rescued ($127.0 \pm 6.8\%$ of baseline; $n = 12$; last 5 min; $p < 0.01$) (Fig. 2A). This potentiation was significantly different from the EPSC changes resulting from PF and CF stimulation in the absence of the drug ($p < 0.01$, Mann-Whitney U test). In the absence of tetanization, AM251 did not alter EPSC amplitudes ($100.9 \pm 3.3\%$; $n = 6$; last 5 min; $p > 0.05$) (Fig. 2B). The opposite strategy is to test whether PF tetanization alone at 8 Hz for 15 s can still elicit LTP when CB receptors are tonically activated. Bath application of the CB receptor agonist WIN55,212-2 ($2 \mu\text{M}$) caused a pronounced reduction in EPSC amplitudes ($37.2 \pm 5.1\%$ of baseline; $n = 7$; last 5 min; $p < 0.01$) (Fig. 3A), which was associated with a significant increase in the PPF ratio ($123.8 \pm 8.5\%$; $n = 7$; last 5 min; $p < 0.01$) (Fig. 3B), indicating that the drug acts on presynaptic CB receptors to reduce transmitter release. When WIN55,212-2 was present in the bath, application of the otherwise LTP-inducing PF tetanization protocol did not cause a potentiation ($96.1 \pm 3.5\%$; $n = 17$; last 5 min; $p > 0.05$) (Fig. 3C). This blockade was significantly different from the LTP seen under control conditions ($p < 0.01$, Mann-Whitney U test). Together, the results obtained from the CB1 receptor antagonist (AM251) and the CB receptor agonist (WIN55,212-2) experiments suggest that activation of presynaptic CB1 receptors blocks the induction of presynaptic PF-LTP and that this pathway can be recruited by CF activity.

CB1 receptor activation can inhibit adenylyl cyclase activity and can modify K- and Ca-selective channels (Ameri, 1999). It has been shown that the induction of presynaptic PF-LTP involves the activation of adenylyl cyclase (Salin et al., 1996; Storm et al., 1998). Therefore, we next examined whether, under our experimental conditions, receptor activation would interfere with the adenylyl cyclase pathway. To do so, we bath applied the adenylyl cyclase activator forskolin ($50 \mu\text{M}$). Forskolin application resulted in a strong potentiation of EPSCs ($178.4 \pm 17.7\%$ of baseline; $n = 6$; last 5 min; $p < 0.01$) (Fig. 4A), which was associated with a significant reduction in the PPF ratio ($89.2 \pm 4.7\%$; $n = 6$; last 5 min; $p < 0.01$) (Fig. 4B). In contrast, when forskolin was added to the bath in the presence of WIN55,212-2, no subsequent enhancement of EPSC amplitudes could be observed ($99.9 \pm 3.8\%$; $n = 6$; last 5 min) (Fig. 4C). This effect was significantly different from the potentiation seen in the absence of WIN55,212-2 ($p < 0.01$; Mann-Whitney U test). As forskolin

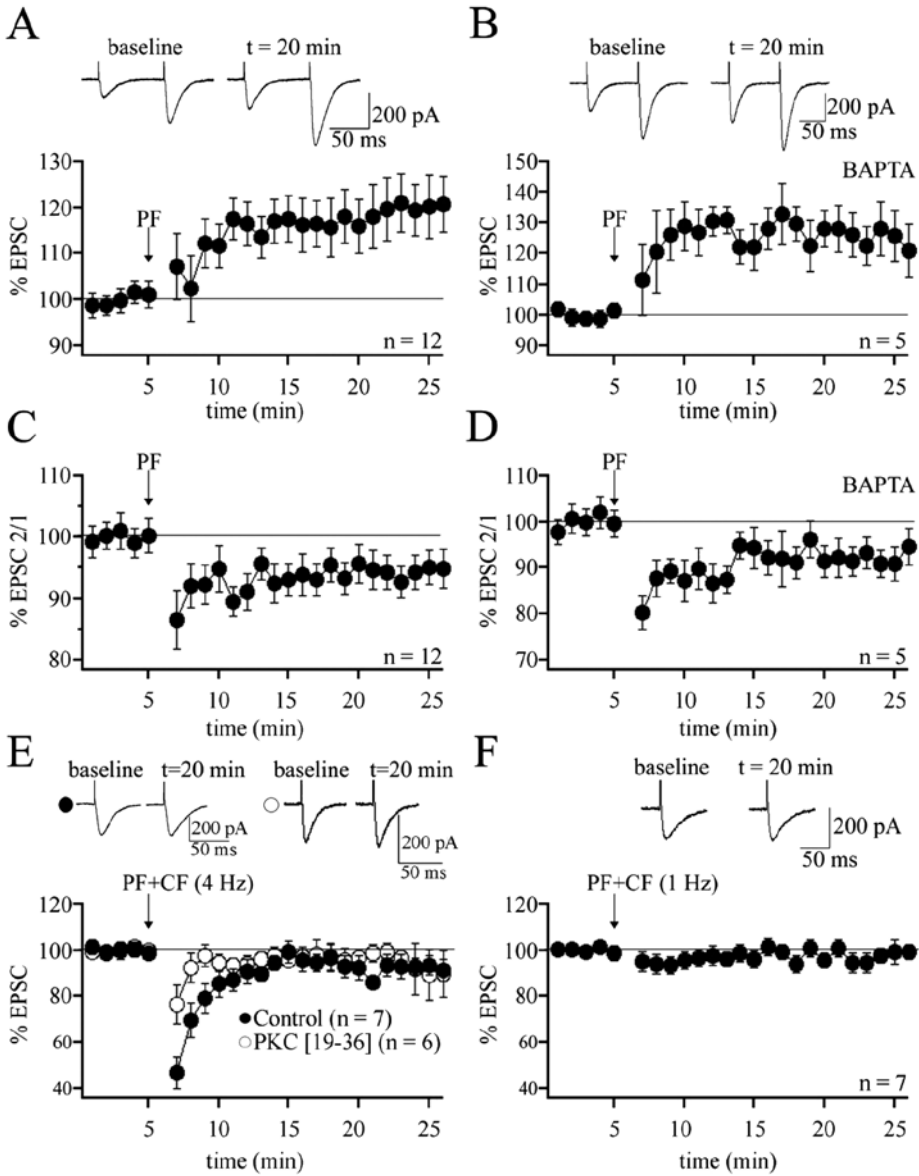


Figure 1: CF activity suppresses the induction of presynaptic PF-LTP. **A**, PF-LTP can be induced by PF stimulation at 8 Hz for 15 s ($n = 12$). Each data point represents the average of three successive test responses evoked at 0.05 Hz. The traces on top show EPSCs before and after LTP induction. The arrow indicates the onset of tetanization. **B**, PF-LTP can be induced when BAPTA (30 μ M) is added to the internal saline ($n = 5$). **C**, PPF ratio (EPSC 2/EPSC 1) from the LTP group shown in **A**. **D**, PPF ratio from the BAPTA group shown in **B**. **E**, PF-LTP is abolished when 8 Hz PF stimulation is paired with 4 Hz CF stimulation ($n = 7$). LTP suppression using paired CF stimulation can also be observed when PKC [19-36] (100 μ M) is added to the internal saline ($n = 6$). **F**, PF-LTP is blocked when the 8 Hz PF stimulation is paired with CF stimulation at 1 Hz ($n = 7$). Error bars indicate SEM.

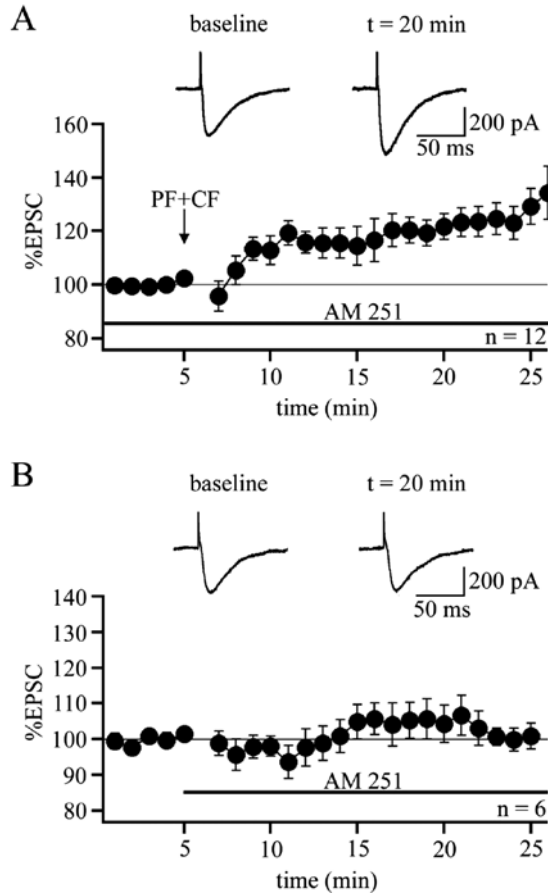


Figure 2: The CB1 receptor antagonist AM251 rescues PF-LTP. *A*, PF-LTP is observed when PF and CF synapses are coactivated in the presence of AM251 (5 μ m; n = 12). *B*, Bath application of AM251 does not alter EPSC amplitudes (n = 6). The horizontal bar indicates the period in which AM251 was bath applied. Error bars indicate SEM.

activates adenylyl cyclase and thus acts downstream of K⁻ or Ca⁻ selective ion channels, the blockade of the forskolin-mediated EPSC potentiation by WIN55,212-2 suggests that the CB receptor agonist indeed interferes at the level of adenylyl cyclase activation.

DISCUSSION

The main finding of this study is that activity of the heterosynaptic CF input suppresses the induction of a presynaptically expressed form of PF-LTP through retrograde cannabinoid signaling. Derivatives of the cannabinoid Δ^9 -tetrahydrocannabinol, the primary psychoactive component of the cannabis plant, are powerful modulators of synaptic transmission. In the

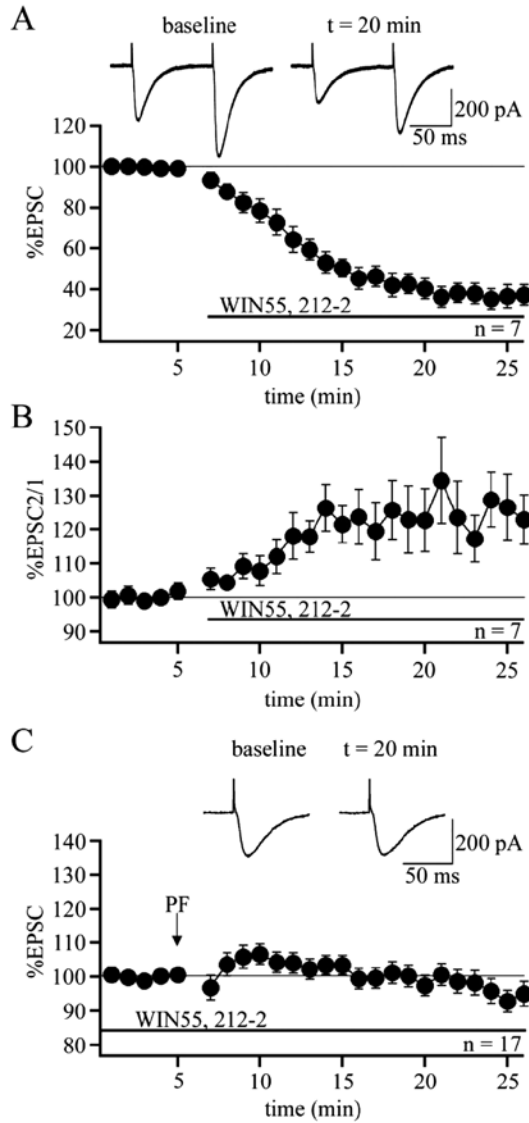


Figure 3: The CB receptor agonist WIN55,212-2 blocks PF-LTP. A, Bath application of WIN55,212-2 (2 μ m) depresses PF-EPSCs (n = 7). **B,** PPF ratio (EPSC 2/EPSC 1) from the group shown in A. The horizontal bar indicates the presence of WIN55,212-2 in the bath. **C** PF-LTP induced by 8 Hz PF stimulation for 15 s is abolished in the presence of WIN55,212-2 (n = 17). Error bars indicate SEM.

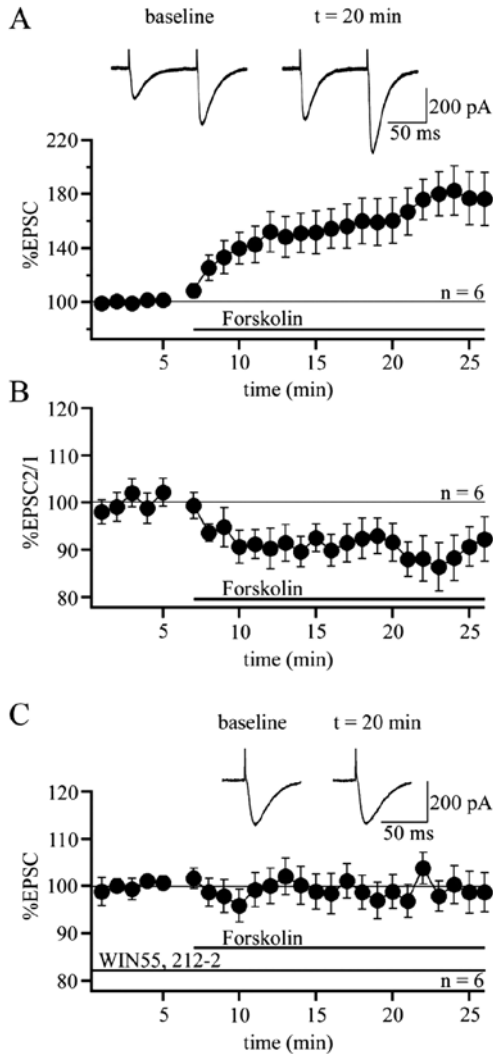


Figure 4: WIN55,212-2 prevents the activation of adenylyl cyclases by forskolin. **A**, Bath application of the adenylyl cyclase activator forskolin ($50 \mu\text{M}$) enhances PF-EPSCs ($n = 6$). **B**, PPF ratio (EPSC 2/EPSC 1) from the group shown in **A**. **C**, WIN55,212-2 ($2 \mu\text{M}$) abolishes the forskolin-mediated enhancement of PF-EPSCs ($n = 6$). The horizontal bars indicate the presence of WIN55,212-2 and forskolin, respectively, in the bath. Error bars indicate SEM.

brain, the endocannabinoids anandamide and 2-arachidonylglycerol function as modulators of transmitter release by binding to G-protein-coupled CB1 receptors, which are located on synaptic terminals. CB1 receptor activation can both inhibit adenylyl cyclases and modify K- and Ca-selective channels (Ameri, 1999). The latter mode of action has been shown to be involved in the acute effects of CB1 receptor activation on PF-EPSPs (Daniel et al., 2004) and DSEs (Brown

et al., 2004). The resulting downregulation of transmitter release has consequences for LTP/LTD induction: cannabinoids impair LTP as well as LTD induction at glutamatergic synapses (Levenes et al., 1998; Misner and Sullivan, 1999) but have also been reported to facilitate the induction of LTD (Gerdeman et al., 2002). Moreover, cannabinoids have been described to reduce GABA release (Chevaleyre and Castillo, 2003). This effect likely explains the observation that endocannabinoids can, through heterosynaptic interaction, also facilitate LTP induction (Carlson et al., 2002; Chevaleyre and Castillo, 2004). The effects of CB1 receptor activation on K- and Ca-selective ion channels and adenylyl cyclases might interfere with presynaptic forms of long-term plasticity as well. For example, it has been shown that presynaptic LTD at neocortical synapses requires CB1 receptor activation (Sjöström et al., 2003).

Here, we report that endocannabinoid signaling can be triggered by CF activity and that the subsequent activation of CB1 receptors impairs presynaptic PF-LTP. Endocannabinoid signaling is well suited to mediate this CF-evoked suppression because it can be triggered in a calcium-dependent way (Kreitzer and Regehr, 2001; Ohno-Shosaku et al., 2001; Wilson and Nicoll, 2001; Brenowitz and Regehr, 2003), and because CB1 receptors are located at PF terminals. Our data show that cannabinoids indeed act as mediators of the CF effect. When the PF and CF inputs were coactivated, bath application of the CB1 receptor antagonist AM251 could rescue PF-LTP. Moreover, effects of CF stimulation could be mimicked by tonically activating CB1 receptors with bath application of WIN55,212-2, which impaired LTP induction. Agonists of CB1 receptors have been reported previously to reduce transmitter release (Levenes et al., 1998; Takahashi and Linden, 2000; Daniel et al., 2004). Activation of CB1 receptors has several effects, which all result in a reduction of transmitter release: (1) it can lead to a downregulation of voltage-dependent calcium channels; (2) it can cause an upregulation of K channels; and (3) it can interfere with the activation of adenylyl cyclases and thus with the PF-LTP induction cascade. All three mechanisms could account for the observed effects. By showing that in the presence of the CB receptor agonist WIN55,212-2 the adenylyl cyclase activator forskolin no longer potentiates PF-EPSCs, we confirm that CB receptor activation indeed suppresses the activity of adenylyl cyclase. This finding does not exclude the possibility that Ca- or K-selective channels are also modified, but it suggests that during tetanization, the activation of CB1 receptors blocks the adenylyl cyclase–PKA signaling cascade that otherwise leads to the induction of presynaptic LTP through phosphorylation of the PKA substrate RIM1 α (Castillo et al., 2002; Lonart et al., 2003).

The observed endocannabinoid-mediated suppression of presynaptic PF-LTP occurs under conditions that also favor the induction of postsynaptically expressed LTD (paired PF and CF activity). However, when LTD induction was blocked by adding the PKC inhibitory peptide PKC [19-36], CF coactivation was still able to suppress presynaptic LTP, suggesting that LTD does not simply mask LTP. Rather, the CF-evoked suppression of presynaptic LTP might provide a safety lock, which prevents that LTP is expressed presynaptically, while LTD is expressed postsynaptically. The signaling cascades involved partially overlap with those described for DSE; CF activity causes complex spike-associated calcium transients that trigger the release of endocannabinoids (Brenowitz and Regehr, 2005). It is remarkable

that the CF apparently controls all forms of PF plasticity. Simultaneous CF activity postsynaptically promotes the induction of PF-LTD by providing a large calcium transient, whereas postsynaptically expressed PF-LTP is triggered by smaller calcium transients in the absence of CF activity (Coemans et al., 2004). Postsynaptic PF-LTP depends on the activation of protein phosphatases PP1, PP2A, and PP2B (Belmeguenai and Hansel, 2005), whereas PF-LTD depends on the activation of PKC (for review, see Hansel et al., 2001). Thus, it can be argued that CF activity, by promoting the PKC cascade, has a tight grip on the polarity of postsynaptic PF plasticity. Our observation that CF activity additionally suppresses the induction of presynaptic PF-LTP supports the notion that the CF input heterosynaptically controls all forms of PF synaptic plasticity.

The suppressive effect of CF coactivation was not only observed with CF stimulation at 4 Hz, but also at 1 Hz, suggesting the possibility that presynaptic LTP is permanently suppressed under resting conditions. In our recordings, spike activity is prevented in PCs by constant current injection. CF stimulation at 1 Hz thus provides a transient increase in PC activity that might trigger endocannabinoid release only under these *in vitro* conditions. Even if endocannabinoids were released under resting conditions *in vivo*, there are physiological activity patterns favoring presynaptic LTP because complex spikes are not constantly fired at 1 Hz. Transient inhibition of CFs by elevated cerebellar activity has been shown to facilitate the extinction of conditioned eyelid responses (Medina et al., 2002) and might create time windows without complex spike activity during which LTP can be induced.

Previous reports have suggested that cannabinoids interfere with the induction of PF-LTD. A previous study has shown that cannabinoid signaling impairs PF-LTD induction, which was explained by reduced transmitter release during tetanization (Levenes et al., 1998). The opposite effect was reported recently, showing that cannabinoid signaling is permissive for PF-LTD induction (Safo and Regehr, 2005). The resulting paradox that a retrograde messenger modifies the induction probability of postsynaptic LTD was addressed by suggesting that CB1 receptor activation might trigger NO release from PF terminals. Because NO has been suggested to be required for LTD induction, CB1 receptor activation could promote LTD induction, despite an accompanying transient reduction in transmitter release. The study by Safo and Regehr (2005) and ours complement each other and, in fact, provide two sides of the same coin. Whereas these authors demonstrated that cannabinoid signaling is required for the induction of PF-LTD (which is postsynaptically expressed), we demonstrate here that cannabinoid signaling suppresses a presynaptic form of PF-LTP. This LTP suppression might well provide a better explanation for the endocannabinoid-mediated promotion of PF-LTD than NO signaling as suggested by Safo and Regehr (2005). First, it has recently been shown that NO might indeed be involved in LTD induction; however, it is not released from PF terminals, but rather from interneurons (Shin and Linden, 2005). Second, simultaneous induction of presynaptic LTP would counteract postsynaptic LTD. It is likely that the CF-evoked calcium transients in PC dendrites can postsynaptically promote LTD and, through the release of endocannabinoids, presynaptically suppress LTP at the same time. The latter effect would facilitate LTD induction and enhance the observed LTD magnitude.

ACKNOWLEDGEMENTS

This work was supported by a grant from NWO-VIDI (The Netherlands Organization for Scientific Research) to C.H. We thank members of the Hansel laboratory for helpful discussions.



REFERENCES

1. Ameri A (1999) The effects of cannabinoids on the brain. *Prog Neurobiol* 58:315–348.
2. Belmeguenai A, Hansel C (2005) A role for protein phosphatases 1, 2A, and 2B in cerebellar long-term potentiation. *J Neurosci* 25:10768–10772.
3. Brenowitz SD, Regehr WG (2003) Calcium dependence of retrograde inhibition by endocannabinoids at synapses onto Purkinje cells. *J Neurosci* 23:6373–6384.
4. Brenowitz SD, Regehr WG (2005) Associative short-term synaptic plasticity mediated by endocannabinoids. *Neuron* 45:419–431.
5. Brown SP, Safo PK, Regehr WG (2004) Endocannabinoids inhibit transmission at granule cell to Purkinje cell synapses by modulating three types of presynaptic calcium channels. *J Neurosci* 24:5623–5631.
6. Carlson G, Wang Y, Alger BE (2002) Endocannabinoids facilitate the induction of LTP in the hippocampus. *Nat Neurosci* 5:723–724.
7. Castillo PE, Schoch S, Schmitz F, Südhof TC, Malenka RC (2002) RIM1 α is required for presynaptic long-term potentiation. *Nature* 415:327–330.
8. Chen C, Regehr WG (1997) The mechanism of cAMP-mediated enhancement at a cerebellar synapse. *J Neurosci* 17:8687–8694.
9. Chevaleyre V, Castillo PE (2003) Heterosynaptic LTD of hippocampal GABAergic synapses: a novel role of endocannabinoids in regulating excitability. *Neuron* 38:461–472.
10. Chevaleyre V, Castillo PE (2004) Endocannabinoid-mediated metaplasticity in the hippocampus. *Neuron* 43:871–881.
11. Coesmans M, Weber JT, De Zeeuw CI, Hansel C (2004) Bidirectional parallel fiber plasticity in the cerebellum under climbing fiber control. *Neuron* 44:691–700.
12. Daniel H, Rancillac A, Crepel F (2004) Mechanisms underlying cannabinoid inhibition of presynaptic Ca²⁺ influx at parallel fiber synapses of the rat cerebellum. *J Physiol (Lond)* 557:159–174.
13. Diana MA, Levenes C, Mackie K, Marty A (2002) Short-term retrograde inhibition of GABAergic synaptic currents in rat Purkinje cells is mediated by endogenous cannabinoids. *J Neurosci* 22:200–208.
14. Gerdeman GL, Ronesi J, Lovinger DM (2002) Postsynaptic endocannabinoid release is critical to long-term depression in the striatum. *Nat Neurosci* 5:446–451.
15. Hansel C, Linden DJ, D'Angelo E (2001) Beyond parallel fiber LTD: the diversity of synaptic and non-synaptic plasticity in the cerebellum. *Nat Neurosci* 4:467–475.
16. Ito M (2001) Cerebellar long-term depression: characterization, signal transduction, and functional roles. *Physiol Rev* 81:1143–1194.
17. Jacoby S, Sims RE, Hartell NA (2001) Nitric oxide is required for the induction and heterosynaptic spread of long-term potentiation in rat cerebellar slices. *J Physiol (Lond)* 535:825–839.
18. Kreitzer AC, Regehr WG (2001) Retrograde inhibition of presynaptic calcium influx by endogenous cannabinoids at excitatory synapses onto Purkinje cells. *Neuron* 29:717–727.
19. Levenes C, Daniel H, Soubrie P, Crepel F (1998) Cannabinoids decrease excitatory synaptic transmission and impair long-term depression in rat cerebellar Purkinje cells. *J Physiol (Lond)* 510:867–879.
20. Lev-Ram V, Wong ST, Storm DR, Tsien RY (2002) A new form of cerebellar long-term potentiation is postsynaptic and depends on nitric oxide but not cAMP. *Proc Natl Acad Sci USA* 99:8389–8393.
21. Linden DJ (1997) Long-term potentiation of glial synaptic currents in cerebellar culture. *Neuron* 18:983–994.
22. Llano I, Leresche N, Marty A (1991) Calcium entry increases the sensitivity of cerebellar Purkinje cells to applied GABA and decreases inhibitory synaptic currents. *Neuron* 6:565–574.
23. Lonart G, Schoch S, Kaeser PS, Larkin CJ, Südhof TC, Linden DJ (2003) Phosphorylation of RIM1 α by PKA triggers presynaptic long-term potentiation at cerebellar parallel fiber synapses. *Cell* 115:49–60.
24. Medina JF, Nores WL, Mauk MD (2002) Inhibition of climbing fibres is a signal for the extinction of conditioned eyelid responses. *Nature* 416:330–333.
25. Misner DL, Sullivan JM (1999) Mechanism of cannabinoid effects on long-term potentiation and depression in hippocampal CA1 neurons. *J Neurosci* 19:6795–6805.

26. Ohno-Shosaku T, Maejima T, Kano M (2001) Endogenous cannabinoids mediate retrograde signals from depolarized postsynaptic neurons to presynaptic terminals. *Neuron* 29:729–738.
27. Pitler TA, Alger BE (1992) Postsynaptic spike firing reduces synaptic GABA_A responses in hippocampal pyramidal cells. *J Neurosci* 12:4122–4132.
28. Safo PK, Regehr WG (2005) Endocannabinoids control the induction of cerebellar LTD. *Neuron* 48:647–659.
29. Salin PA, Malenka RC, Nicoll RA (1996) Cyclic AMP mediates a presynaptic form of LTP at cerebellar parallel fiber synapses. *Neuron* 16:797–803.
30. Shin JH, Linden DJ (2005) An NMDA receptor/nitric oxide cascade is involved in cerebellar LTD but is not localized to the parallel fiber terminal. *J Neurophysiol* 94:4281–4289.
31. Sjöström PJ, Turrigiano GG, Nelson SB (2003) Neocortical LTD via coincident activation of presynaptic NMDA and cannabinoid receptors. *Neuron* 39:641–654.
32. Storm DR, Hansel C, Hacker B, Parent A, Linden DJ (1998) Impaired cerebellar long-term potentiation in type I adenylyl cyclase mutant mice. *Neuron* 20:1199–1210.
33. Takahashi KA, Linden DJ (2000) Cannabinoid receptor modulation of synapses received by cerebellar Purkinje cells. *J Neurophysiol* 83:1167–1180.
34. Wilson RI, Nicoll RA (2001) Endogenous cannabinoids mediate retrograde signaling at hippocampal synapses. *Nature* 410:588–592.
35. Wilson RI, Kunos G, Nicoll RA (2001) Presynaptic specificity of endocannabinoid signaling in the hippocampus. *Neuron* 31:453–462.

**PURKINJE CELL-SPECIFIC
KNOCKOUT
OF THE PROTEIN
PHOSPHATASE PP2B
IMPAIRS POTENTIATION
AND CEREBELLAR MOTOR
LEARNING**

M. Schonewille^{1†}, A. Belmeguenai^{1,2†},
S.K. Koekkoek^{1†}, S.H. Houtman^{1†},
H.J. Boele¹, B.J. van Beugen¹,
Z. Gao¹, A. Badura¹, G. Ohtsuki¹
, W.E. Amerika¹, E. Hosity¹,
F.E. Hoebeek¹, Y. Elgersma¹,
C. Hansel¹ and C.I. De Zeeuw^{3,1}

¹ Department of Neuroscience, Erasmus MC, 3000
DR Rotterdam, The Netherlands

² Laboratoire de Physiologie Intégrative Cellulaire et
Moléculaire, Université Claude Bernard Lyon, 69622
Villeurbanne Cedex, France

³ Netherlands Institute for Neuroscience, Royal
Academy of Sciences (KNAW), Meibergdreef 47,
1105 BA Amsterdam, The Netherlands

† These authors contributed equally

IV

ABSTRACT

Cerebellar motor learning is required to obtain procedural skills. Studies have provided supportive evidence for a potential role of kinase-mediated long-term depression (LTD) at the parallel fiber to Purkinje cell synapse in cerebellar learning. Recently, phosphatases have been implicated in the induction of potentiation of Purkinje cell activities *in vitro*, but it remains to be shown whether and how phosphatase-mediated potentiation contributes to motor learning. Here, we investigated its possible role by creating and testing a Purkinje cell specific knockout of calcium/calmodulin-activated protein-phosphatase-2B (L7-PP2B). The selective deletion of PP2B indeed abolished postsynaptic long-term potentiation in Purkinje cells and their ability to increase their excitability, whereas LTD was unaffected. The mutants showed impaired *gain-decrease* and *gain-increase* adaptation of their VOR as well as impaired *acquisition* of classical delay conditioning of their eyeblink response. Thus, our data indicate that PP2B may mediate indeed potentiation in Purkinje cells and contribute prominently to cerebellar motor learning.

INTRODUCTION

At excitatory synapses onto hippocampal or neocortical synapses, protein phosphatases are required for postsynaptic LTD induction, whereas kinases are required for postsynaptic LTP induction (Lisman and Zhabotinsky, 2001; Mulkey et al., 1993). In these regions protein phosphatase 1 (PP1), the activity state of which is indirectly controlled by calcium/calmodulin-activated protein phosphatase 2B (calcineurin or PP2B), has been suggested to act in concert with the α isoform of calcium/calmodulin-dependent kinase II (α CaMKII) to provide a molecular switch regulating the phosphorylation state of AMPA receptors (Lisman and Zhabotinsky, 2001; Malleret et al., 2001). In contrast, at cerebellar PF synapses onto Purkinje cells LTD induction is PKC α - (Leitges et al., 2004), cGKI- (Feil et al., 2003) and α/β CaMKII-dependent (Hansel et al., 2006; van Woerden et al., 2009), whereas LTP requires the activation of PP1, PP2A, and calcineurin (Belmeguenai and Hansel, 2005). Interestingly, changes in LTD and LTP induction can be associated with changes in intrinsic excitability in the hippocampus and cerebellum (Armano et al., 2000; Lu et al., 2000), and calcineurin has indeed been associated differentially with changes in intrinsic excitability in pyramidal cells and Purkinje cells (Misonou et al., 2004 and personal communication, respectively). Thus, cerebellar Purkinje cells operate in general inversely to their hippocampal counterparts in that downstream kinase and phosphatase activity can push the balance towards LTD and LTP, respectively (Coemans et al., 2004; Jorntell and Hansel, 2006), even though the activity of these enzymes themselves can be regulated by proteins of the opposite category upstream (Eto et al., 2002; Launey et al., 2004).

Over the past decades, attempts to determine the cellular mechanisms underlying cerebellar motor learning have focused virtually exclusively on the impact of LTD (Aiba et al., 1994; De Zeeuw et al., 1998; De Zeeuw and Yeo, 2005; Steuber et al., 2007). Genetic interference with kinase-mediated LTD induction and/or maintenance in Purkinje cells has been reported to be associated with impaired motor learning such as defects in VOR gain adaptation or eyeblink conditioning (Boyden et al., 2006; De Zeeuw et al., 1998; Feil et al., 2003; Hansel et al., 2006; cf Welsh et al., 2005). Some of these studies have encouraged scientists to hypothesize that LTD is specifically responsible for gain *increases* in VOR adaptation (Boyden and Raymond, 2003) and *acquisition* of conditioned eyeblink responses (De Zeeuw and Yeo, 2005; Koekkoek et al., 2003) raising the possibility that potentiation might be responsible for gain-*decrease* VOR adaptations and *extinction* of conditioned responses (Boyden and Raymond, 2003). However, no transgenic mouse mutants have been created yet, which allow us to investigate specifically the possible contribution of potentiation in Purkinje cells. Since calcineurin is required for PF-PC LTP and increases in intrinsic excitability (Belmeguenai and Hansel, 2005 and personal communication, respectively), this protein forms an ideal molecular target to genetically manipulate potentiation in Purkinje cells, and to investigate for the first time a potential role of potentiation in cerebellar motor learning. Thus, here we created mutant mice (L7-PP2B), in which calcineurin activity is selectively impaired in Purkinje cells by crossing

floxed CNB1 mice (regulatory subunit of calcineurin) (Zeng et al., 2001) with a Purkinje cell specific (L7-)cre-line (Barski et al., 2000) (Figure 1A), and we subsequently investigated them at the cell physiological and behavioral level.

RESULTS

IV

L7-PP2B mice lack calcineurin but show normal histology

Immunocytochemical analysis of the L7-PP2B mice with antibodies directed against the CNB1 subunit showed that calcineurin is indeed specifically deleted in Purkinje cells (Figure 1B). Density analyses showed that PP2B staining intensity was significantly lower in Purkinje cell bodies and primary dendrites ($p = 0.003$ and 0.034 , respectively; t-test), but not in granule cells or the neuropil of the molecular layer ($p > 0.6$ for both parameters). Thionine and Golgi stainings revealed that the mutation did not affect the foliation of the cerebellar cortex or the cyto-architecture of Purkinje cells, respectively (Figure 1C). Moreover, electron microscopic examinations of calbindin-stained sections of the cerebellar cortex of L7-PP2B mice showed that the number and size of synaptic inputs from PFs onto Purkinje cells were not significantly different from those of littermate controls ($p > 0.26$ for all parameters, i.e. PSD length, PSD area, and density of synapses; t-test) (Figure 1D). Moreover, the area covered by the Purkinje cell dendrites as well as the thickness of the different layers of the cerebellar cortex was also unaffected ($p > 0.49$ for both parameters; t-test).

L7-PP2B mice show specific defects in parallel fiber to Purkinje cell plasticity

As predicted by our previous pharmacological *in vitro* studies in cerebellar rat tissue (Belmeguenai and Hansel, 2005), our cell physiological examination of 10-24 week-old L7-PP2B mice indeed showed that LTP induction following parallel fiber stimulation alone was blocked ($p = 0.027$; t-test) (Figure 2A). In contrast, LTD induction following paired PF and climbing fiber (CF) stimulation was unaffected in adult L7-PP2B mice ($p = 0.96$; t-test) (Figure 2C). In wild type littermates, both LTP and LTD were successfully induced (Figures 2A and C). The inability of L7-PP2B mutants to potentiate their parallel fiber input did not depend on the temperature, age or type of induction protocol, while it could be rescued by the addition of active PP2B (Figures S1 and S2). Moreover, EPSPs and intracellular calcium concentrations during the tetanus did not differ (Figure 2B), arguing against the possibility that these factors were responsible for the observed deletion of parallel fiber potentiation.

Climbing fiber elimination, paired-pulse ratios and inhibition are not affected in Purkinje cells of L7-PP2B mice

Since the presence or absence of CF activity is critical for the induction of depression and potentiation in Purkinje cells, respectively (Coesmans et al., 2004; Lev-Ram et al., 2002), we also examined whether deletion of calcineurin in Purkinje cells directly affects the developmental elimination of surplus CF inputs, as previously observed for mutant mice lacking PKC (De Zeeuw et al., 1998) or α CaMKII activity (Hansel et al., 2006). CF

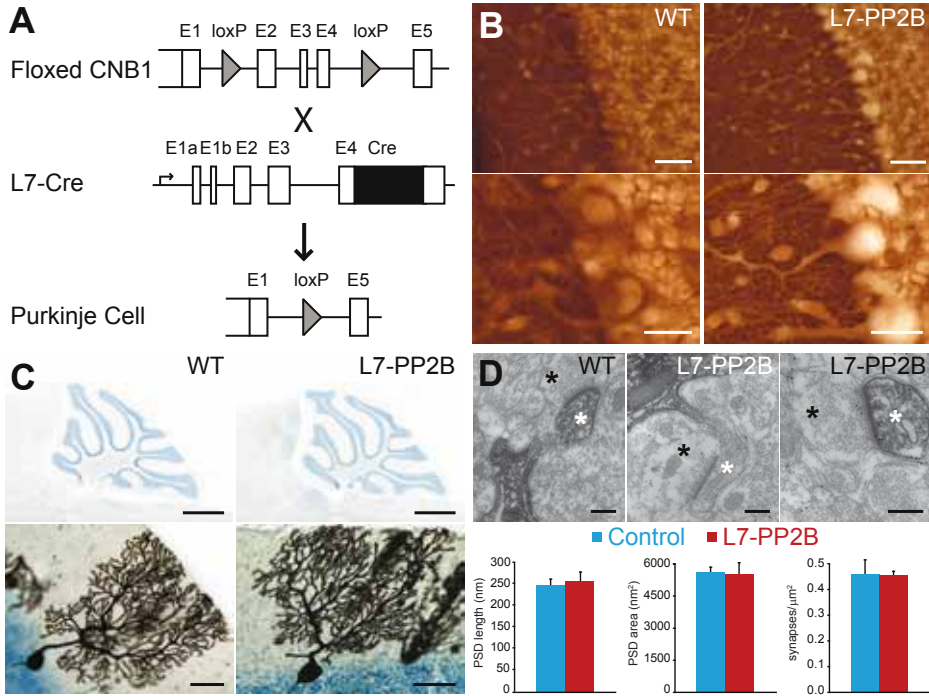


Figure 1: The L7-PP2B mutant: Creation and morphology. A, The L7-PP2B mutant mice were created by crossing a floxed calcineurin line with a L7-Cre line. B, Calcineurin (B subunit) stainings of the cerebellar cortex confirm the selective deletion of PP2B in Purkinje cells in L7-PP2B mice ($n = 4$); note the normal expression of PP2B in the parallel fibers of the molecular layer in which the unstained Purkinje cell dendrites stand out (right panels). C, Thionin (upper panel) and Golgi (lower panel) stainings of sagittal sections of the vermis showed no morphological or cyto-architectural differences between control ($n = 4$) and L7-PP2B mice ($n = 4$) ($p > 0.49$; t -test). D, Electron micrographic quantification of parallel fiber contacts with calbindin stained Purkinje cell dendrites in the molecular layer revealed no significant differences between control ($n = 3$) and L7-PP2B mice ($n = 3$) in PSD length, PSD area, and density of synapses ($p > 0.26$ for all parameters; t -test). Scale bars indicate $50 \mu\text{m}$ (upper panels) and $25 \mu\text{m}$ (lower panels) in B, $1000 \mu\text{m}$ (upper panels) and $50 \mu\text{m}$ (lower panels) in C, and 200nm (upper panels) in D. Black asterisks indicate parallel fiber terminals, and white asterisks indicate Purkinje cell spines in D.

elimination in adult L7-PP2B mice (10-24 weeks), however, appeared normal, and is therefore unlikely to have affected synaptic input patterns that could indirectly impair plasticity in Purkinje cells of L7-PP2B mice (Figure 3A). Likewise, we did not detect differences in the paired-pulse depression (PPD) ratio at CF synapses and the paired-pulse facilitation (PPF) ratio at PF synapses, respectively (Figure 3B and C). In fact, even in the presence of NBQX or lower extracellular calcium the PPF did not differ (Figure 3C). These findings suggest that the observed effects on plasticity were postsynaptic, but they don't allow us to conclude that presynaptic changes were completely absent. Finally, we found no

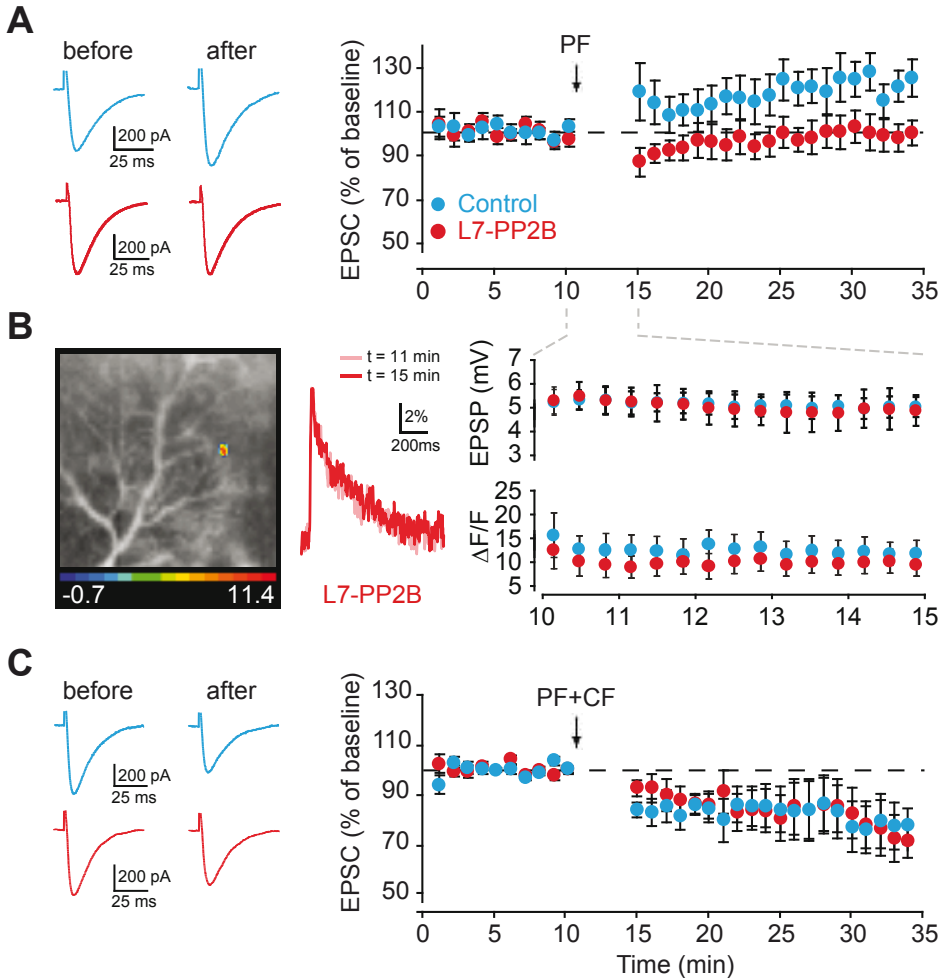


Figure 2: L7-PP2B mice show impaired parallel fiber – Purkinje cell potentiation. A, Induction of LTP at the parallel fiber to Purkinje cell synapse was significantly ($p < 0.03$; t -test) impaired in slices of adult L7-PP2B mice (8 cells from 5 mice) compared to those of controls (7 cells from 6 mice). B, Voltage responses (EPSP, average of 20 stimuli at 1 Hz) and changes in calcium transients (500 ms scans at 0.05 Hz) during the tetanus were not different (both $p > 0.5$; ANOVA for repeated measurements) between controls ($n = 13$ and 5, respectively) and L7-PP2B mice ($n = 10$ and 5). Left, sample image of parallel fiber stimulation induced Ca^{2+} -signal. Middle, example trace of PF-stimulation elicited calcium transients (average of 3). C, Induction of LTD at the parallel fiber to Purkinje cell synapse was not affected ($p = 0.96$; t -test) (7 and 9 cells in 5 mutants and 5 controls, respectively). PF-PC LTP was induced by PF stimulation at 1 Hz for 5 min, while LTD was induced by paired PF and CF stimulation at 1 Hz for 5 min. Traces on the left side show EPSCs before (left) and after (right) induction of plasticity. See also Figure S1-2.

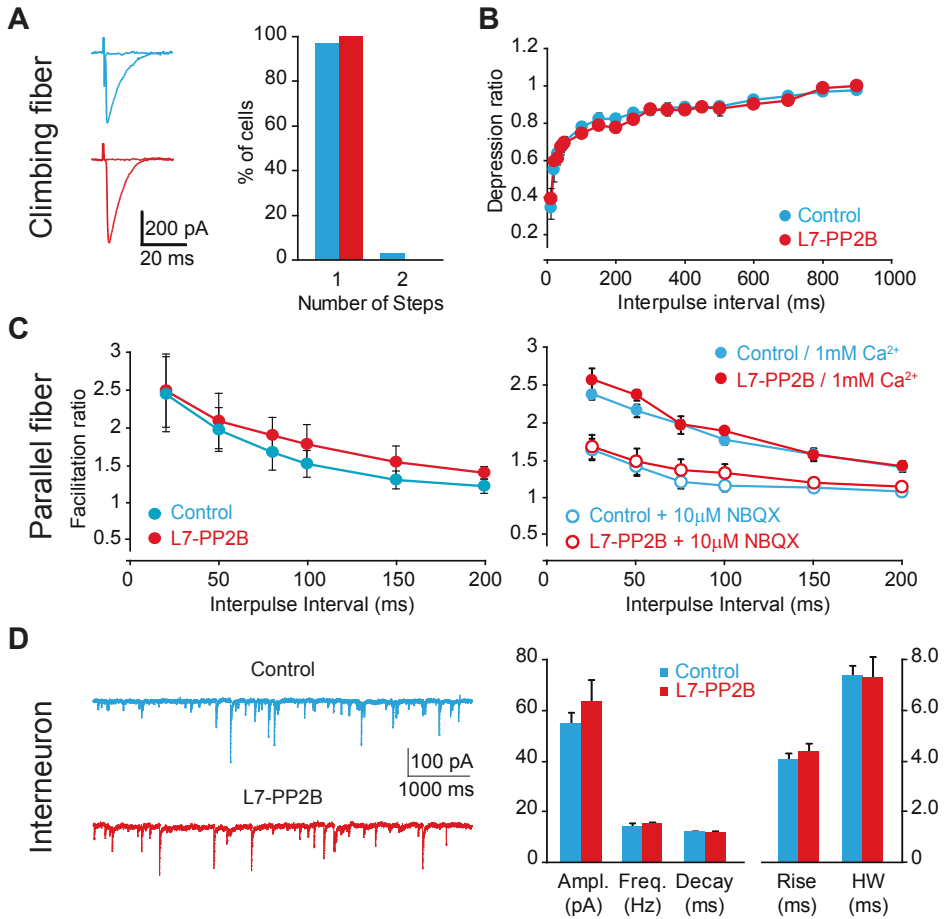


Figure 3: Climbing fiber elimination and basal state of excitatory and inhibitory input to Purkinje cells is unaffected in L7-PP2B mutant mice. A, All-or-none climbing fiber EPSCs were evoked at increasing stimulus intensities. Traces show EPSCs above and below threshold. Climbing fiber elimination is nearly complete in Purkinje cells of both controls and L7-PP2B mutants at 20-24 wks (33 cells from 12 control mice; 12 cells from 4 mutants). B and C, We did not detect differences in the paired-pulse depression (PPD) ratio at CF synapses (B) and the paired-pulse facilitation (PPF) ratio at PF synapses (C), respectively. PPF ratios were determined for the indicated stimulus intervals in both wild type ($n = 8$) and mutant mice ($n = 5$) and no differences are found ($p = 0.163$; ANOVA for repeated measurements). PPF ratios also did not differ in conditions of lower external calcium ($p = 0.213$; $n = 6$ vs. 6, control vs. L7-PP2B) or in the presence of NBQX ($p = 0.314$; $n = 5$ vs. 8). Insets show sample traces. D, Characterization of sIPSCs revealed no differences in frequency, amplitude, rise time, half width and decay time (all $p > 0.34$; $n = 11$ vs. 6, control vs. L7-PP2B; t -test). Sample traces on the left. Error bars indicate SEM.

differences in frequency, amplitude, rise/decay time and half width of spontaneous IPSCs in Purkinje cells (Figure 3D). Together, these data suggest that the basic synaptic transmission of both excitatory and inhibitory inputs to Purkinje cells is unaffected in L7-PP2B mice.

L7-PP2B mice show defects in intrinsic plasticity of Purkinje cells

In addition to synaptic parallel fiber potentiation, also non-synaptic Purkinje cell intrinsic excitability can be potentiated. This intrinsic potentiation could be readily induced in wild types, but not in the L7-PP2B mutants ($p = 0.007$; ANOVA for repeated measurements) (Figure 4A). Notably, we also observed differences in baseline intrinsic excitability. Linear fits of the current-frequency curves showed that the slope of L7-PP2B mice is less steep ($p = 0.002$; t-test) (Figure 4B). This difference suggests that the cells are less excitable, which is confirmed by a lower maximum firing frequency ($p < 0.001$; t-test) (Table S1).

A lack of PP2B affects regularity but not average firing frequency of simple spike activities in vivo

To test whether the deficits in PF-PC LTP and plasticity of intrinsic excitability affect Purkinje cell activity *in vivo* we performed extracellular recordings in awake mice ($n = 25$ vs. 30 for control vs. L7-PP2B). Firing frequencies of simple spikes and complex spikes were both normal ($p = 0.94$ and $p = 0.54$, respectively; t-test), but the inter-simple spike interval distribution was sharper with less high-frequency spiking and concomitant higher regularity in L7-PP2B mutants (Figure 4C). Thus, the changes in intrinsic excitability and potentiation in L7-PP2B mice correlate with a loss of high-frequency simple spike activity, but do not alter the average firing frequency of Purkinje cells. We therefore conclude that the deficits in potentiation in the L7-PP2B mice may selectively affect their spatiotemporal firing patterns of simple spike activities.

L7-PP2B mice show defects in adaptation of the vestibulo-ocular reflex

In the open field or during footprint analysis L7-PP2B mice did not show obvious signs of ataxia (Figure S3). To explore their specific capabilities for cerebellar motor learning, we first subjected the mice to compensatory eye movement tests, in particular VOR adaptation tests, which are controlled by the vestibulocerebellum (De Zeeuw et al., 1998; Hansel et al., 2006; Wulff et al., 2009) (Figure 5). Measurements of basic performance parameters including the gain (amplitude) and phase (timing) of the optokinetic reflex (OKR) and/or VOR showed overall that the motor performance of the L7-PP2B mutants was moderately, but significantly, affected (Figures 5B-D, Figure S4A-C). For OKR and VVOR the gain of L7-PP2B mutants were significantly lower than those of wild type littermates (both OKR and VVOR $p < 0.001$; ANOVA for repeated measurements) (Figure 5B-C), while their phase values were significantly lagging those of the wild types (OKR $p < 0.01$; VVOR $p < 0.001$; ANOVA for repeated measurements). In contrast, for VOR the gain of L7-PP2B mutants was significantly greater than that of wild type littermates ($p < 0.001$; ANOVA for repeated measurements) (Figure 5D), while their phase values were also significantly lagging those of the wild types ($p < 0.01$; ANOVA for repeated measurements) (Figure S4). The differences among mutants

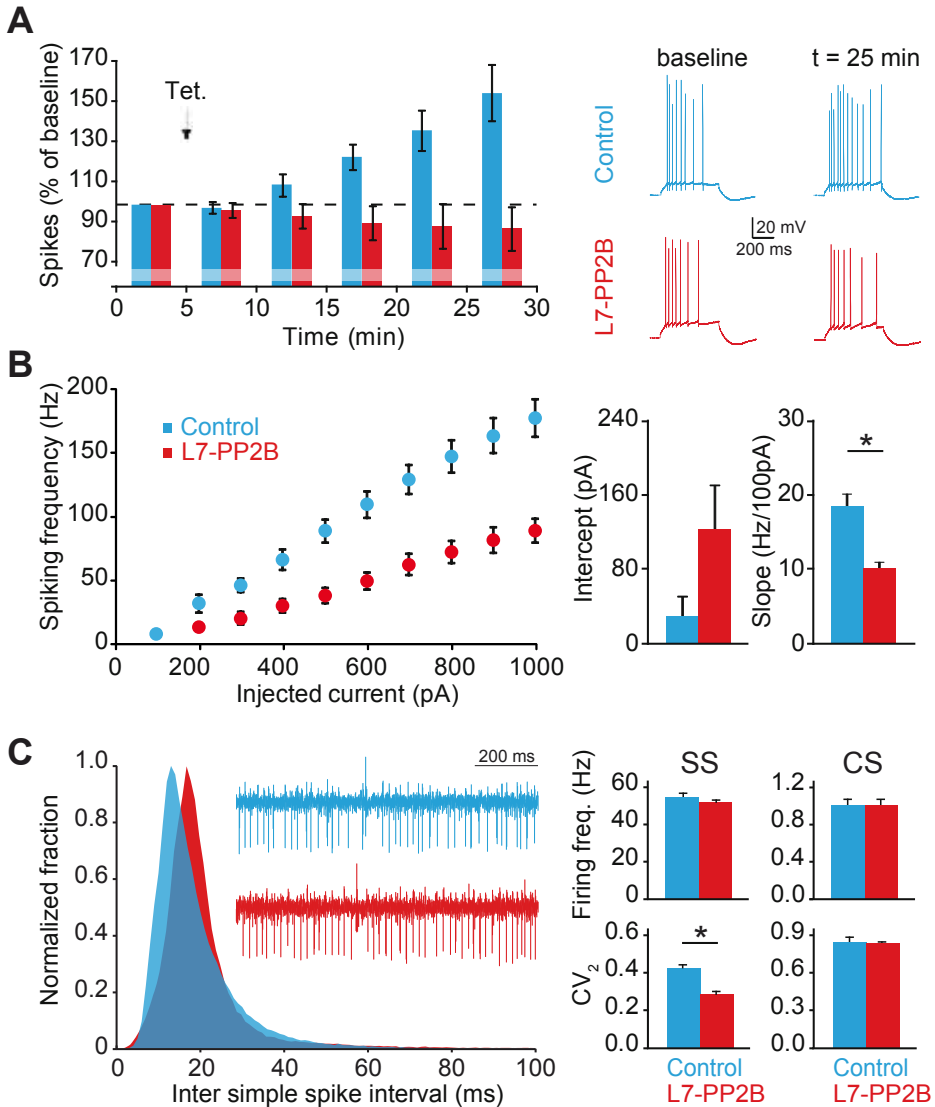
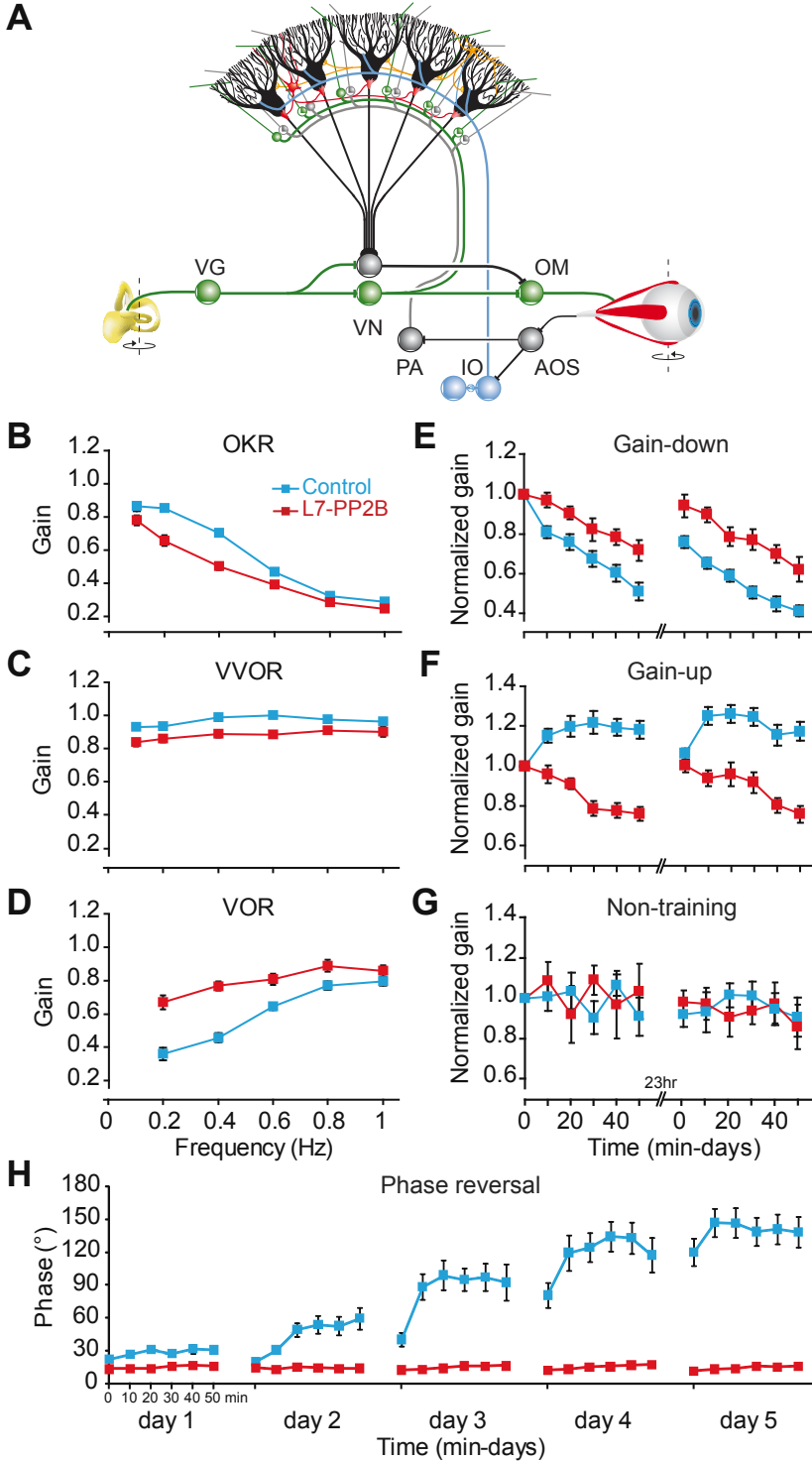


Figure 4: Intrinsic excitability and spiking activity in L7-PP2B mice. A, Following tetanization (150-300 pA at 5 Hz for 3 s) the spike rate evoked with 550 ms depolarizing current pulses of 100-200 pA increased in wild types ($n = 9$), but not in the L7-PP2B mutants ($n = 16$; $p = 0.007$; ANOVA for repeated measurements)(Figure 4A). Right, sample traces before and after induction. B, Basal intrinsic excitability is significantly lower in L7-PP2B mice ($n = 7$ vs. $n = 10$ for controls), quantified by slope ($p = 0.002$; t -test) and intercept with the x-axis ($p = 0.07$; t -test). C, Purkinje activity in vivo is characterized by a sharper inter-simple spike interval distribution (left) and concomitant higher regularity of spiking (i.e. CV_2 , $p < 0.001$), but the average frequencies of simple spikes and complex spikes were normal (both $p > 0.5$; t -test). Inset shows sample traces. See also Table S1.

and wild types during OKR and VVOR were not caused by differences in vision itself, because the latencies of the eye movement responses to the onset of the optokinetic stimuli were unaffected in the mutants ($p = 0.55$, ANOVA for repeated measurements) (Figure S5).

A prominent phenotype of the L7-PP2B mice was observed when we subjected the animals to the mismatch learning paradigms. In a two-day visuo-vestibular training paradigm aimed at reducing the gain of the VOR, learning was significantly impaired in the mutants (Figure 5E) ($p < 0.0002$ for both days; ANOVA for repeated measurements). In the opposite training paradigm, which was aimed at increasing the gain, the gain values of the mutants even showed a decrease (Figure 5F; comparison among mutants and controls $p < 0.000001$ for both days, ANOVA for repeated measurements). Control experiments revealed that this decrease was not due to aspecific effects, because exposure to a normal, non-training paradigm for the same duration did not result in any decrease ($p = 0.83$ and $p = 0.90$ for day 1 and day 2, respectively, ANOVA for repeated measurements) (Figure 5G). Phase changes are minimal during these gain adaptation paradigms (Figure S4D-F), but phase, like gain, can also be adapted. In this respect the ability of the mutants to learn was affected in such a profound way that they were completely unable to adapt their phase during a long-term 5-day phase reversal training paradigm (Figure 5H). In contrast, wild type littermates were able to reverse their phase towards 180 degrees in five consecutive training sessions (5th day, comparison among L7-PP2B mutants and wild type mice; $p < 0.000001$, ANOVA for repeated measurements). Thus, the Purkinje cell-specific PP2B knockout mice

Figure 5 (on the next page): VOR adaptation is affected in L7-PP2B mice. A, Schematic drawing of the vestibulo-cerebellar system. Purkinje cells (black) in the flocculus of the vestibulo-cerebellum converge upon neurons in the vestibular nuclei (VN), through which they can influence the output of the oculomotor neurons (OM) that drive the eye movements. The Purkinje cells are innervated by two main inputs: they receive vestibular and eye movement signals through the mossy fiber - parallel fiber system (represented by green and grey inputs), and retinal slip signals through climbing fibers derived from the inferior olive (IO; blue). The parallel fibers, which all originate from the granule cells, innervate the dendritic trees of the Purkinje cells. VG, AOS and PA indicate vestibular ganglion cells, accessory optic system, and pontine areas, respectively. B, C and D, Motor performance during the optokinetic reflex (OKR), and the vestibulo-ocular reflex in the light (VVOR) and the dark (VOR) revealed moderate aberrations in L7-PP2B mice ($n = 15$) compared to controls ($n = 19$) (for OKR, VOR as well as VVOR $p < 0.001$; ANOVA for repeated measurements). E and F, Motor learning in L7-PP2B mice was severely affected; during two days of mismatch training so as to either decrease (E) or increase (F) their VOR gain the L7-PP2B mice ($n = 9$) learned significantly less than controls ($n = 10$) ($p < 0.0002$ and $p < 0.000001$ for gain-decrease and gain-increase paradigm, respectively; ANOVA for repeated measurements). Note that gain-increase training resulted in a decrease of the gain in the L7-PP2B mice. G, Without mismatch training stimuli as in E or F, no differences were observed ($p = 0.83$ on day 1 and $p = 0.90$ on day 2; ANOVA for repeated measurements). H, When the L7-PP2B mice ($n = 8$) were subjected during four consecutive days (days 2 to 5) to a mismatch training paradigm aimed at reversing the phase of their VOR, they learned significantly less ($p < 0.000001$; ANOVA for repeated measurements) than their controls ($n = 8$). On the day (day 1) preceding this reversal protocol the animals were subjected to the standard in-phase gain-decrease paradigm. Error bars indicate SEM. See also Figure S3-5.



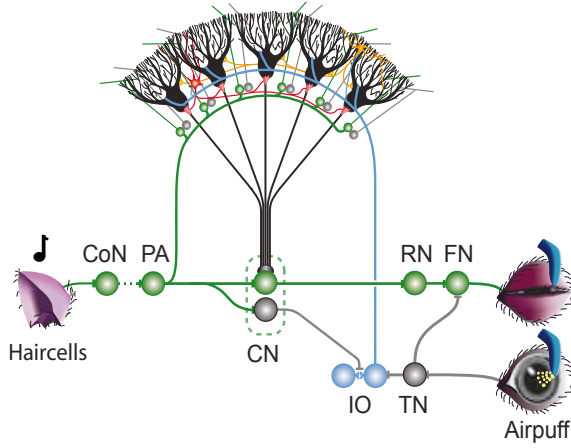
were moderately affected in the performance of their basic compensatory eye movements and markedly affected in all forms of VOR adaptation tested.

L7-PP2B mice show impaired eyeblink conditioning

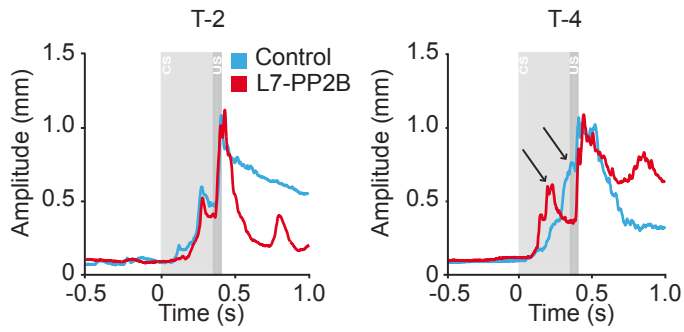
Next, to find out whether the learning deficits in the L7-PP2B mutants are limited to abnormalities in VOR adaptation, which is controlled by the vestibulocerebellum, or whether they reflect a more global deficit in cerebellar motor learning, we also subjected them to a training paradigm that is controlled by a different region of the cerebellum: classical conditioning of eyeblink responses, which in mice is controlled by lobulus simplex in the hemisphere and lobule VI in the vermis (Van Der Giessen et al., 2008) (for underlying circuitry see Figure 6A). The eyeblink responses of the mice were conditioned using a tone and an air-puff as the conditioned stimulus (CS) and unconditioned stimulus (US), respectively (Koekkoek et al., 2003). After 4 paired training sessions (T-1 to T-4), the L7-PP2B mutants showed significantly less conditioned responses than their wild type littermates (comparison between L7-PP2B mice and wild type littermates at T4: $p < 0.05$, t-test), while this difference was absent during the first training session (at T1: $p = 0.82$, t-test) (Figures 6B and C). In fact, the L7-PP2B mutant mice did not show any significant change in percentage of conditioned eyeblink responses over consecutive days of training (e.g. T4 versus T1, $p = 0.52$; one way within subjects ANOVA). The timing of the conditioned responses in the mutants was also affected in that the average peak latency of their CS-alone responses at T4 was significantly shorter ($p < 0.02$; t-test) than that of controls (Figure 6C; for peaks in paired trials, see also

Figure 6 (on the next page): Eyeblink conditioning is impaired in L7-PP2B mutants. A, Neuro-anatomical circuitry involved in eyeblink conditioning. Purkinje cells in the cerebellar cortex form a central site where signal convergence of the unconditioned stimulus (US) and conditioned stimulus (CS) takes place. The US consists of a mild corneal air puff and the CS of an auditory tone. US signals reach the Purkinje cells via the inferior olive (IO) by climbing fibers, while mossy fiber projections from the pontine area (PA) relay the CS. Repeated paired presentation of the CS and US results in conditioned responses (CR), during which the eyelid closes in response to the tone. B, Representative traces of paired CS-US trials from an L7-PP2B knockout (red) and a littermate control (blue) during training sessions T2 and T4. CS onset occurs at time 0, while US follows 325 ms later. Note that the L7-PP2B knockout is not able to improve the timing of the CR (left arrow), whereas the control demonstrates a well-timed CR at T4 (right arrow). C, The percentage of CRs in L7-PP2B knockout mice ($n = 9$) does not significantly increase over the four training sessions ($p = 0.52$; t-test). Instead, the control littermates ($n = 9$) demonstrate a clear learning curve ($p < 0.01$; t-test) and at T4 they show significantly more CRs than L7-PP2B knockouts ($p < 0.05$). In addition, the quality of the CR does not improve in L7-PP2B knockout mice. Where controls demonstrate well timed CRs during training session 4 (e.g. T4 versus T2, $p < 0.001$; t-test), L7-PP2B knockout mice do not improve their timing (e.g. at T4 L7-PP2B versus controls, $p < 0.02$; t-test). D, Kinetics of the eyelid responses are not affected in L7-PP2B knockout mice. Onset, peak amplitude and velocity of the eyelid response to the air puff in the mutants do not differ from those of controls ($p > 0.4$ in all comparisons; t-test) indicating that kinetics of the eyelid are the same for both groups. Abbreviations: CN Cerebellar Nuclei; CoN Cochlear Nucleus; FN Facial Nucleus; RN Red nucleus; TN Trigeminal Nucleus. All error bars indicate SEM.

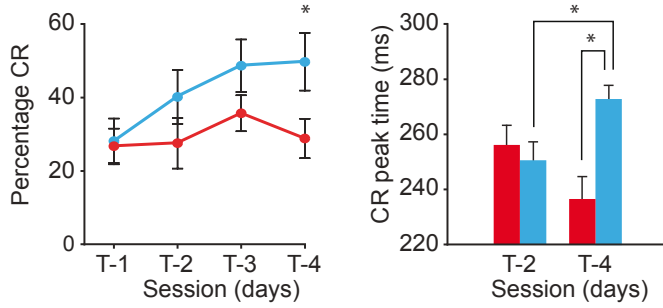
A



B



C



D

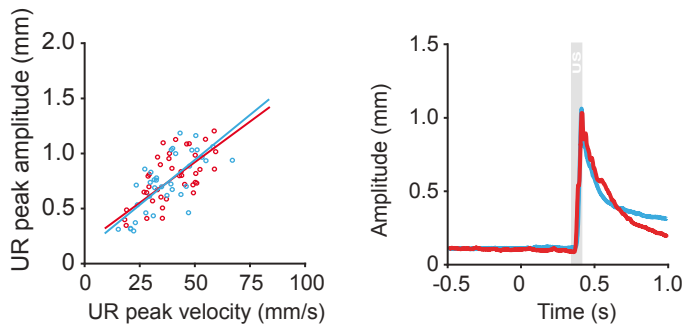


Figure 6B). In contrast, the kinetics of the unconditioned eyeblink responses in the L7-PP2B mutants were indistinguishable ($p > 0.4$ for onset, peak amplitude as well as velocity of UR; t-test) from those in controls (Figure 6D). Thus, our eyeblink tests showed that the L7-PP2B mice have a specific impairment in their conditioned responses rather than a general deficit in the motor component of all their eyeblink responses. Together with the VOR gain adaptation tests, we conclude that the L7-PP2B mutants have severe deficits in hallmark features of cerebellar learning functions: The fine-tuning of sensorimotor gains and the fast adaptation of motor output in response to changing behavioral needs.

DISCUSSION

The current study is the first to specifically address the role of potentiation of Purkinje cell activities in cerebellar motor learning. Guided by the original ideas of Albus (1971), and Ito (2001), virtually all previous studies that were aimed at identifying the molecular and cellular mechanisms underlying cerebellar motor learning focused on depression (for review see De Zeeuw and Yeo, 2005; Ito, 2001). These studies provided supportive evidence that kinases such as PKC (De Zeeuw et al., 1998), cGKI (Feil et al., 2003), CaMKIV (Boyden et al., 2006) and α/β CaMKII (Hansel et al., 2006; van Woerden et al., 2009) are essential for both LTD at the parallel fiber to Purkinje cell synapse and motor learning. The idea has been put forward that gain-increase adaptations of the VOR may be mediated predominantly by LTD, while gain-decrease adaptations may result from potentiation of Purkinje cells (Boyden and Raymond, 2003). Likewise, it has been suggested that LTD is required for the acquisition of well-timed conditioned responses (De Zeeuw and Yeo, 2005; Koekkoek et al., 2003; cf Welsh et al., 2005), raising the possibility that the extinction is mediated by potentiation of Purkinje cells. This latter option is supported by the finding that the extinction process requires activation of the GABAergic input to the inferior olive (Medina et al., 2002), which in principle could reduce climbing fiber activities and thereby shift the balance at the Purkinje cell level from depression to potentiation (Coemans et al., 2004). Based on these hypotheses, one might have expected that L7-PP2B mice are specifically impaired in learning VOR gain decreases and in extinction of conditioned eyeblink responses. Instead, we observed, next to deficits in gain decreases, profound deficits in VOR gain increases and a virtual absence of phase reversal learning, while the acquisition of conditioned eyeblink responses and their timing were also affected. In fact, the *acquisition* of the conditioning process was such prominently affected that there was no difference in the number of CRs between the last and the first training session making it impossible to estimate a potential contribution of Purkinje cell potentiation to *extinction*. By comparison the behavioral deficits of the potentiation-deficient L7-PP2B mice exceed those of the depression-deficient kinase mutants both during VOR adaptation and eyeblink conditioning (De Zeeuw et al., 1998; Feil et al., 2003; Hansel et al., 2006; Koekkoek et al., 2003). Moreover, a possible functional role for LTP at the parallel fiber to Purkinje cell synapse in our daily motor behavior is further supported by the finding that natural cycles

may influence this form of plasticity just like VOR adaptation itself (Andreescu et al., 2007). Thus, Purkinje cell potentiation may not only have been neglected over the past decades, it may even be one of the most dominant players in cerebellar learning.

The approach of the current study has the advantage of simultaneously tackling the two major forms of Purkinje cell potentiation, i.e. PF-PC LTP and PC intrinsic plasticity, in a single animal model and rendering prominent behavioral phenotypes. At the same time, it is not possible to determine to what extent both types of plasticity interact, and which of the two impaired types of potentiation in the L7-PP2B mice is more relevant for which parts of their behavioral phenotypes. Since both types can be induced at physiologically relevant temperatures in wild types, we expect both to contribute, but future studies will have to segregate the two.

Although the kinetics of the unconditioned eyeblink responses in the L7-PP2B mutants were unaffected and therefore unlikely to have contributed to their reduced level of conditioning, we cannot exclude the possibility that the moderate deficits in eye movement performance did contribute to the deficits in VOR adaptation. However, we recently investigated other Purkinje cell specific mutants with comparable performance deficits, and these mutants had no gain learning deficits (Wulff et al., 2009). Thus, a performance deficit does not necessarily induce a deficit in gain increase and/or gain decrease learning per se.

The robust behavioral phenotypes in our calcineurin-deficient mutants are in line with a recent adaptive-filter model of Porrill and Dean (2008). This model is based on the covariance learning rule, implicating a preponderance of silent PF synapse, which has been experimentally observed (Chadderton et al., 2004; Isope and Barbour, 2002). Consequently, their model suggests that LTP is likely to initiate new motor learning, whereas LTD depresses synapses active in the pre-learning situation, a process controlled by the climbing fiber (Dean and Porrill, 2008). This way, the cerebellum optimizes the weight of each relevant PF to Purkinje cell synapse given their relative amount of signal and noise. Thus, PP2B-mediated LTP might set the appropriate weights at the PF to Purkinje cell synapses and together with related levels of intrinsic plasticity generate the appropriate spatiotemporal patterns of simple spike activities that are required for cerebellar motor learning. Such an operating scenario could be supported by various other pre- and postsynaptic forms of potentiation at the GABAergic molecular layer interneuron to Purkinje cell synapse (Dean and Porrill, 2008; Jorntell and Ekerot, 2002) allowing temporal pattern formation without affecting the average firing frequency (Wulff et al., 2009). By combining optimally learned levels of potentiated excitation and feed-forward inhibition Purkinje cells are probably equipped with a push-pull mechanism so as to convey and consolidate appropriately formed patterns of spikes and/or pauses that may be read out in the cerebellar nuclei provided that they occur coherently in ensembles of cells (De Zeeuw et al., 2008; Gauck and Jaeger, 2000; Telgkamp and Raman, 2002; Wulff et al., 2009). We therefore suggest that potentiation in Purkinje cells complements other forms of cerebellar plasticity in controlling synaptic input strengths and excitability in a dynamic manner, and that the cerebellum uses these plasticity mechanisms to shape the spike activity patterns of the inhibitory Purkinje cell output required for motor learning.

EXPERIMENTAL PROCEDURES

Generation of L7-PP2B mice. Mutant mice in which calcineurin was selectively deleted from Purkinje cells (L7-PP2B mutant) were obtained using the Cre-loxP-system, with loxP sites flanking the regulatory subunit (CNB1) of calcium / calmodulin-activated protein phosphatase 2B (referred to as PP2B-loxP) (Zeng et al., 2001). Mice heterozygous for PP2B-loxP were crossed with mice heterozygous for both PP2B-loxP and the L7-Cre transgene (Barski et al., 2000). Mice of the following genotypes (PP2B-loxP / L7-Cre) were used for the experiments: homozygous / + (referred to as L7-PP2B) and homozygous / -, wild type / + and wild type / - (littermate controls). All preparations described below were done with approval of the European Communities Council Directive (86/609/EEC).

Immunohistochemistry and electron microscopy. Immunocytochemistry of L7-PP2B was performed on free-floating 40 μm thick frozen sections from 3-5 month's old mice, employing a standard avidin-biotin-immunoperoxidase complex method (ABC, Vector Laboratories, USA) with PP2B as the primary antibody and diaminobenzidine (0.05%) as the chromogen (Hansel et al., 2006). For electron microscopy, sections were stained for calbindin immunocytochemistry with rabbit anti-calbindin antibody (Swant), osmicated, embedded in Durcupan, and processed for electron microscopy (De Zeeuw et al., 1998). Electron micrographs and other photographs were stored and analyzed using Adobe PhotoShop (San Jose, CA). Surface areas and thickness of layers for light microscopic data were determined using NeuroLucida software (MicroBrightfield). For electron microscopy 16 micrographs were taken randomly in each mouse from the molecular layer at a magnification of 19,000 and the density of parallel fiber to Purkinje cell synapses and the morphology of the PSDs was determined using MetaVue 4.6 (Metavue Corporation).

In vitro electrophysiology. Sagittal slices of the cerebellar vermis of 10 to 24 wk old mice (adult) or p16 – p21 mice (young) were kept in ACSF containing (in mM): 124 NaCl, 5 KCl, 1.25 Na_2HPO_4 , 2 MgSO_4 , 2 CaCl_2 , 26 NaHCO_3 , 20 D-Glucose and bicuculline methiodide, bubbled with 95% O_2 and 5% CO_2 (all drugs are purchased from Sigma-Aldrich, unless stated otherwise). Whole-cell patch-clamp recordings were performed at room temperature or physiological temperatures (as indicated in the text) using an EPC-10 amplifier (HEKA Electronics, Germany). The patch pipettes were filled with intracellular solution containing (in mM): 120 K-Gluconate, 9 KCl, 10 KOH, 3.48 MgCl_2 , 4 NaCl, 10 HEPES, 4 Na_2ATP , 0.4 Na_3GTP and 17.5 sucrose (pH 7.25). Test responses were evoked at a frequency of 0.05 Hz with the use of patch pipettes filled with ACSF at 1-4 μA for 500 μs (LTP) or 700 μs (LTD). Holding potentials in the range of -60 to -75 mV were chosen to prevent spontaneous spike activity, and cells were switched to current-clamp mode for tetanization. PF-LTD was induced by paired PF and CF stimulation at 1 Hz for 5 min in current-clamp mode, while PF-LTP was induced by PF stimulation alone at 1 Hz for 5 min unless indicated otherwise (Belmeguenai and Hansel, 2005). For the experiments on intrinsic excitability and plasticity recordings were performed in current-clamp mode, again using an EPC-10 amplifier (HEKA Electronics). Intrinsic excitability was monitored during the test periods

by injection of brief (550 ms) depolarizing current pulses (100-200 pA) adjusted to evoke 5-15 spikes. Intrinsic plasticity was induced by tetanization of the Purkinje cell with 150-300 pA current pulses at 5 Hz for 3 s. The spike count was taken as a measure of excitability. Input resistance (R_i) was measured by injection of hyperpolarizing test currents (200 pA; 100 ms) and was calculated from the voltage transient towards the end of current injection. Recordings were excluded if the series or input resistance varied by >15%. To test whether CF elimination was delayed in L7-PP2B mice, we recorded CF-EPSCs in voltage-clamp mode in 10 to 24 wk old animals, while increasing the stimulus intensity and counting the number of all-or-none steps in the EPSC amplitude. The paired-pulse ratios at CF and PF synapses, respectively, were examined in voltage-clamp mode, by applying stimulus pairs at varying intervals. The paired-pulse ratio was calculated as the ratio of EPSC 2 / EPSC 1. Inhibitory transmission was examined by recording spontaneous IPSCs using an internal solution (pH 7.3) containing (in mM): 150 CsCl, 15 CsOH, 1.5 MgCl₂, 0.5 EGTA, 10 HEPES, 4 Na₂ATP and 0.4 Na₃GTP. Purkinje cells were voltage clamped at -70 mV at 34 ± 1 °C in the presence of 10 μM NBQX (Tocris Cookson, Bristol, UK).

Calcium imaging. Patch-clamp recordings were made from Purkinje cells as described above with a calcium indicator dye added to the solution (Oregon Green BAPTA-2, 200μM). After patch formation the calcium dye was allowed to passively diffuse into the distal dendrites for a minimal of 30 min. Once the entire dendritic tree was visible, the stimulus electrode was positioned at a remote dendritic site to avoid congruent climbing fiber activation. To standardize recordings between both groups, PFs were stimulated to elicit EPSCs of approximately 300pA. Fluorescence recordings were performed using a NeuroCCD-SMQ camera (80x80 pixels) and NeuroPlex software (both RedShirtImaging, Decatur, GA) for data acquisition. The fluorophore was excited using a 100W Xenon arc lamp (Cairn Research Ltd, Faversham, UK). During the tetanus-protocol (PF-stimulation for 5 minutes at 1Hz) the elicited calcium-signals were monitored every 20 seconds. Data was acquired at 2kHz for sweep durations of 500ms. Fluorescence changes were normalized to resting levels and expressed as the ratio $(t) = \frac{F(t)}{F}$, where $F(t)$ is the fluorescence value at time t , and F is the averaged fluorescence obtained during the baseline period preceding the stimulus application. To correct for dye-bleaching, an exponential curve was fitted to the recording and subtracted. After acquisition, recordings were filtered using a Gaussian low-pass filter with a cut-off at 150Hz. The region of interest was set such that it gave the maximal response.

Eye movement recordings. Mice, aged 10-26 wks, were equipped with a pedestal under anaesthesia and investigated as described before (Hoebeek et al., 2005). In short, after recovery the mice were placed in a restrainer and fixed onto the centre of a turntable, which was surrounded by a visual screen. The (V)VOR and OKR were evoked by rotating the turntable and/or surrounding screen, respectively, with an amplitude of 5° at different frequencies. Gain and phase learning capabilities were studied by applying protocols for two consecutive days that were aimed either at reducing the gain of the VOR by subjecting the mice to 5 x 10 min periods of sinusoidal *in phase* drum and table rotation at 0.6 Hz (both with an amplitude of 5°) or at increasing the gain by subjecting them to *out of phase* drum

and table stimulation at 1.0 Hz (both with an amplitude of 1.6°). Phase reversal was tested by applying an *in phase* stimulation on day 1 and subsequently reversing the phase on days 2, 3, 4 and 5 by subjecting the animals to 5 x 10 min periods of sinusoidal *in phase* drum and table rotation at 0.6 Hz, but with drum amplitudes of 7.5° (days 2) and 10° (days 3, 4 and 5), while the amplitude of the turntable remained 5°. The animals were kept in the dark in between all recording days. A CCD camera was fixed to the turntable in order to monitor the eyes of the mice. The eye movements were recorded at 240 Hz using an eye-tracking device (ISCAN Inc.). Video calibrations and subsequent eye movement computations were performed as described previously (Hoebeek et al., 2005).

Eyeblink conditioning. Mice, aged 11-30 wks, were anesthetized, surgically prepared and investigated with the use of MDMT as described before (Koekkoek et al., 2003). A magnet was glued to the lower eyelid and a GMR sensor chip was placed over the upper eyelid such that the axis of sensitivity was aligned with the north-south axis of the magnet. The eyelid responses of the wild type mice and L7-PP2B mutants were conditioned to a tone as the CS (10 kHz, gradually increased over 25 ms to 73 dB) during daily training sessions of 8 blocks of 8 trials. The blocks consisted of 1 US-alone trial, 6 paired trials, and 1 CS-alone trial, and the trials were separated by a random intertrial interval in the range of 20 to 40 s. In paired group the onsets of the CS and US were separated by an inter-stimulus interval of 350 ms.

Data Analyses. Off-line analyses of eye movements and eyeblink responses were performed in Matlab (MathWorks, Natick, MA) as described before (Hoebeek et al., 2005; Koekkoek et al., 2003). Statistical tests were performed with SPSS 13 (SPSS Inc., Chicago, IL). Data were compared using a two-tailed unpaired Student's *t*-test, Mann-Whitney U-test or two-way repeated-measures ANOVA, as appropriate. The level of significance was set at $p < 0.05$.

ACKNOWLEDGEMENTS

We kindly thank J. van der Burg, E. Haasdijk, E. Galliano, R. de Avila Freire, E. Goedknecht and M. Rutteman for their excellent technical assistance; we kindly thank S. Tonegawa for providing the floxed calcineurin mice; and we kindly thank the Dutch Organization for Medical Sciences (ZonMw; YE, CIDZ), Life Sciences (ALW; ABe, FEH, CH, CIDZ), Senter (Neuro-Bsik; YE, CIDZ), Erasmus University Fellowship (MS), NIH (#NS62771; CH), Prinses Beatrix Fonds (CIDZ), and the SENSOPAC, CEREBNET and C7 programs of the European Community (CIDZ) for their financial support.

REFERENCE LIST

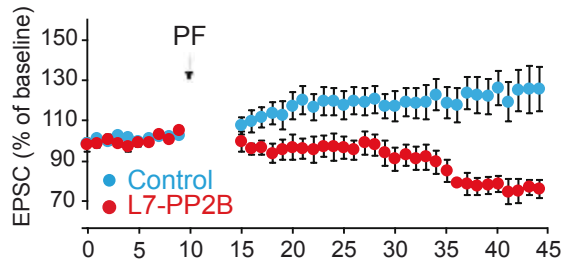
1. Aiba, A., Kano, M., Chen, C., Stanton, M.E., Fox, G.D., Herrup, K., Zwingman, T.A., and Tonegawa, S. (1994). Deficient cerebellar long-term depression and impaired motor learning in mGluR1 mutant mice. *Cell* 79, 377-388.
2. Albus, J.S. (1971). A theory of cerebellar function. *Math. Biosci.* 10, 25-61.
3. Andreescu, C.E., Milojkovic, B.A., Haasdijk, E.D., Kramer, P., De Jong, F.H., Krust, A., De Zeeuw, C.I., and De Jeu, M.T. (2007). Estradiol improves cerebellar memory formation by activating estrogen receptor beta. *J Neurosci* 27, 10832-10839.
4. Armano, S., Rossi, P., Taglietti, V., and D'Angelo, E. (2000). Long-term potentiation of intrinsic excitability at the mossy fiber-granule cell synapse of rat cerebellum. *J Neurosci* 20, 5208-5216.
5. Barski, J.J., Dethleffsen, K., and Meyer, M. (2000). Cre recombinase expression in cerebellar Purkinje cells. *Genesis* 28, 93-98.
6. Belmeguenai, A., and Hansel, C. (2005). A role for protein phosphatases 1, 2A, and 2B in cerebellar long-term potentiation. *J Neurosci* 25, 10768-10772.
7. Boyden, E.S., Katoh, A., Pyle, J.L., Chatila, T.A., Tsien, R.W., and Raymond, J.L. (2006). Selective engagement of plasticity mechanisms for motor memory storage. *Neuron* 51, 823-834.
8. Boyden, E.S., and Raymond, J.L. (2003). Active reversal of motor memories reveals rules governing memory encoding. *Neuron* 39, 1031-1042.
9. Chadderton, P., Margrie, T.W., and Hausser, M. (2004). Integration of quanta in cerebellar granule cells during sensory processing. *Nature* 428, 856-860.
10. Coesmans, M., Weber, J.T., De Zeeuw, C.I., and Hansel, C. (2004). Bidirectional parallel fiber plasticity in the cerebellum under climbing fiber control. *Neuron* 44, 691-700.
11. De Zeeuw, C.I., Hansel, C., Bian, F., Koekkoek, S.K., van Alphen, A.M., Linden, D.J., and Oberdick, J. (1998). Expression of a protein kinase C inhibitor in Purkinje cells blocks cerebellar LTD and adaptation of the vestibulo-ocular reflex. *Neuron* 20, 495-508.
12. De Zeeuw, C.I., Hoebeek, F.E., and Schonewille, M. (2008). Causes and consequences of oscillations in the cerebellar cortex. *Neuron* 58, 655-658.
13. De Zeeuw, C.I., and Yeo, C.H. (2005). Time and tide in cerebellar memory formation. *Curr Opin Neurobiol* 15, 667-674.
14. Dean, P., and Porrill, J. (2008). Adaptive-filter Models of the Cerebellum: Computational Analysis. *Cerebellum* 7, 567-571.
15. Eto, M., Bock, R., Brautigam, D.L., and Linden, D.J. (2002). Cerebellar long-term synaptic depression requires PKC-mediated activation of CPI-17, a myosin/moesin phosphatase inhibitor. *Neuron* 36, 1145-1158.
16. Feil, R., Hartmann, J., Luo, C., Wolfsgruber, W., Schilling, K., Feil, S., Barski, J.J., Meyer, M., Konnerth, A., De Zeeuw, C.I., and Hofmann, F. (2003). Impairment of LTD and cerebellar learning by Purkinje cell-specific ablation of cGMP-dependent protein kinase I. *J Cell Biol* 163, 295-302.
17. Gauck, V., and Jaeger, D. (2000). The control of rate and timing of spikes in the deep cerebellar nuclei by inhibition. *J Neurosci* 20, 3006-3016.
18. Hansel, C., de Jeu, M., Belmeguenai, A., Houtman, S.H., Buitendijk, G.H., Andreev, D., De Zeeuw, C.I., and Elgersma, Y. (2006). alphaCaMKII Is essential for cerebellar LTD and motor learning. *Neuron* 51, 835-843.
19. Hoebeek, F.E., Stahl, J.S., van Alphen, A.M., Schonewille, M., Luo, C., Rutteman, M., van den Maagdenberg, A.M., Molenaar, P.C., Goossens, H.H., Frens, M.A., and De Zeeuw, C.I. (2005). Increased noise level of purkinje cell activities minimizes impact of their modulation during sensorimotor control. *Neuron* 45, 953-965.
20. Isope, P., and Barbour, B. (2002). Properties of unitary granule cell->Purkinje cell synapses in adult rat cerebellar slices. *J Neurosci* 22, 9668-9678.
21. Ito, M. (2001). Cerebellar long-term depression: characterization, signal transduction, and functional roles. *Physiol Rev* 81, 1143-1195.
22. Jorntell, H., and Ekerot, C.F. (2002). Reciprocal bidirectional plasticity of parallel fiber receptive fields in cerebellar Purkinje cells and their afferent interneurons. *Neuron* 34, 797-806.
23. Koekkoek, S.K., Hulscher, H.C., Dortland, B.R., Hensbroek, R.A., Elgersma, Y., Ruigrok, T.J., and De Zeeuw, C.I. (2003). Cerebellar LTD and learning-dependent timing of conditioned eyelid responses. *Science* 301, 1736-1739.

- IV
24. Launey, T., Endo, S., Sakai, R., Harano, J., and Ito, M. (2004). Protein phosphatase 2A inhibition induces cerebellar long-term depression and declustering of synaptic AMPA receptor. *Proc Natl Acad Sci U S A* *101*, 676-681.
 25. Leitges, M., Kovac, J., Plomann, M., and Linden, D.J. (2004). A unique PDZ ligand in PKC α confers induction of cerebellar long-term synaptic depression. *Neuron* *44*, 585-594.
 26. Lev-Ram, V., Wong, S.T., Storm, D.R., and Tsien, R.Y. (2002). A new form of cerebellar long-term potentiation is postsynaptic and depends on nitric oxide but not cAMP. *Proc Natl Acad Sci U S A* *99*, 8389-8393.
 27. Lisman, J.E., and Zhabotinsky, A.M. (2001). A model of synaptic memory: a CaMKII/PP1 switch that potentiates transmission by organizing an AMPA receptor anchoring assembly. *Neuron* *31*, 191-201.
 28. Lu, Y.M., Mansuy, I.M., Kandel, E.R., and Roder, J. (2000). Calcineurin-mediated LTD of GABAergic inhibition underlies the increased excitability of CA1 neurons associated with LTP. *Neuron* *26*, 197-205.
 29. Malleret, G., Haditsch, U., Genoux, D., Jones, M.W., Bliss, T.V., Vanhooose, A.M., Weitlauf, C., Kandel, E.R., Winder, D.G., and Mansuy, I.M. (2001). Inducible and reversible enhancement of learning, memory, and long-term potentiation by genetic inhibition of calcineurin. *Cell* *104*, 675-686.
 30. Medina, J.F., Nores, W.L., and Mauk, M.D. (2002). Inhibition of climbing fibres is a signal for the extinction of conditioned eyelid responses. *Nature* *416*, 330-333.
 31. Misonou, H., Mohapatra, D.P., Park, E.W., Leung, V., Zhen, D., Misonou, K., Anderson, A.E., and Trimmer, J.S. (2004). Regulation of ion channel localization and phosphorylation by neuronal activity. *Nat Neurosci* *7*, 711-718.
 32. Mulkey, R.M., Herron, C.E., and Malenka, R.C. (1993). An essential role for protein phosphatases in hippocampal long-term depression. *Science* *261*, 1051-1055.
 33. Porrill, J., and Dean, P. (2008). Silent synapses, LTP, and the indirect parallel-fibre pathway: computational consequences of optimal cerebellar noise-processing. *PLoS Comput Biol* *4*, e1000085.
 34. Steuber, V., Mittmann, W., Hoebeek, F.E., Silver, R.A., De Zeeuw, C.I., Hausser, M., and De Schutter, E. (2007). Cerebellar LTD and pattern recognition by Purkinje cells. *Neuron* *54*, 121-136.
 35. Telgkamp, P., and Raman, I.M. (2002). Depression of inhibitory synaptic transmission between Purkinje cells and neurons of the cerebellar nuclei. *J Neurosci* *22*, 8447-8457.
 36. Van Der Giessen, R.S., Koekkoek, S.K., van Dorp, S., De Gruijl, J.R., Cupido, A., Khosrovani, S., Dortland, B., Wellershaus, K., Degen, J., Deuchars, J., *et al.* (2008). Role of olivary electrical coupling in cerebellar motor learning. *Neuron* *58*, 599-612.
 37. van Woerden, G.M., Hoebeek, F.E., Gao, Z., Nagaraja, R.Y., Hoogenraad, C.C., Kushner, S.A., Hansel, C., De Zeeuw, C.I., and Elgersma, Y. (2009). betaCaMKII controls the direction of plasticity at parallel fiber-Purkinje cell synapses. *Nat Neurosci* *12*, 823-825.
 38. Welsh, J.P., Yamaguchi, H., Zeng, X.H., Kojo, M., Nakada, Y., Takagi, A., Sugimori, M., and Llinas, R.R. (2005). Normal motor learning during pharmacological prevention of Purkinje cell long-term depression. *Proc Natl Acad Sci U S A* *102*, 17166-17171.
 39. Wulff, P., Schonewille, M., Renzi, M., Viltono, L., Sassoe-Pognetto, M., Badura, A., Gao, Z., Hoebeek, F.E., van Dorp, S., Wisden, W., *et al.* (2009). Synaptic inhibition of Purkinje cells mediates consolidation of vestibulo-cerebellar motor learning. *Nat Neurosci* *12*, 1042-1049.
 40. Zeng, H., Chattarji, S., Barbarosie, M., Rondi-Reig, L., Philpot, B.D., Miyakawa, T., Bear, M.F., and Tonegawa, S. (2001). Forebrain-specific calcineurin knockout selectively impairs bidirectional synaptic plasticity and working/episodic-like memory. *Cell* *107*, 617-629.

SUPPLEMENTARY MATERIALS

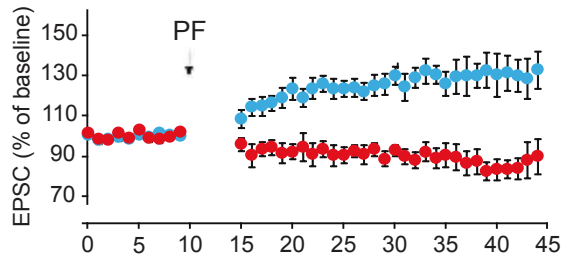
A

LTP
 PF at 1Hz for 5 min
 Adult mice
 $34 \pm 1^\circ \text{C}$



B

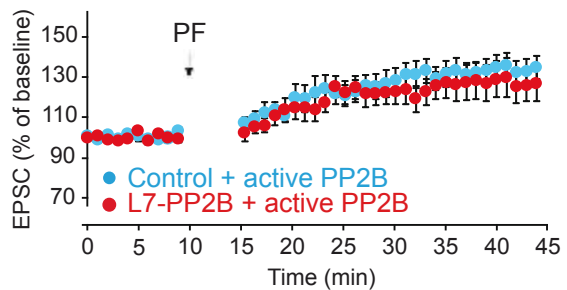
LTP
 PF at 1Hz for 5 min
 Young mice
 $34 \pm 1^\circ \text{C}$



C

LTP
 PF at 1Hz for 5 min
 Adult mice
 $34 \pm 1^\circ \text{C}$

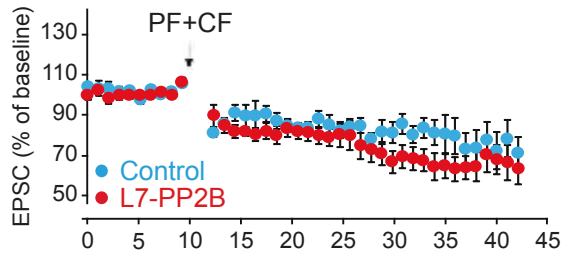
with active PP2B



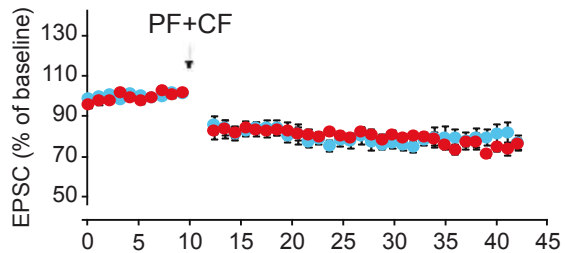
Supplementary Figure 1: Induction of PF-PC LTP under different experimental conditions, related to Figure 2. A, PF-PC LTP was induced in adult mice at 34°C using parallel fiber stimulation at 1 Hz for 5 min (similar to Figure 2A). We observed an increase in EPSC amplitude in control mice ($n = 13$), but not in the L7-PP2B mice ($n = 10$), and this difference was significant ($p = 0.019$; t -test). B, When we repeated this experiment in young, 3 week old, control ($n = 10$) and L7-PP2B ($n = 7$) mice, this difference was even larger ($p = 0.002$; t -test). C, However, addition of active PP2B in the recording pipette abolished this difference ($p = 0.52$; t -test); both control ($n = 8$) and mutant ($n = 8$) mice showed a clear potentiation. All EPSCs are expressed as percentage of baseline, calculated as the average of the last 5 min before tetanus. Error bars indicate SEM.

A

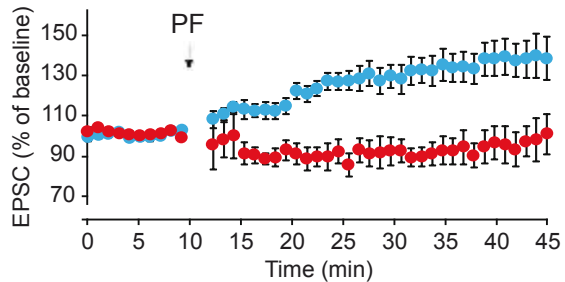
LTD
 5x PF + 1x CF at 0.5 Hz
 for 100 s
 Adult mice
 $34 \pm 1^\circ \text{C}$

**B**

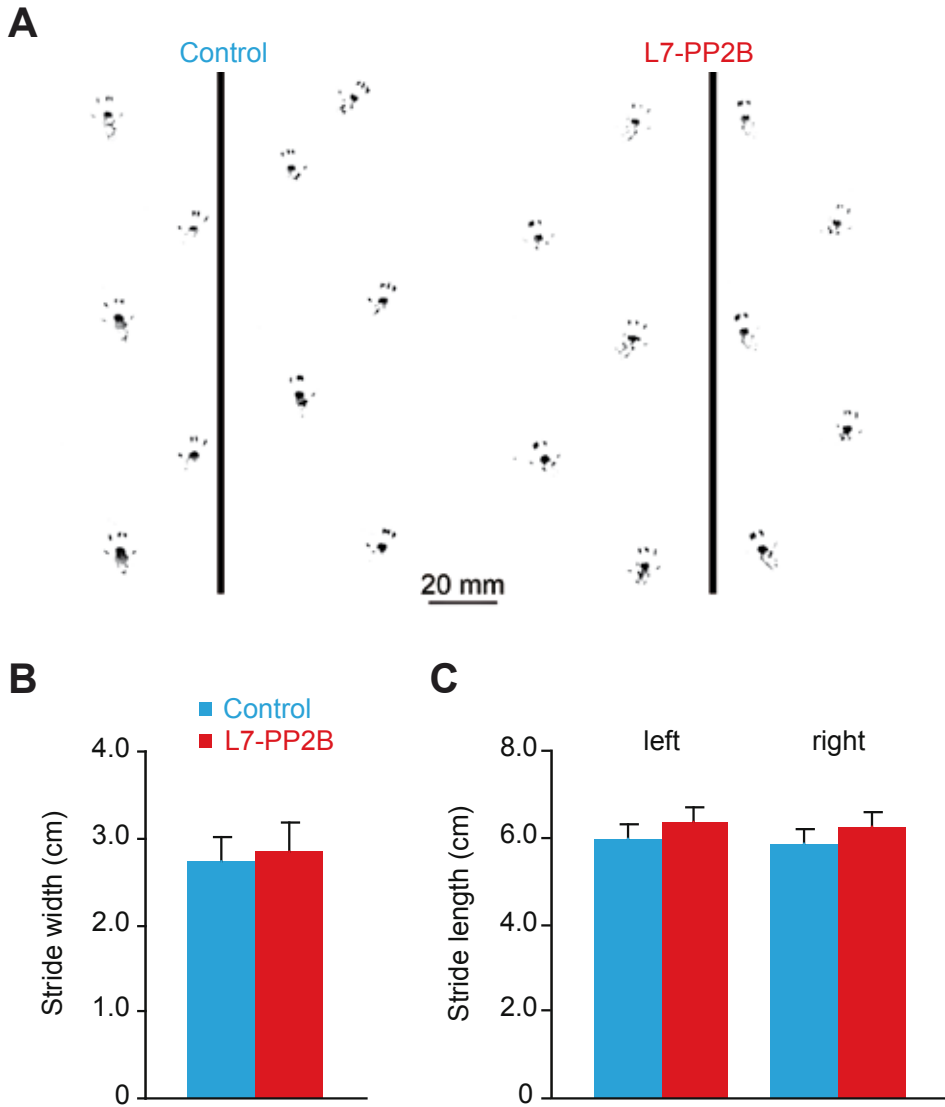
LTD
 PF+CF at 1Hz for 2 min
 Adult mice
 $34 \pm 1^\circ \text{C}$

**C**

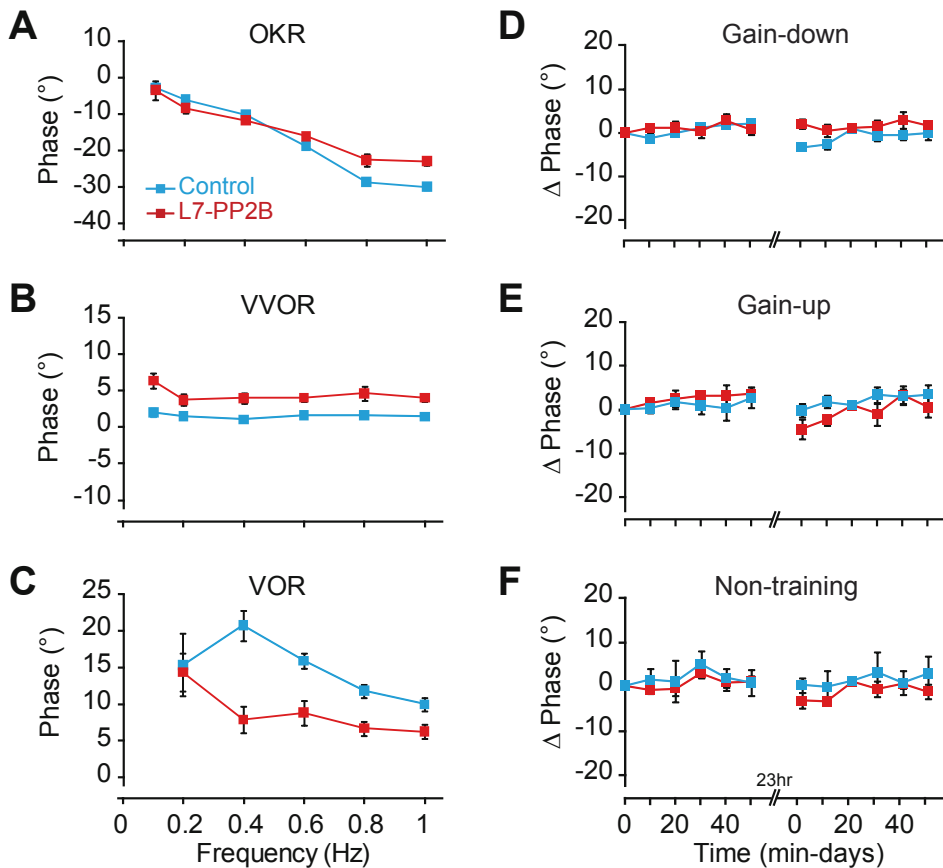
LTP
 PF at 1Hz for 2 min
 Adult mice
 $23 \pm 1^\circ \text{C}$



Supplementary Figure 2: Induction of PF-PC plasticity with different induction protocols, related to Figure 2. To confirm that LTP-selectivity of the mutation was independent from the induction protocol, we tested LTD and LTP using different induction protocols. A, PF-PC LTD was induced in adult mice at 34°C with an alternative induction protocol (see Wang, Denk & Häusser, 2000), consisting of 50 pairings of 5 PF stimuli at 100 Hz followed 150 ms later by a single CF stimulus. This induction protocol resulted in a decrease in EPSC amplitude in L7-PP2B ($n = 7$) mice that was not significantly different ($p = 0.37$; t -test) from that in controls ($n = 8$). B, In addition, we used another LTD induction protocol (Feil et al., 2003) consisting of 120 pairings at 1 Hz of simultaneous PF and CF stimuli. We again found no difference ($p = 0.47$; t -test) between control ($n = 12$) and L7-PP2B mice ($n = 6$). C, In contrast, the latter protocol, but now without the CF stimulus, was able to induce LTP in control mice ($n = 7$), but not in L7-PP2B mice ($n = 9$); this difference was significant ($p = 0.011$; t -test). Error bars indicate SEM.



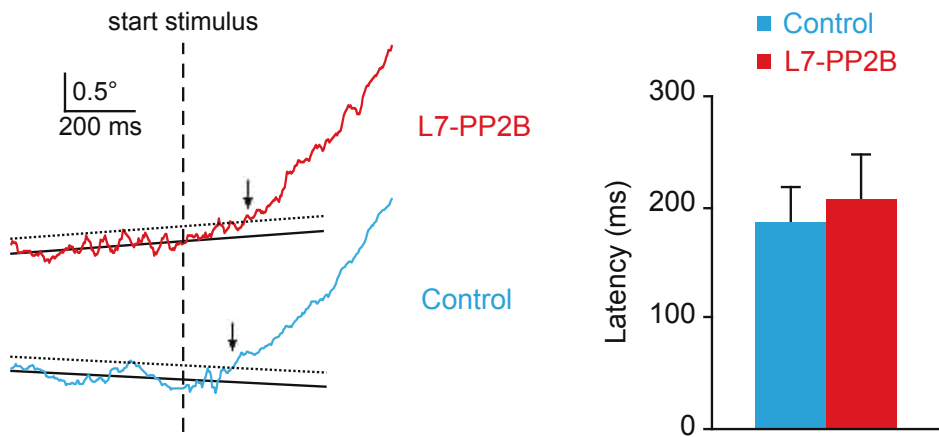
Supplementary Figure 3: L7-PP2B mutant mice are not ataxic, related to Figure 5. A and B, The walking pattern of L7-PP2B mice was evaluated with the use of footprint analysis (A). Evaluation of hind limb walking pattern revealed no significant differences in stride width (B) or length (C) (all $p > 0.15$; t -test). Data are obtained from 4 wild-type and 4 L7-PP2B mice. Error bars indicate SEM.



Supplementary Figure 4: Phase data for compensatory eye movement experiments, related to Figure 5. A-C, The differences in VVOR and VOR gain, as depicted in Figure 5, are accompanied by differences in phase (OKR, $p = 0.010$; VVOR, $p < 0.001$; VOR, $p = 0.008$; ANOVA for repeated measurements). D-F, All (non-)training sessions aimed at changing the gain have only minor effects on the phase. Absolute phase change (Δ phase) was significantly different between control and L7-PP2B mice on the second day of gain-down training ($p = 0.046$; for first day $p = 0.71$; ANOVA for repeated measurements) (D), but not on either day for gain-up training (both $p > 0.24$) (E) or control non-training (both $p > 0.21$) (F). For number of animals used, see legends of Figure 5. Error bars indicate SEM.

Supplementary Table 1. *In vivo* spiking characteristics, related to Figure 4.

	Control (n = 10) mean \pm sem	L7-PP2B (n = 7) mean \pm sem	t-test
Maximum firing frequency (Hz)	199 \pm 14	108 \pm 9	0.000
Peak amplitude (mV)	41 \pm 3	47 \pm 2	0.135
Afterhyperpolarization (mV)	-7.2 \pm 1.0	-10.2 \pm 1.4	0.076
Half width (ms)	0.26 \pm 0.02	0.27 \pm 0.02	0.838
Input resistance (M Ω) (recorded at room temperature)	146 \pm 10	147 \pm 18	0.518



Supplementary Figure 5: Latency data for OKR, related to Figure 5. The latency of the eye movement response to the optokinetic stimulus in the L7-PP2B mutants (n = 7) was not significantly different from that in the wild types (n = 7) ($p = 0.69$; t-test). Traces on the left show samples of individual animals. The moment of onset of the optokinetic response was determined by the crossing of the eye movement trace through the (dotted) line that was 2 SD above the average before the start of the stimulus (dashed line) for at least 10 ms.

**ENHANCED AMPA
RECEPTOR FUNCTION
PROMOTES CEREBELLAR
LONG-TERM DEPRESSION
RATHER THAN
POTENTIATION**

**Boeke J. van Beugen^{1,2}, Xin Qiao¹
& Christian Hansel^{1,2}**

¹Department of Neuroscience, Erasmus University
Medical Center, 3000 DR Rotterdam, The
Netherlands.

²Department of Neurobiology, University of Chicago,
Chicago, Illinois 60637, USA.



ABSTRACT

Ampakines facilitate hippocampal long-term potentiation (LTP) and learning, and have been considered for the treatment of cognitive and memory deficits. Here, we show that the ampakine CX546 raises the amplitude and slows the decay time of excitatory postsynaptic currents (EPSCs) at cerebellar parallel fiber (PF) to Purkinje cell synapses, thus resembling CX546 effects described at hippocampal synapses. Using the fluorescent calcium indicator dye Oregon Green BAPTA-2 and an ultra high-speed CCD camera, we also monitored calcium transients in Purkinje cell dendrites. In the presence of CX546 in the bath, PF-evoked calcium transients were enhanced and prolonged, suggesting that CX546 not only enhances synaptic transmission, but also boosts dendritic calcium signaling at cerebellar synapses. In contrast to previous observations in the hippocampus, however, CX546 applied during cerebellar recordings facilitates long-term depression (LTD) rather than LTP at PF synapses. These findings challenge the view that potentiation generally results from high activity patterns and provide tools for the selective manipulation of synaptic memories.

INTRODUCTION

At glutamatergic synapses onto hippocampal and neocortical pyramidal cells, respectively, coincident pre- and postsynaptic activity elicits long-term potentiation (LTP), which typically requires the activation of N-methyl-D-aspartate (NMDA) receptors (1). Long-term depression (LTD), in contrast, may or may not require NMDA receptor activation, but results from activity patterns that activate the postsynaptic neuron in a less efficient, or less well-timed manner (2, 3). It has been suggested that LTP requires a larger calcium signal amplitude for its induction than LTD (4-6). It seems likely that other calcium signaling parameters are crucial as well (7, 8), but the amplitude of calcium signaling might be the one parameter that most faithfully reflects synaptic input strength during the induction phase. Efforts to develop memory-enhancing drugs have thus focused on the strategy that the magnitude and induction probability of LTP might be enhanced by drugs that boost synaptic transmission and calcium signaling. Ampakines, which are allosteric modulators of AMPA receptors that enhance transmission by slowing both desensitization and deactivation of AMPA receptors (9), have indeed been shown to facilitate LTP induction (10, 11). These observations demonstrate that a selective manipulation of synaptic activation strength can affect the LTP induction probability. Moreover, ampakines positively affect memory encoding and recall in humans (12-14), and reduce effects of sleep deprivation on cognitive performance (15). These data show that enhancing synaptic transmission using drugs that interfere with AMPA receptor function can positively affect synaptic plasticity as well as cognitive performance and learning.

To elucidate the general applicability of this strategy to all types of glutamatergic synapses, we examined the effects of the ampakine CX546 on synaptic plasticity at cerebellar parallel fiber (PF) to Purkinje cell synapses. These synapses provide an exceptional case regarding LTP / LTD induction rules, in that a higher calcium threshold needs to be reached for LTD than for LTP induction (16). Here, we address the question whether enhancing AMPA-mediated synaptic transmission facilitates LTP induction (as in the hippocampus), or promotes LTD (because of the higher calcium threshold).

RESULTS

To examine the effects of CX546 on PF synaptic transmission, we performed whole-cell patch-clamp recordings from Purkinje cells in P18-25 rat cerebellar slices (200-250 μ m). At concentrations of 200 μ M and 300 μ M, respectively, bath-applied CX546 enhanced both the peak amplitude (200 μ M: 162.4 \pm 34.1% of baseline \pm SEM; n=4; p<0.05; 300 μ M: 160.9 \pm 17.1%; n=5; p<0.05; t=30min; Fig. 1A) and the area of PF-EPSCs (200 μ M: 262.4 \pm 53.2%; n=4; p<0.05; 300 μ M: 374.5 \pm 43.8%; n=5; p<0.05; t=30min; Fig. 1A+B). The observed slowed decay time of PF-EPSCs is in line with the note that CX546 acts by destabilizing the desensitized receptor conformation (17). There was no change in the paired-pulse facilitation (PPF) ratio of peak EPSC amplitudes (EPSC 2/1; 200 μ M: 92.8 \pm 6.8%; n=4; p>0.05; 300 μ M: 102.9 \pm 4.2%; n=5; p>0.05; t=30min; Supplementary Figure 1), confirming

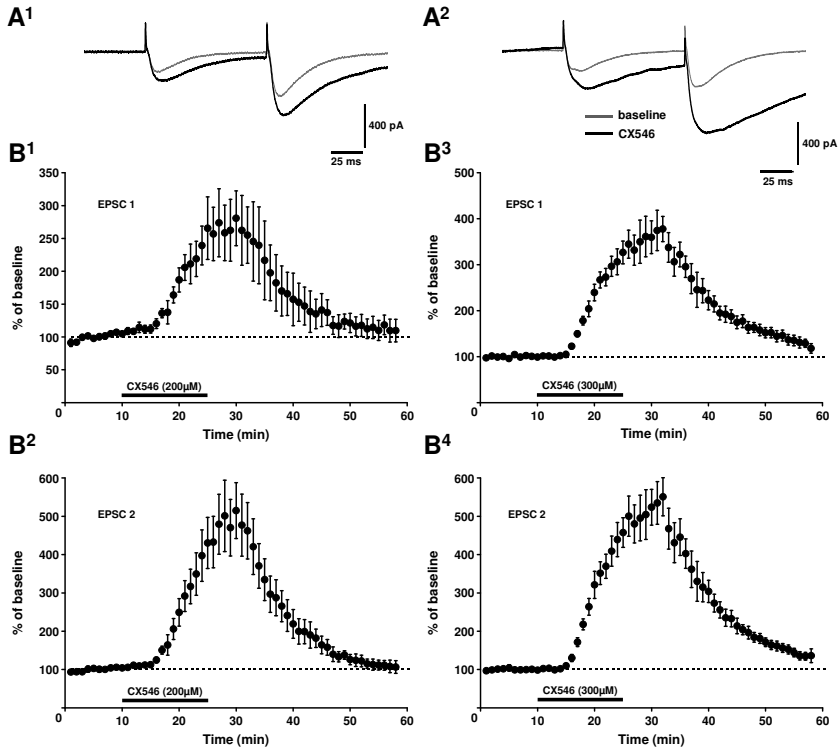


Figure 1: The ampakine CX546 enhances and prolongs PF-EPSCs. (A+B) At concentrations of $200\mu\text{M}$ (left column; $n=4$) and $300\mu\text{M}$ (right column; $n=5$), respectively, CX546 increases the peak amplitude and slows the decay time of PF-EPSCs. (A) Typical traces recorded upon wash-in of $200\mu\text{M}$ CX546 (left) and $300\mu\text{M}$ CX546 (right), respectively. (B) Top: time graph showing changes in the EPSC1 integral when CX546 is bath-applied (bar), bottom: time graph showing the integral of EPSC2. Error bars are mean \pm SEM.

that CX546 acted postsynaptically. These results show that CX546 enhances and prolongs EPSCs at cerebellar PF synapses, thus boosting basic synaptic transmission the same way as previously observed at hippocampal synapses (17, 18).

The ultimate goal of this study was to examine how ampakines affect cerebellar synaptic plasticity, which, like hippocampal synaptic plasticity, is under the control of dendritic calcium signaling (19, 20). To examine whether bath application of CX546 enhances calcium transients in Purkinje cell dendrites, we performed fluorometric calcium imaging experiments using an ultra high-speed CCD camera (NeuroCCD-SMQ; RedShirtImaging, Decatur, GA), and the fluorescent calcium indicator dye Oregon Green BAPTA-2 ($200\mu\text{M}$). PF stimulation evoked dendritic calcium transients that were localized to specific branches (see also 21, 22). This spatial restriction is illustrated in Fig. 2: in this example, PF stimulation that is sufficiently strong to evoke PF-EPSCs of about 300pA (600pA for

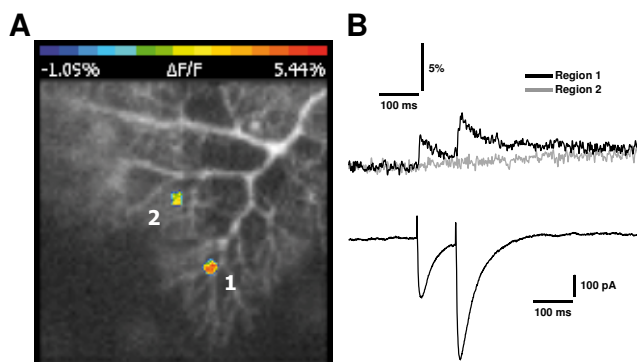


Figure 2: PF stimulation elicits spatially restricted calcium transients. (A) Original image showing two regions of interest (ROI) indicating spatial restriction of calcium transient hotspots (false-color coding). Calcium transients are reported as normalized fluorescence changes ($\Delta F/F$). (B) PF-EPSCs (bottom) and associated calcium transients (top) recorded from regions 1 and 2 as shown in (A). Fluorescence measurements were performed using an ultra high-speed CCD camera (NeuroCCD-SMQ; RedShirtImaging) and the fluorescent calcium indicator Oregon Green BAPTA-2 (200 μ M).

EPSC2) elicits a calcium transient in a small region of interest (ROI) located on a dendritic branch (region 1; Fig. 2), but not in a ROI on a neighboring branch (region 2; Fig. 2). In the following recordings, we routinely monitored calcium signals from those ROI's that showed the most pronounced calcium transients.

To assess the effect of CX546 bath-application on PF-evoked calcium signaling, we monitored calcium transients during a 5min baseline period, washed-in CX546 (200 μ M) for 5min, and recorded calcium signals in the presence of CX546 for at least five more minutes. During the wash-in period, data acquisition was discontinued to limit the amount of light exposure and phototoxicity, and thus to allow for long-term recordings of calcium transients under stable baseline fluorescence conditions (23, 24). In the presence of CX546, the calcium transients were enhanced ($203.5 \pm 37.9\%$; $n=5$, $t=13-15$ min; $p<0.01$; Fig. 3; Supplementary Fig. 2C). These calculations are based on the area under the curve (100ms time window) of the calcium transient evoked by the second stimulus to take advantage of the more pronounced and more stable calcium signals. There was no change in the paired-pulse ratio of the calcium transients (peak of calcium transient 2/1; $117.8 \pm 10.7\%$; $n=5$; $t=13-15$ min; $p>0.05$). In the absence of CX546, the calcium transients remained stable ($99.6 \pm 12.0\%$; $n=6$; $p>0.05$; $t=13-15$ min; Fig. 3C; Supplementary Fig. 2A+B). These results show that CX546 not only enhances and prolongs PF-EPSCs, but also boosts dendritic calcium transients.

Ampakines have received attention as potential memory enhancers following the discovery that they facilitate the induction of hippocampal LTP (9, 10). More recently, this LTP-enhancing effect has also been demonstrated specifically for CX546 (11). As cerebellar LTP and LTD are governed by induction rules that differ from those described in hippocampal and neocortical circuits (19, 20), we tested whether enhancing AMPA

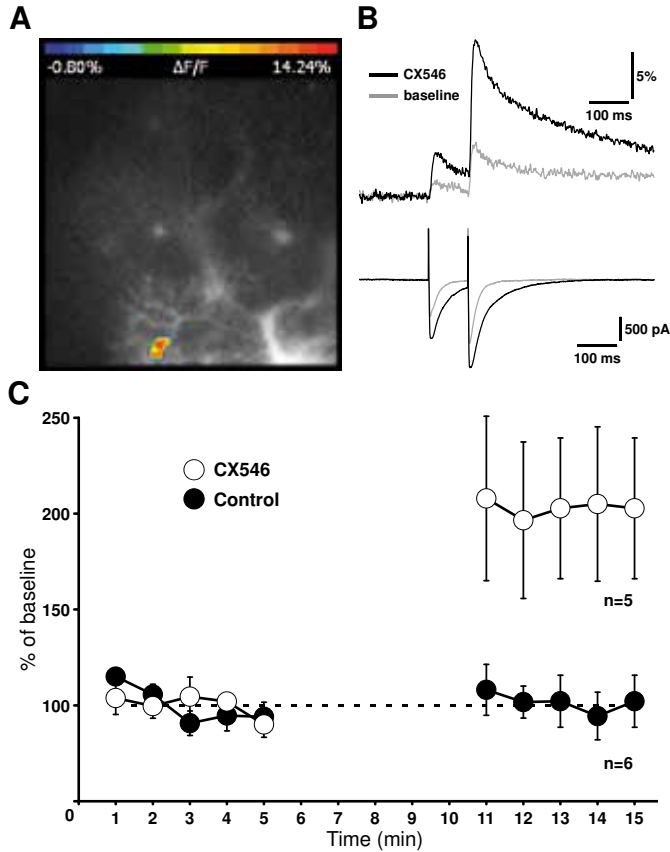


Figure 3: CX546 enhances PF-evoked calcium transients. (A) Original image with false-color coded ROI. (B) PF-EPSCs (bottom) and calcium transients (top) before (grey line) and after wash-in of CX546 (black line). (C) Time graph showing the area under the curve of the calcium transients under control conditions (closed dots; $n=6$) and when CX546 was applied to the bath (open dots; $n=5$). In these recordings, data acquisition was limited to three sweeps per minute to reduce the amount of light exposure. The traces shown are averages over three subsequent sweeps. During wash-in of CX546, data acquisition was discontinued (5min). Error bars are mean \pm SEM.

receptor-mediated PF-EPSCs by CX546 bath application (200 and 300 μ M, data were pooled) affects PF synaptic plasticity. Under control conditions, PF stimulation at 1Hz for 5min elicited a weak, but significant potentiation (120.1 \pm 5.7%; $t=20-30$ min; $n=8$; $p<0.05$ / $t=30-40$ min: 111.8 \pm 7.0%; $n=8$; $p<0.05$; Fig. 4). In contrast, in the presence of CX546 in the bath, application of the same PF stimulation protocol caused LTD (83.3 \pm 11.8%; $t=20-30$ min; $n=8$; $p>0.05$ / $t=30-40$ min: 73.0 \pm 10.8%; $n=8$; $p<0.05$; Fig. 4). The change in the PF-EPSC amplitude in the presence of CX546 was significantly different from that observed under control conditions (Mann-Whitney U test; $t=30-40$ min; $p<0.05$). Thus,

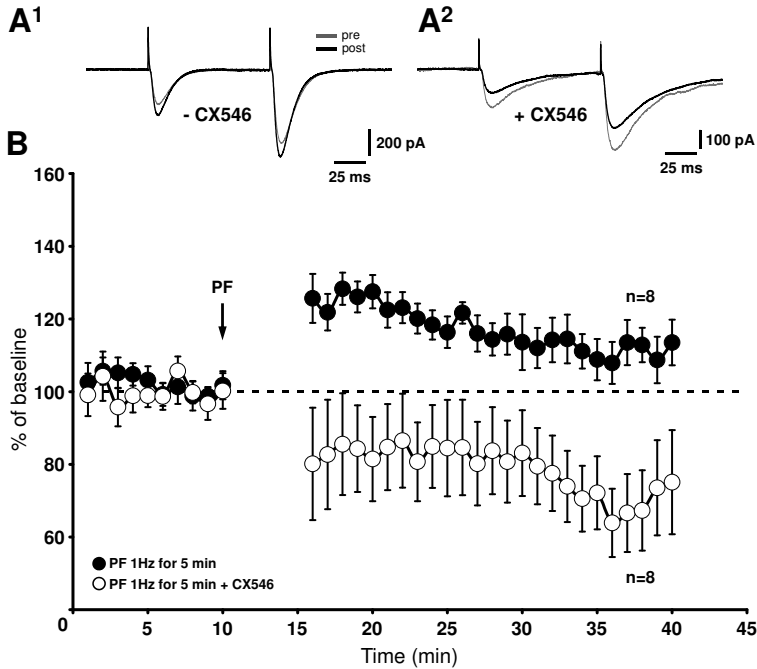


Figure 4: CX546 enhances the probability for LTD induction. (A) Time graph showing changes in the amplitude of EPSC1. Under control conditions, PF stimulation at 1Hz for 5min causes a potentiation (closed dots; n=8). In the presence of CX546, application of the same PF stimulation protocol causes LTD instead (open circles; n=8). (B) Typical traces obtained in the absence (top) and in the presence (bottom) of CX546. Error bars are mean \pm SEM.

while ampakines facilitate LTP induction at hippocampal synapses (10, 11), at cerebellar PF synapses we observe the opposite effect: application of a weak LTP induction protocol results in the induction of LTD instead.

DISCUSSION

In hippocampal and neocortical circuits, ampakines enhance synaptic transmission and promote the induction of LTP (9). Our study shows that in cerebellar circuits, the basic mode of action (slowing desensitization / deactivation of AMPA receptors) is the same, but the consequences of enhanced transmission are fundamentally different, as CX546 promotes LTD rather than LTP induction. At both types of synapses, the change in induction probabilities is likely due to an increase in calcium signaling, resulting from a stronger AMPA receptor-mediated depolarization and facilitated activation of voltage-gated calcium channels, which we could demonstrate in this study at cerebellar PF synapses. However, in contrast to its hippocampal and neocortical counterparts, cerebellar LTD requires higher calcium transients for induction than LTP (16). This difference might explain why



V

ampakines promote LTP in the hippocampus, but LTD in the cerebellum. Ultimately, the outcome might well be the same, as LTD is currently seen as the cellular correlate of forms of motor learning (25), and thus assumes the role in synaptic memory formation that is assigned to LTP in the hippocampus. This difference between hippocampal and cerebellar synapses points towards a general problem when attempting to develop drugs for the treatment of memory deficits: LTP does not simply equal learning and memory formation. Rather, LTP and LTD co-exist at most types of synapses and play very specific roles in information storage (26). These specific roles need to be considered when interfering with the balance of LTP and LTD mechanisms using ampakines or other memory-enhancing drugs. Likewise, it needs to be taken into consideration that excessive AMPA receptor activation can promote excitotoxicity (27). At cerebellar PF synapses, LTD is induced upon PF and CF co-activation and thus results when PF activity coincides with error signals conveyed by the CF input (28, 29). LTP, in contrast, is induced by PF stimulation alone and provides a reversal mechanism for LTD (formally, LTD can also provide a reversal mechanism for LTP; 19). As demonstrated here, ampakines can shift the balance of cerebellar LTD / LTP towards a higher LTD induction probability and might thus be useful candidate drugs for the treatment of cerebellar dysfunctions that are related to deficits in LTD induction / maintenance. The majority of mouse mutants, in which LTD is impaired (e.g. mGluR1 knock-out mice, mice with a Purkinje cell-specific overexpression of a PKC inhibitory peptide, or α CaMKII knock-out mice), also show severe motor coordination and / or motor learning deficits (for review, see 19, 30). These observations do not provide a complete explanation of the cellular basis of cerebellar ataxias, but they do suggest that deficits in LTD induction constitute one component of the ataxia phenotype. It is therefore conceivable that, with the limitations discussed above, ampakines might be useful candidate drugs for the treatment of cerebellar dysfunctions, as in cerebellar ataxias.

Our study shows that ampakines enhance PF synaptic transmission and dendritic calcium signaling, but promote LTD, rather than LTP induction. Thus, these findings challenge the view that enhanced synaptic activity generally equals a higher probability for LTP induction. Rather, different brain circuits and different types of synapses use synaptic plasticity mechanisms, such as LTP and LTD, in ways that are uniquely adapted. As a consequence, therapeutic treatments based on drugs interfering with memory processes need to be tailored to the specific types of memory deficits.

MATERIALS AND METHODS

Slice preparation: Sagittal slices of the cerebellar vermis (200–250 μ m) were prepared from P18–25 Sprague-Dawley rats in ice-cold artificial cerebrospinal fluid (ACSF), and were kept at room temperature for a maximum of six hours in ACSF containing (in mM): 124 NaCl, 5 KCl, 1.25 Na_2HPO_4 , 2 MgSO_4 , 2 CaCl_2 , 26 NaHCO_3 , and 10 D-glucose bubbled with 95% O_2 and 5% CO_2 . Slices were continuously perfused with ACSF throughout recording. All drugs were purchased from Sigma (St. Louis, MO), except for Oregon Green BAPTA-2 (Invitrogen, Carlsbad, CA).

Electrophysiology: Whole-cell patch-clamp recordings were performed at room temperature using an EPC-10 amplifier (HEKA Electronics, Lambrecht/Pfalz, Germany). Currents were filtered at 3kHz, digitized at 8kHz, and acquired using PULSE software (HEKA). Patch pipettes (2.5-5.0 M Ω) were filled with a solution containing (in mM): 9 KCl, 10 KOH, 120 K-gluconate, 3.48 MgCl₂, 10 HEPES, 4 NaCl, 4 Na₂ATP, 0.4 Na₃GTP, and 17.5 sucrose (pH 7.25-7.35). Purkinje cells were voltage-clamped at holding potentials in the range of -65 to -70mV. Picrotoxin (5 μ M) was added to the ACSF to block GABA_A receptors. To evoke EPSCs, parallel fibers were activated using glass electrodes that were filled with ACSF. These electrodes were placed in the upper 1/3 of the molecular layer to reduce the risk of unintentional climbing fiber stimulation. In all experiments, test responses were elicited using paired-pulse stimulation (interval 50-100ms) at a frequency of 0.05Hz with stimulus currents in the range of 0.5-2 μ A. The paired-pulse facilitation (PPF) ratio was determined to confirm the postsynaptic origin of alterations. The PPF ratio was calculated as EPSC2/EPSC1. The protocol for inducing LTP consisted of parallel fiber stimulation at 1Hz for 5min. For tetanization, the recording mode was switched from voltage- to current-clamp. Series and input resistance were monitored throughout the experiment by applying a hyperpolarizing voltage step (-10mV) at the end of each sweep. Recordings were excluded from the study if the series or the input resistance varied by >15% over the course of the experiments. All values are shown as % of baseline (calculated from the last 5min of baseline recording) \pm SEM. For statistical analysis, we used the Student's t-test (paired/unpaired) and the Mann-Whitney U test, when appropriate.

Calcium imaging: Microfluorometric recordings were performed using a NeuroCCD-SMQ camera (80x80 pixels) and NeuroPlex software (both RedShirtImaging, Decatur, GA) for data acquisition. Fluorescence was sampled at 2kHz for sweep durations of 750ms. Fluorescence was excited using a 100W Xenon arc lamp (Cairn Research Ltd, Faversham, UK). Recordings started >30min after patch formation to allow for the calcium indicator dye (Oregon Green BAPTA-2; 200 μ M) to diffuse into the distal dendrites. The stimulus electrode was placed under visual guidance to activate fine dendritic branchlets. Fluorescence changes were normalized to resting levels and expressed as the ratio $(t) = \frac{F(t) - F}{F}$, where F(t) is the fluorescence value at time t, and F is the averaged fluorescence obtained during the baseline period preceding the stimulus application.

ACKNOWLEDGMENTS

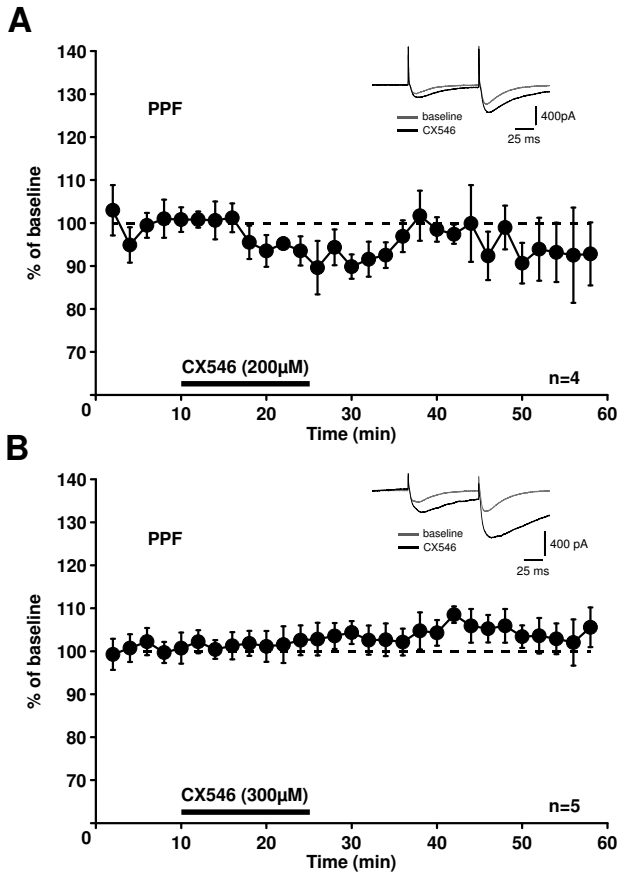
We are grateful to members of the Hansel laboratory for invaluable comments on the manuscript. This work was supported by grants from the Hersenstichting Nederland, the Netherlands Organization for Scientific Research (NWO-ALW), and a National Institutes of Health (NIH) grant NS62771 to C.H.

REFERENCES

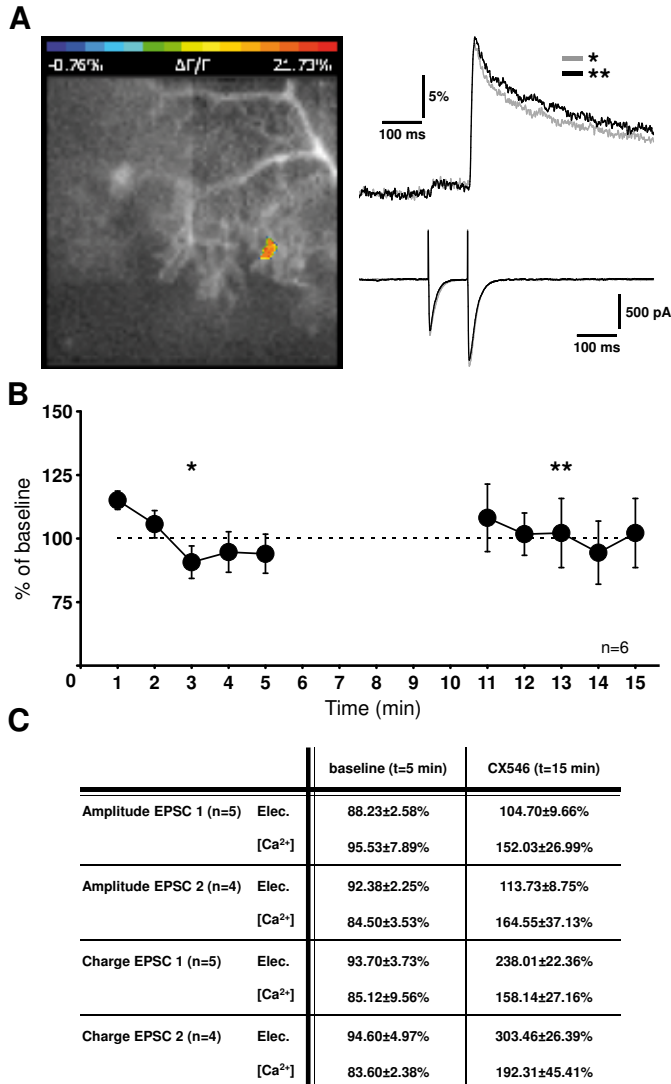
1. Bliss TVP, Collingridge GL (1993) A synaptic model of memory: long-term potentiation in the hippocampus. *Nature* 361: 31-39.
2. Artola A, Singer W (1993) Long-term depression of excitatory synaptic transmission and its relationship to long-term potentiation. *Trends Neurosci.* 16: 480-487.
3. Kirkwood A, Dudek SM, Gold JT, Aizenman CD, Bear MF (1993) Common forms of synaptic plasticity in the hippocampus and neocortex in vitro. *Science* 260: 1518-1521.
4. Bienenstock EL, Cooper LN, Munro PW (1982) Theory for the development of neuron selectivity: orientation specificity and binocular interaction in visual cortex. *J. Neurosci.* 2: 32-48.
5. Bear MF, Cooper LN, Ebner FF (1987) A physiological basis for a theory of synaptic modification. *Science* 237: 42-48.
6. Hansel C, Artola A, Singer W (1997) Relation between dendritic Ca²⁺ levels and the polarity of synaptic long-term modifications in rat visual cortex neurons. *Eur. J. Neurosci.* 9: 2309-2322.
7. Neveu D, Zucker RS (1996) Postsynaptic levels of [Ca²⁺]_i needed to trigger LTD and LTP. *Neuron* 16: 619-629.
8. Nevian T, Sakmann B (2006) Spine Ca²⁺ signaling in spike-timing-dependent plasticity. *J. Neurosci.* 26: 11001-11013.
9. Lynch G (2002) Memory enhancement: the search for mechanism-based drugs. *Nat. Neurosci.* 5: 1035-1038.
10. Stäubli, U. et al. (1994) Centrally active modulators of glutamate receptors facilitate the induction of long-term potentiation in vivo. *Proc. Natl. Acad. Sci. USA* 91: 11158-11162.
11. Arai AC, Xia YF, Susuki E (2004) Modulation of AMPA receptor kinetics differentially influences synaptic plasticity in the hippocampus. *Neuroscience* 123: 1011-1024.
12. Lynch G et al. (1997) Evidence that a positive modulator of AMPA-type glutamate receptors improves delayed recall in aged humans. *Exp. Neurol.* 145: 89-92.
13. Ingvar M et al. (1997) Enhancement by an ampakine of memory encoding in humans. *Exp. Neurol.* 146: 553-559.
14. Lynch G, Gall CM (2006) Ampakines and the threefold path to cognitive enhancement. *Trends Neurosci.* 29: 554-562.
15. Porrino LJ et al. (2005) Facilitation of task performance and removal of the effects of sleep deprivation by an ampakine (CX717) in nonhuman primates. *PLOS Biology* 3: 1639-1652.
16. Coesmans M, Weber JT, De Zeeuw CI, Hansel C (2004) Bidirectional parallel fiber plasticity in the cerebellum under climbing fiber control. *Neuron* 44: 691-700.
17. Nagarajan N et al. (2001) Mechanism and impact of allosteric AMPA receptor modulation by the ampakine CX546. *Neuropharmacology* 41: 650-663 (2001).
18. Arai AC, Xia YF, Rogers G, Lynch G, Kessler M (2002) Benzamide-type AMPA receptor modulators form two subfamilies with distinct modes of action. *J. Pharmacol. Exp. Ther.* 303: 1075-1085.
19. Jörntell H, Hansel C (2006) Synaptic memories upside down: bidirectional plasticity at cerebellar parallel fiber-Purkinje cell synapses. *Neuron* 52: 227-238.
20. Hansel C, Bear MF (2008) LTD-Synaptic depression and memory storage. In *Molecular Mechanisms of Memory*, ed. Sweatt, J.D., Vol. 4 of *Learning and Memory: A Comprehensive Reference*, ed. Byrne, J. (Oxford, Elsevier), pp. 327-366.
21. Denk W, Sugimori M, Llinas R (1995) Two types of calcium response limited to single spines in cerebellar Purkinje cells. *Proc. Natl. Acad. Sci. USA* 92: 8279-8282.
22. Eilers J, Augustine GJ, Konnerth A (1995) Subthreshold synaptic Ca²⁺ signaling in fine dendrites and spines of cerebellar Purkinje neurons. *Nature* 373: 155-158.
23. Weber JT, De Zeeuw CI, Linden DJ, Hansel C (2003) Long-term depression of climbing fiber-evoked calcium transients in Purkinje cell dendrites. *Proc. Natl. Acad. Sci. USA* 100: 2878-2883.
24. Yasuda R, Sabatini BL, Svoboda K (2003) Plasticity of calcium channels in dendritic spines. *Nat. Neurosci.* 6: 948-955.
25. Ito M (2001) Cerebellar long-term depression: characterization, signal transduction, and functional roles. *Physiol. Rev.* 3: 1143-1194 (2001).
26. Malenka RC, Bear MF (2004) LTP and LTD: an embarrassment of riches. *Neuron* 44: 5-21.

27. Yamada KA (1998) Modulating excitatory synaptic neurotransmission: potential treatment for neurological disease? *Neurobiology of Disease* 5: 67-80.
28. Ito M, Sakurai M, Tongroach P (1982) Climbing fibre induced depression of both mossy fibre responsiveness and glutamate sensitivity of cerebellar Purkinje cells. *J. Physiol.* 324: 113-134.
29. Ito M, Kano M (1982) Long-lasting depression of parallel fiber-Purkinje cell transmission induced by conjunctive stimulation of parallel fibers and climbing fibers in the cerebellar cortex. *Neurosci. Lett.* 33: 253-258.
30. De Zeeuw CI, Yeo CH (2005) Time and tide in cerebellar memory formation. *Curr. Opin. Neurobiol.* 15: 667-674.

SUPPLEMENTARY MATERIALS



Supplementary Figure 1: CX546 does not affect the paired-pulse facilitation (PPF) ratio. (A) Time graph of the PPF ratio (PF-EPSC 2/1) when CX546 was bath applied at 200 μ M ($n=4$). (B) Time graph of the PPF ratio when CX546 was bath applied at 300 μ M ($n=5$). The bars indicate the presence of CX546 in the bath. All values are mean \pm SEM.



Supplementary Figure 2: Stability of calcium transients under control conditions. (A) Left: Original image of a Purkinje cell filled with Oregon Green BAPTA-2 (200 μ M). The false-color coded area indicates the ROI from which calcium transients were recorded that are shown on the right. Right: PF-EPSCs (bottom) and calcium transients (top) recorded with a delay of 10min. (B) Time graph of the control experiments (n=6; same as in Fig. 2C). Data acquisition was discontinued for 5min after baseline recording, to match the conditions that were applied in the CX546 experiments. The stars indicate the time periods at which traces were taken for display in (A). All values are mean \pm SEM. (C) Table showing CX546 effects on PF-EPSCs and associated calcium transients. Parameters that were monitored were the peak amplitudes of EPSC1 and EPSC2, as well as the corresponding calcium transients. Moreover, the area under the curve ('charge') of both EPSCs and calcium transients was determined. The table summarizes values taken during the baseline (t=5min) and after wash-in of CX546 (t=15min). All values are mean \pm SEM.

V

GENERAL DISCUSSION

Boeke J. van Beugen

parts of this general discussion are adapted from
Gao, van Beugen and De Zeeuw, 2012

VI

VI. GENERAL DISCUSSION

6.1. Implications of low release probability at the PF-PC synapse on cerebellar function

As discussed in chapter one, PF terminals that project to PCs have a low initial release probability and activity patterns in granule cells exceed the release capacity. This is a remarkable finding, as the MF-GrC is specialized to perform with high temporal precision. While this temporal precision is not crucial downstream for transmission between PFs and PCs, it might still be important for signalling between MLI and PC and influence burst timing in GrCs. At the PF-PC synapse, however, it serves to overcome a low release probability to ensure signalling with lower temporal precision.

A heterogenic distribution of release probability between individual terminals likely reflects the difference between depressed and potentiated synapses. While depressed synapses will only signal consistently during prolonged activation, even potentiated terminals remain far too unreliable to convey temporally coded information, despite a much facilitated release.

By itself, an unreliable, stochastic relay cannot serve any purpose in the direct control of movement. However, this behaviour reveals an important characteristic of cerebellar processing; while the input of an individual connection is meaningless, grouped activity of multiple PFs displays a linear characteristic between the duration of activity and the size of the response. Grouping of activity is controlled by spatiotemporal activity in the granule cell layer, creating spatiotemporal maps of granule cell activity. Combined with unresponsiveness to individual connections, cerebellar computing filters noise at the level of the granule cells layer and at the PF-PC synapse, creating a noise-free, coordinated spike timing in PCs.

6.2. Behavioural implication of reversible plasticity at PF-PC synapse

For a long time, theories about cerebellar motor learning were based on the idea that adaptation results from weakening the relevant connections between the PFs and PCs (postsynaptic PF-PC LTD), ultimately leading to reduced inhibition from the cerebellar cortex onto the cerebellar nuclei (Marr, 1969; Albus, 1971; Ito, 1982). This creates a timed window of opportunity in which relevant sensory input can be passed onto relevant brain regions downstream. Supported by experimental data showing the involvement of PF-PC LTD in cerebellar learning (Ito, 1984), this hypothesis has long dominated the direction of cerebellar research. However, a system based on this principle would suffer from 2 major problems: 1) the ability to further adapt would saturate once every synapse is depressed and 2) once adapted, neither extinction nor reversal can occur (Jörntell and Hansel, 2006). Recent studies have shown that, in addition to LTD, the PF-PC synapse can also express LTP and that the direction of plasticity depends on an activity dependent balance between kinases and phosphatases (Lev-Ram, 2002; Coesmans et al., 2004; Belmeguenai and Hansel, 2005). Here, we show that LTP is both involved in the Pavlovian conditioned response, as well as motor adaptation. The finding that LTD-dependent 'gain-decrease' is partially impaired suggest that LTP might serve to prevent saturation. However, the finding that

both ‘gain-increase’ and ‘phase-reversal’ show no effect at all, suggests that LTP also serves a more direct function in cerebellar motor learning.

6.3. Network formation under CF control

6.3.1. *Endocannabinoids assist climbing fiber driven plasticity at the PF-PC synapse*

In chapter 2 and 3 we discuss two mechanisms by which the climbing fiber exerts its influence and controls bidirectional plasticity at the PF-PC synapse; while its presence or absence directly controls the direction of postsynaptic plasticity at this synapse by affecting postsynaptic calcium signals (Coemans et al., 2004), in parallel, it can also activate the release of retrograde acting endocannabinoids to influence presynaptic plasticity accordingly. This property further sharpens the effectiveness with which the CF directs plasticity at the PF-PC synapse. Previous work has suggested that endocannabinoids can serve a protective function to suppress PF input onto Purkinje cells during sustained activity and prevent damage from over-excitation (Kreitzer and Regehr, 2001). However, our results suggest that, more likely, endocannabinoids assist climbing fiber driven plasticity at the PF-PC synapse. These findings further emphasize the importance the CF has on directing plasticity at this synapse.

However, CF-control stretches far beyond the PF-PC synapse and likely creates grouped activity in the granule cell layer and selects inputs to Golgi cells, MLI and PCs in the molecular layer. In this manner, presence or absence of CF activity directs plasticity throughout the cerebellum, forming functional modules.

6.3.2. *Function of the Purkinje cell network: Creating output by selecting input*

The granule cell network provides enormous diversity in signal coding to Purkinje cell dendrites in the molecular layer (D’Angelo, 2011), even when the mossy fibre input is relatively uniform (Arenz et al., 2008). The huge diversity of parallel fiber codings, widely distributed over the molecular layer, has the advantage that guiding signals (provided by climbing fibers) can select and sculpt those codings that are needed to improve behaviour as required in a particular spatiotemporal context (De Zeeuw et al., 2011). The climbing fibers achieve this through the presence and absence of heterosynaptic effects, either directly or via spillover. Climbing fiber activity may not only reduce Purkinje cell activity by inducing LTD at the parallel fiber–Purkinje cell synapse, but also by promoting potentiation at the parallel fiber–molecular-layer interneuron synapse and molecular-layer interneuron–Purkinje cell synapse, and probably even at the parallel fiber–Golgi cell synapse. Conversely, the absence of climbing fibers can increase Purkinje cell activity by permitting LTP at the parallel fiber–Purkinje cell synapse, by increasing the intrinsic excitability of Purkinje cell dendrites, and by promoting LTD at parallel fiber–interneuron synapses. For the VOR phase reversal learning paradigm this implies that multiple forms and sites of plasticity will be actively involved once the direction of the retinal slip and thereby that of the climbing fiber modulation is reversed. For example, when retinal slip is reversed towards the left during training, a specific set of parallel fiber–Purkinje cell synapses is probably potentiated

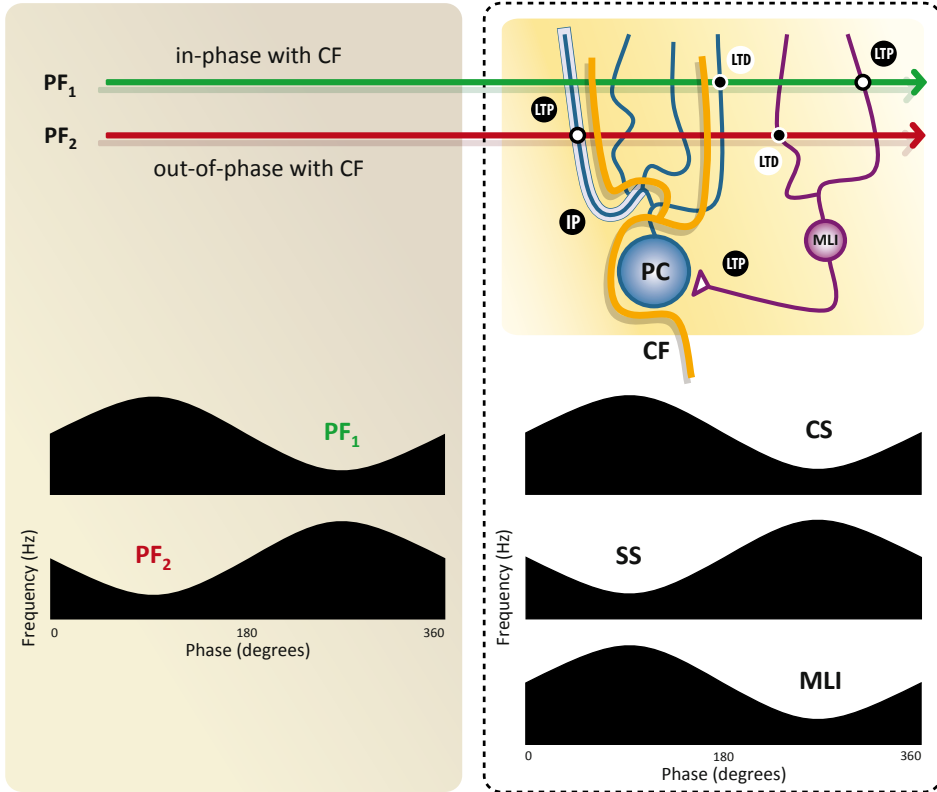


Fig 1 Discussion: Creating output by selecting input in the Purkinje cell network. By controlling the direction of plasticity at multiple synapses, climbing fibre (CF) activity links the parallel fibre (PF) that has the appropriate phase to the desired target. When CF activity is in-phase with PF activity (PF₁), it will promote LTP at the PF-MLI synapse, LTD at the PF-PC synapse, and rebound potentiation at the MLI-PC synapse (for simplicity the rebound potentiation is here also indicated as LTP). Conversely, when CF activity is absent (i.e. out-of-phase with PF activity (PF₂)), LTD is induced at the PF-MLI synapse, whereas LTP is induced at the PF-PC synapse together with intrinsic plasticity (IP) in the PC (depicted as a 'halo' around dendritic membrane). Thus, because the inductions of these forms of plasticity are dependent on the direction of the periodic CF stimuli, CF activity can induce opposite phases in the MLI versus the PC. As a result of the above mechanisms, simple-spike activity in PCs is determined directly by excitatory inputs from out-of-phase PFs (PF₂) and by suppression from in-phase PFs (PF₁), and the simple-spike (SS) output of PCs will thus be out-of-phase with CF activity (indicated as complex spikes (CS)). As the route of information through the molecular-layer interneurons is parallel to the route through the Purkinje cells, we predict that the various forms of plasticity in either one of these routes can compensate at least in part for deficits in the other route.

in the left flocculus, whereas the synapses of the same parallel fibers onto interneurons are depressed (Hoebeek et al., 2005; Schonewille et al., 2010). Conversely, when the retinal slip is moving towards the right a different set of parallel fiber synapses with the same Purkinje cells is subject to depression, whereas the synapses of these parallel fibers onto interneurons are potentiated. As these depressing and potentiating effects (which work in synergy) are all timing-dependent in the sense that they all depend on whether or not climbing fiber activity coincides (within a particular time frame) with parallel fiber activity (Bell et al., 1997; Coesmans et al., 2004; Han et al., 2000; Wang et al., 2000), it is crucial that parallel fibers carry sufficient variety in temporal coding. This variety allows the climbing fibers to shape the simple-spike modulation of the Purkinje cells in any direction, even to a phase that is opposite to that of the mossy fibers. Interestingly, such an opposite phase in mossy fiber activity and Purkinje cell simple-spike activity is exactly what has been observed in various experiments. For example, during VOR the majority of vestibular simple-spike responses of Purkinje cells in vertical-axis zones of the floccular complex in primates show a phase that is opposite to that of the majority of the corresponding mossy fiber inputs (Lisberger and Fuchs, 1978a, b; Miles et al., 1980). Likewise, during smooth-pursuit eye movement the percentage of Purkinje cell simple-spike responses that are excited for rotation of the ipsilateral eye to the ipsilateral side of recording is higher than that of corresponding mossy fiber responses (Lisberger and Fuchs, 1978a, b). If the climbing fibers dominate the periodicity of the simple-spike activity by regulating multiple forms of plasticity in the molecular layer, one expects that selectively reversing the laterality of the climbing fibers from a contralateral to an ipsilateral projection reverses the simple-spike modulation even when the laterality of the mossy fiber projection is unaffected; this prediction indeed holds (Badura et al., 2010). Moreover, as VOR phase reversal learning in effect also reverses the climbing fiber modulation, one expects that manipulating simultaneously multiple forms of climbing fiber mediated forms of plasticity induces the most prominent deficits in this paradigm (reversal of the phase of the climbing fiber signals induces potentiation at parallel fiber–Purkinje cell synapses and the parallel fiber synapses onto interneurons that were in a silent or depressed state before the reversal and it depresses the parallel fiber–Purkinje cell and parallel fiber–interneuron synapses that were potentiated in the initial state); this prediction indeed also holds. We therefore argue that climbing fiber-guided selection in the molecular layer provides a powerful mechanism to create the appropriate Purkinje cell simple-spike output by simultaneously inducing several forms of plasticity.

6.3.3. *Distributed synergistic plasticity*

Plasticity in the granule cell network may increase the diversity of coding, whereas plasticity in the Purkinje cell network may facilitate the selection of the appropriate coding and transfer it to the output domain that controls the appropriate movement. The combination of the different forms of plasticity in these networks during learning can be referred to as distributed synergistic plasticity; distributed, because it includes various types of synaptic and intrinsic plastic effects in various types of neurons and superimposed interneurons

in both the granular and molecular layer under compatible induction protocols; and synergistic, because the different forms of long-term plasticity in the cerebellar cortex act synergistically: forms of plasticity that occur in serial fashion (*i.e.* plasticity in granule cell network and plasticity in Purkinje cell network) and forms of plasticity that occur in parallel fashion (*i.e.* plasticity at parallel fiber–Purkinje cell synapses and that at parallel fiber–interneuron synapses) in effect enhance one another through precise and periodic timing in the climbing fiber system relative to the mossy fiber system. This configuration implies that memory formation and storage in the olivocerebellar system is created in a distributed and synergistic fashion across the networks, allowing continuous expansion and fine-tuning to the changing bodily and environmental conditions.

The processes — such as plasticity at the mossy-fiber–granule-cell synapse or intrinsic plasticity of granule cells — that modify activity in the granule cell network and may serve to enhance, fine-tune and maintain diversity of parallel fiber coding probably depend predominantly on activity in the mossy fibers and Golgi cells. By contrast, the processes that modify activity in the Purkinje cell network are mainly regulated by climbing fiber activity. The climbing fibers play a crucial role in all of these processes by inducing various forms of heterosynaptic plasticity when they are active, and by permitting various forms of homosynaptic plasticity when they are silent (Badura et al., 2010). The various forms of climbing fiber dependent plasticity are bidirectional (that is, they have depressing and potentiating effects) and are reinforcing in a parallel fashion, in the sense that the potentiating and depressing effects of climbing fibers at the inputs onto and output of superimposed interneurons act in synergy with the direct depressing and potentiating effects, respectively, of the climbing fibers at the parallel fiber inputs to the Purkinje cells. As the routes of information through the interneurons are parallel to the routes of information through the Purkinje cells, the various forms of plasticity in either one of these routes can compensate at least in part for deficits in the other route.

This conceptual model of distributed synergistic plasticity elaborates upon concepts initiated by Marr, Albus, Ito and others (Albus, 1971; Dean et al., 2010; Fujita, 1982; Ito, 1982; Kawato et al., 1987; Marr, 1969; Roberts, 2007). However, this hypothesis states that, while LTD may still be crucial for correct cerebellar functioning, potentiation of granule cells and potentiation of Purkinje cells are, at least initially, the dominant type of plasticity during visuovestibular learning. LTD at the inputs to these cells might contribute at various levels during ongoing learning, might compensate for deficits in potentiation at synapses with opposite polarity, and/or might avoid saturation of synapses by noise and so prevent overexcitation or underexcitation (Coemans et al., 2004; Jörntell and Hansel, 2006). However, it does not appear to be essential for visuovestibular motor learning. By speculating that LTP and intrinsic changes in the excitability of granule cells and Purkinje cells are, initially, the fundamental mechanisms underlying procedural memory formation, we follow the notion that the cerebellum has an excessive number of granule cells and even more parallel fibre varicosities, the vast majority of which has been reported to be rather silent during rest (Brunel et al., 2004; Chadderton et al., 2004; Isope and Barbour,

2002) and, therefore, tends initially to be more sensitive to potentiation than depression (Le Guen and De Zeeuw, 2010). By contrast, interneurons have been reported to be more active relative to granule cells during rest (Barmack and Yakhnitsa, 2008), and their inputs and outputs may therefore initially be more prone to depression. If potentiation of granule cells and Purkinje cells and depression of interneurons are indeed the main initial forms of plasticity underlying learning, one may predict that during the execution of learned motor skills the activity of granule cells increases, whereas that of interneurons decreases; this indeed turns out to be the case for locomotion (Wang, S.S.; unpublished observations). However, as different cerebellar lobules and zones show different levels of intrinsic activity that may lead to different propensities for potentiation and depression (Wadiche and Jahr, 2005), different learning behaviours controlled by different regions may show different propensities for plasticity. In this respect, it will be interesting to investigate the extent to which the concept of distributed synergistic plasticity applies to other forms of cerebellar learning, such as Pavlovian eye blink conditioning, locomotion conditioning, fear conditioning and spatial navigation (Bissiere et al., 2011; Boele et al., 2010; Rochefort et al., 2011; Van Der Giessen et al., 2008). The similarities in the presence and absence of phenotypes of mouse mutants that have been subjected to multiple cerebellar learning tests suggest that Pavlovian conditioning is subject to the same principles as visuovestibular motor learning (Schonewille et al., 2010; Schonewille et al., 2011; Wada et al., 2007).

Owing to the abundance and distributed variety of different forms of plasticity in the cerebellar cortex and the room for compensation, probably none of them is essential by itself. Thus, the concept of distributed synergistic plasticity predicts that none of the individual forms of plasticity is absolutely essential, even though some forms of plasticity may be more efficient than their counterparts in the initial stages of various forms of cerebellar learning. In this respect, one could hypothesize that the superimposed interneurons, which may have arisen later in evolution than their target neurons (*i.e.* the Purkinje cells and granule cells), have endowed the cerebellar cortex with a wide range of possibilities to compensate for potential deficits in one of the forms of plasticity in the target neurons themselves. This development would by itself emphasize how important the role of the cerebellar cortex in learning and consolidation has become during evolution. Thus, the options provided by distributed synergistic plasticity in the cerebellar cortex are sufficiently rich to modify phases of activity and behaviour in any direction, and that these acquired behaviours can be maintained for a lifetime in the sets of modified inputs to granule cells and Purkinje cells as well as their superimposed interneurons, even when failures at particular forms of plasticity occur. These memories may remain stored in the cerebellar cortex independently from the “copy transfer” to the cerebellar and vestibular nuclei that may facilitate retrieval of the memories after consolidation (Kassardjian et al., 2005; Kellett et al., 2010; Shutoh et al., 2006).

The fact that a stored procedural memory or cognitive procedure should in principle be retrievable for the rest of one’s life demands a mechanism that can last forever. In this respect the molecular mechanisms underlying distributed synergistic plasticity in the cerebellar cortex may differ from those underlying plasticity in the hippocampus, which is required for

declarative memory formation — a type of memory that is formed more rapidly, with more readily available options for extinction (Morris et al., 1986; Myers et al., 2006). Procedural memories formed at a young age can indeed last forever (Stahl et al., 2006) and the ability to form new procedural memories is affected by aging (Woodruff-Pak et al., 2010), and it will be interesting to find out whether the capacity for modifying parallel-fibre synapses both at Purkinje cells and interneurons is diminished over time and whether or not analogous changes in the capacity for plasticity can be observed in the hippocampus (Douyard et al., 2007; Kessels and Malinow, 2009). In particular, it will be interesting to investigate whether a change in capacity for synaptic plasticity is reflected in the amount of particular stabilizing receptor subunits at the end of life and whether there is a difference between the target neurons and interneurons in this respect (Douyard et al., 2007; Kessels and Malinow, 2009).

6.4 Ampakines: the potential to promote cerebellar learning

In the outdated Marr-Albus-Ito hypothesis, in which PF LTD solely is responsible for cerebellar learning, promoting the likelihood of LTD through ampakine treatment could benefit cerebellar learning and therefore improve motor control. Considering the simultaneous expression of plasticity at multiple sites following the hypothesis of distributed synergistic plasticity, this assumption is not at all straightforward. However, ampakines will only affect AMPA-driven activity and thus, its effect is restricted to MF, PF and CF output. At the MF-GrC synapse the increased postsynaptic Ca²⁺ might facilitate the induction of LTP; at the PF-MLI, ampakines will likely promote LTD in those synapses that express GluR2-lacking AMPAR, but will have no effect on readily depressed synapses that express calcium-impermeable GluR2-containing AMPAR; increased postsynaptic calcium transients in PCs might favour rebound potentiation and strengthen inhibitory projections from MLI onto PCs.

Ultimately, ampakines will weaken out-of-phase PF-activity and promote in-phase MLI-PC activity. Indeed, together these effects might facilitate cerebellar learning and therefore it will be interesting to see if ampakines will benefit motor performance *in vivo*.

REFERENCES

1. Albus, J.S. (1971). A theory of cerebellar function. *Math Biosci* 10, 25-61.
2. Arenz, A., Silver, R.A., Schaefer, A.T., and Margrie, T.W. (2008). The contribution of single synapses to sensory representation in vivo. *Science* 321, 977-980.
3. Badura, A., Schonewille, M., Vinuesa Veloz, M.F., Renier, N., Chedotal, A., and De Zeeuw, C.I. (2010). Disruption in cerebellar circuitry causes more profound impairment than having no cerebellar output at all. In 7th FENS (Amsterdam).
4. Barmack, N.H., and Yakhnitsa, V. (2008). Functions of interneurons in mouse cerebellum. *J Neurosci* 28, 1140-1152.
5. Bell, C.C., Han, V.Z., Sugawara, Y., and Grant, K. (1997). Synaptic plasticity in a cerebellum-like structure depends on temporal order. *Nature* 387, 278-281.
6. Belmeguenai, A. and Hansel, C. (2005) A role for protein phosphatases 1, 2A and 2B in cerebellar long-term potentiation. *J Neurosci* 25(46), 10768-10772.
7. Bissiere, S., Zelikowsky, M., Ponnusamy, R., Jacobs, N.S., Blair, H.T., and Fanselow, M.S. (2011). Electrical synapses control hippocampal contributions to fear learning and memory. *Science* 331, 87-91.
8. Boele, H.J., Koekkoek, S.K., and De Zeeuw, C.I. (2010). Cerebellar and extracerebellar involvement in mouse eyeblink conditioning: the ACDC model. *Front Cell Neurosci* 3, 19.
9. Brunel, N., Hakim, V., Isope, P., Nadal, J.P., and Barbour, B. (2004). Optimal information storage and the distribution of synaptic weights: perceptron versus Purkinje cell. *Neuron* 43, 745-757.
10. Chadderton, P., Margrie, T.W., and Hausser, M. (2004). Integration of quanta in cerebellar granule cells during sensory processing. *Nature* 428, 856-860.
11. Coesmans, M., Weber, J.T., De Zeeuw, C.I., and Hansel, C. (2004). Bidirectional parallel fiber plasticity in the cerebellum under climbing fiber control. *Neuron* 44, 691-700.
12. D'Angelo, E. (2011). Neural circuits of the cerebellum: hypothesis for function. *Journal of integrative neuroscience* 10, 317-352.
13. De Zeeuw, C.I., Hoebeek, F.E., Bosman, L.W., Schonewille, M., Witter, L., and Koekkoek, S.K. (2011). Spatiotemporal firing patterns in the cerebellum. *Nat Rev Neurosci*.
14. Dean, P., Porrill, J., Ekerot, C.F., and Jörntell, H. (2010). The cerebellar microcircuit as an adaptive filter: experimental and computational evidence. *Nat Rev Neurosci* 11, 30-43.
15. Douyard, J., Shen, L., Huganir, R.L., and Rubio, M.E. (2007). Differential neuronal and glial expression of GluR1 AMPA receptor subunit and the scaffolding proteins SAP97 and 4.1N during rat cerebellar development. *J Comp Neurol* 502, 141-156.
16. Fujita, M. (1982). Adaptive filter model of the cerebellum. *Biol Cybern* 45, 195-206.
17. Han, V.Z., Grant, K., and Bell, C.C. (2000). Reversible associative depression and nonassociative potentiation at a parallel fiber synapse. *Neuron* 27, 611-622.
18. Hoebeek, F.E., Stahl, J.S., van Alphen, A.M., Schonewille, M., Luo, C., Rutteman, M., van den Maagdenberg, A.M., Molenaar, P.C., Goossens, H.H., Frens, M.A., *et al.* (2005). Increased noise level of purkinje cell activities minimizes impact of their modulation during sensorimotor control. *Neuron* 45, 953-965.
19. Isope, P., and Barbour, B. (2002). Properties of unitary granule cell->Purkinje cell synapses in adult rat cerebellar slices. *J Neurosci* 22, 9668-9678.
20. Ito, M. (1982). Cerebellar control of the vestibulo-ocular reflex--around the flocculus hypothesis. *Annu Rev Neurosci* 5, 275-296.
21. Ito, M. (1984). The modifiable neuronal network of the cerebellum. *Jpn J Physiol* 34(5), 781-792
22. Jörntell, H., and Hansel, C. (2006). Synaptic memories upside down: bidirectional plasticity at cerebellar parallel fiber-Purkinje cell synapses. *Neuron* 52, 227-238.
23. Kassardjian, C.D., Tan, Y.F., Chung, J.Y., Heskin, R., Peterson, M.J., and Broussard, D.M. (2005). The site of a motor memory shifts with consolidation. *J Neurosci* 25, 7979-7985.
24. Kawato, M., Furukawa, K., and Suzuki, R. (1987). A hierarchical neural-network model for control and learning of voluntary movement. *Biol Cybern* 57, 169-185.
25. Kellett, D.O., Fukunaga, I., Chen-Kubota, E., Dean, P., and Yeo, C.H. (2010). Memory consolidation in the cerebellar cortex. *PLoS One* 5, e11737.

26. Kessels, H.W., and Malinow, R. (2009). Synaptic AMPA receptor plasticity and behavior. *Neuron* 61, 340-350.
27. Kreitzer, A.C. and Regehr, W.G. (2001). Retrograde inhibition of presynaptic calcium influx by endogenous cannabinoids at excitatory synapses onto Purkinje cells. *Neuron* 29, 717-727.
28. Le Guen, M.C., and De Zeeuw, C.I. (2010). Presynaptic plasticity at cerebellar parallel fiber terminals. *Funct Neurol* 25, 141-151.
29. Lev-Ram, V., Wong, S.T., Storm D.R. and Tsien, R.Y. (2002). A new form of cerebellar long-term potentiation is postsynaptic and depends on nitric oxide but not cAMP. *Proc Natl Acad Sci USA* 99(22), 8389-8393.
30. Lisberger, S.G., and Fuchs, A.F. (1978a). Role of primate flocculus during rapid behavioral modification of vestibuloocular reflex. I. Purkinje cell activity during visually guided horizontal smooth-pursuit eye movements and passive head rotation. *J Neurophysiol* 41, 733-763.
31. Lisberger, S.G., and Fuchs, A.F. (1978b). Role of primate flocculus during rapid behavioral modification of vestibuloocular reflex. II. Mossy fiber firing patterns during horizontal head rotation and eye movement. *J Neurophysiol* 41, 764-777.
32. Marr, D. (1969). A theory of cerebellar cortex. *J Physiol* 202, 437-470.
33. Miles, F.A., Fuller, J.H., Braitman, D.J., and Dow, B.M. (1980). Long-term adaptive changes in primate vestibuloocular reflex. III. Electrophysiological observations in flocculus of normal monkeys. *J Neurophysiol* 43, 1437-1476.
34. Morris, R.G., Hagan, J.J., and Rawlins, J.N. (1986). Allocentric spatial learning by hippocampectomized rats: a further test of the "spatial mapping" and "working memory" theories of hippocampal function. *Q J Exp Psychol B* 38, 365-395.
35. Myers, K.M., Ressler, K.J., and Davis, M. (2006). Different mechanisms of fear extinction dependent on length of time since fear acquisition. *Learn Mem* 13, 216-223.
36. Roberts, P.D. (2007). Stability of complex spike timing-dependent plasticity in cerebellar learning. *J Comput Neurosci* 22, 283-296.
37. Rochefort, C., Arabo, A., Andre, M., Poucet, B., Save, E., and Rondi-Reig, L. (2011). Cerebellum shapes hippocampal spatial code. *Science* 334, 385-389.
38. Schonewille, M., Belmeguenai, A., Koekkoek, S.K., Houtman, S.H., Boele, H.J., van Beugen, B.J., Gao, Z., Badura, A., Ohtsuki, G., Amerika, W.E., *et al.* (2010). Purkinje cell-specific knockout of the protein phosphatase PP2B impairs potentiation and cerebellar motor learning. *Neuron* 67, 618-628.
39. Schonewille, M., Gao, Z., Boele, H.J., Veloz, M.F., Amerika, W.E., Simek, A.A., De Jeu, M.T., Steinberg, J.P., Takamiya, K., Hoebeek, F.E., *et al.* (2011). Reevaluating the role of LTD in cerebellar motor learning. *Neuron* 70, 43-50.
40. Shutoh, F., Ohki, M., Kitazawa, H., Itoharu, S., and Nagao, S. (2006). Memory trace of motor learning shifts transsynaptically from cerebellar cortex to nuclei for consolidation. *Neuroscience* 139, 767-777.
41. Stahl, J.S., James, R.A., Oommen, B.S., Hoebeek, F.E., and De Zeeuw, C.I. (2006). Eye movements of the murine P/Q calcium channel mutant tottering, and the impact of aging. *J Neurophysiol* 95, 1588-1607.
42. Van Der Giessen, R.S., Koekkoek, S.K., van Dorp, S., De Gruijl, J.R., Cupido, A., Khosrovani, S., Dortmund, B., Wellershaus, K., Degen, J., Deuchars, J., *et al.* (2008). Role of olivary electrical coupling in cerebellar motor learning. *Neuron* 58, 599-612.
43. Wada, N., Kishimoto, Y., Watanabe, D., Kano, M., Hirano, T., Funabiki, K., and Nakanishi, S. (2007). Conditioned eyeblink learning is formed and stored without cerebellar granule cell transmission. *Proc Natl Acad Sci U S A* 104, 16690-16695.
44. Wadiche, J.I., and Jahr, C.E. (2005). Patterned expression of Purkinje cell glutamate transporters controls synaptic plasticity. *Nat Neurosci* 8, 1329-1334.
45. Wang, S.S., Denk, W., and Häusser, M. (2000). Coincidence detection in single dendritic spines mediated by calcium release. *Nat Neurosci* 3, 1266-1273.
46. Woodruff-Pak, D.S., Foy, M.R., Akopian, G.G., Lee, K.H., Zach, J., Nguyen, K.P., Comalli, D.M., Kennard, J.A., Agelan, A., and Thompson, R.F. (2010). Differential effects and rates of normal aging in cerebellum and hippocampus. *Proc Natl Acad Sci U S A* 107, 1624-1629.

PUBLICATIONS

Van Beugen, B.J.*, Nagaraja, R.Y.*, and Hansel, C. (2006). Climbing fiber-evoked endocannabinoid signaling heterosynaptically suppresses presynaptic cerebellar long-term potentiation. *J Neurosci* 26, 8289-8294.

Schonewille, M.*, Belmeguenai, A.*, Koekkoek, S.K.*, Houtman, S.H.*, Boele, H.J., **van Beugen, B.J.**, Gao, Z., Badura, A., Ohtsuki, G., Amerika, W.E., *et al.* (2010). Purkinje cell-specific knockout of the protein phosphatase PP2B impairs potentiation and cerebellar motor learning. *Neuron* 67, 618-628.

Gao, Z.*, **van Beugen, B.J.***, and De Zeeuw, C.I. (2012). Distributed synergistic plasticity and cerebellar learning. *Nat Rev Neurosci* 13, 619-635.

Van Beugen, B.J., Qiao, X., and Hansel, C. (Under revision). Enhanced AMPA Receptor Function Promotes Cerebellar Long-Term Depression Rather than Potentiation.

Van Beugen, B.J., Gao, Z., Voges, K., Witter L., Hoebeek, F.E., and de Zeeuw, C.I. (submitted). High Frequency Burst Firing Ensures Vesicular Release at the Parallel Fiber to Purkinje Cell Synapse at the Cost of Temporal Coding.

*These authors contributed equally

ACKNOWLEDGEMENTS

Now that you've read this entire thesis, it's better to stop reading here...

Hmm, you didn't stop. Well, it's your call. But, I mean, I've been hangin' 'round the department for quite some time now, getting to know a lot of people who've become part of this thesis in one form or another and now I'm just gonna be stupid and forget to thank you... Please, spare me the embarrassment, stop reading and let's just both pretend you're name is in this piece of text here somewhere...

But seriously, thanks everybody.

Chris, thanks for making all this possible; it started years back when you and Gerard allowed me to participate in the Masters program. Later, you were the one who suggested I should go work for Jerry. Finally (and this still amazes me), when I started my PhD, you were brave enough to let me decide the topic of my research. I'm still grateful you gave me the opportunity to pursue one of my own ideas, while giving valuable guidance along the way.

Christian, what can I say... you've never really been a supervisor to me, because you immediately became a friend. Sure, you've taught me all I know about electrophysiology. And I remember the many informative discussions we had, while seated in those legendary red chairs in your office, applying both knowledge and logic to come up with the best next step for our project (damn, you'd almost think we behaved like true scientists...). But what I remember even more are the small jokes and that constant presence of irony that you brought to the lab, lessening the burden of imminent failure that is inherently linked to patch clamping to a point where you'd almost start to believe it was all worth it... despite ABBA.

Of course I also have to thank all the brilliant characters that were part of the Hansel lab over the years: the true 'Duderino' John Weber ('ohh, I got sh*t to do, man...'), Matt Schmolesky ('if you look at my data for, for instance, ...'), Michiel Coesmans ('Excellent!'), Martijn de Rooter (ceaselessly yodeling and singing dubious songs about various body parts), Raghu 'the Stache' Nagaraja, Amor Belmeguenai ('***** **** *' some French 'words', not suitable for printing), Eric Hosal (cruisin' together through California in a red Mustang convertible) and Gen Ohsuki (double hours, double patching and still laughing). And of course all the recent members of the Hansel lab at UoC: Claire, Giorgio, Heather and Lorenzo. You made me feel at home from the first day I joined your group. I had a great time in Chicago thanks to you guys.

Jerry, it'd be easy to thank you for all the laughs, discussions and great dinners we had over all those years (I still remember that brilliant steak at Grand Central, ribs 'n jazz at Blue Smoke, burgers at the Waterfront, Thai in Meatpacking, Afghan on Lexington and the list

goes on...). But I feel I really need to thank you for something else; you've been a true tutor. You've taught me NY and you've taught me the cerebellum (and I mean more than just: "the cerebellum compensates for its own absence.").

Also many thanks to all the people at NYU: Robert (Hensbroek), Jun, Tim (Belton), Robert (Thorn), Tim (Blenkinsop), Sarah, Josh, Jim, Dedi. And Mary, of course. You've helped make New York a great experience.

Freek, gozert, het meest wil ik je bedanken voor je support over de laatste jaren. Weinig mensen kunnen een persoonlijke situatie zo goed inschatten als jij, waardoor je altijd de juiste steun kon bieden. En natuurlijk bedankt voor het uitbreiden van mijn muziekbibliotheek met een goeie portie tekno (waar mijn burens je minder dankbaar voor zijn, overigens...). Gao, thanks for all those little things that facilitated daily life in the lab; fixing equipment, giving technical advice and a daily dose of small talk. We've had many heated discussions about new publications and how they would relate to our own work. Remarkably, we hardly ever seemed to agree, but ultimately, that's what made both of us better. Mandy, ook jij bedankt voor al die kleine dingen die je onbaatzuchtig voor anderen doet om alles gesmeerd te laten lopen in het lab. En dank voor je grote mond, die nog altijd kleiner is dan je hart (en dat wil wat zeggen...). Ozz, bedankt voor een overdosis slap geouwehoer, genieten. Lieke, ook jij bedankt.

Elize, altijd als ik iets nodig had of zocht (en dat was verdomd vaak), wist jij me daarmee te helpen. En altijd met een gemeende glimlach, dank je wel. En Erica, ook jij natuurlijk bedankt daarvoor. Tom, allereerst ben je natuurlijk van een nostalgische waarde voor mij, omdat ik mijn eerste medische college kreeg van jou. Maar ook wanneer ik een anatomische vraag had, kon ik steeds een beroep doen op jouw ogenschijnlijk grenzeloze kennis. En je hebt natuurlijk gewoon een geweldig karakter. Daarentegen, Dick, bedankt dat je zo heerlijk gestoord bent. Loes en Edith. Jullie hebben zo veel gedaan, zowel voor als achter de schermen, waarschijnlijk zelfs meer dan waar ik weet van heb. En het was natuurlijk altijd gezellig om even bij jullie langs te lopen... En natuurlijk Elise, heel veel dank voor alles wat je hebt gedaan om mijn promotie te regelen.

Dank aan mijn familie: Pa, Ma, Brechje, Annelijn en Sander. Ik zal geen poging doen te beschrijven hoe diepgaand jullie invloed is geweest, want de grootste superlatieven zullen niets dan een slap understatement blijven. Maar jullie weten hoe belangrijk jullie voor me zijn en bedankt daarvoor...

Many thanks to all the expat Italians and all my friends back in Utrecht for offering a much needed distraction from work.

Many thanks to John Pemberton, Baron Karl von Drais and Thomas McCall; by means of your inventions you've had an immeasurable influence on this thesis, without which it might not have existed in the first place...

I want to thank my committee members Gerard, Hans, and Ype, for taking the time to read my thesis and giving me helpful suggestions.

Finally, I want to thank my paranymphs, Michiel Coesmans and Kajo van der Marel. Not only do we all share a career in neuroscience, more importantly, we share a distorted taste in music and a twisted sense of humor. I'm honored to be flanked by two like-minded friends when I face the committee.

Still, I have the feeling I'm forgetting someone. Ah, right, Elisa. Well, whatever....

